

A COMPARISON BETWEEN NATURAL AND LABORATORY OXIDATION
OF TITANOMAGNETITE IN PILLOW LAVAS

by

Patrick J. C. Ryall

Submitted in partial fulfilment
of the requirements for
the Degree of Doctor of Philosophy
at Dalhousie University

Department of Geology

December 1974

DALHOUSIE UNIVERSITY
FACULTY OF GRADUATE STUDIES

The undersigned hereby certify that they have read and recommend to the Faculty of Graduate Studies for acceptance a thesis entitled "A Comparison Between Natural and Laboratory Oxidation of Titanomagnetite in Pillow Lavas" submitted by Patrick J. C. Ryall in partial fulfilment for the degree of Doctor of Philosophy in the Department of Geology.

External Examiner _____

Committee Member _____

Committee Member _____

Committee Member _____

Committee Member _____

DALHOUSIE UNIVERSITY

Date December 1974

Author Patrick J. C. Ryall

Title A Comparison Between Natural and Laboratory

Oxidation of Titanomagnetite in Pillow Lavas

Department or School Department of Geology

Degree Ph.D. Convocation Spring Year 1975

Permission is herewith granted to Dalhousie University to circulate and to have copied for non-commercial purposes, at its discretion, the above title upon the request of individuals or institutions.

Signature of Author

THE AUTHOR RESERVES OTHER PUBLICATION RIGHTS, AND NEITHER THE THESIS NOR EXTENSIVE EXTRACTS FROM IT MAY BE PRINTED OR OTHERWISE REPRODUCED WITHOUT THE AUTHOR'S WRITTEN PERMISSION.

It cannot be that axioms established by
argumentation can suffice for the discovery
of new works, since the subtlety of nature
is greater many times over than the subtlety
of argument.

Francis Bacon

TABLE OF CONTENTS

I.	INTRODUCTION	
1.	A Brief History	1
2.	Relevant Magnetic Mineralogy	5
3.	Observations from Pillow Lavas	7
4.	Laboratory Alteration	10
5.	This Study	15
II.	STUDY OF PILLOW LAVAS	
1.	Introduction	17
2.	Sampling Technique	19
3.	Characteristics of Pillows	19
3.1	Grain Size	19
3.2	Saturation Magnetization and Curie Temperature	24
3.2.1	Equipment	24
3.2.2	Results: Curie Temperature	29
3.2.3	Results: Cell Edges	31
3.2.4	Results: Saturation Magnetization and Concentration	35
3.3	Natural Remanence	
3.3.1	Variation with Distance into the Pillows	43
3.3.2	Alternating Field Demagnetization	49
3.3.3	Direction of NRM	58
4.	Summary	58

III. LABORATORY ALTERATION

1. Methods	
1.1 Introduction	61
1.2 Apparatus	62
1.3 Experimental Procedure	65
2. Initial Experiment at 150°C	
2.1 Sample	67
2.2 Saturation Magnetization and Curie Temperature	67
2.3 A.F. Demagnetization of Successive TRM's	72
3. Experiment at 210°C	
3.1 Samples	74
3.2 Saturation Magnetization and Curie Temperature	75
3.3 A.F. Demagnetization of Successive TRM's	83
4. Second Experiment at 150°C	
4.1 Introduction	91
4.2 Samples	91
4.3 Saturation Magnetization and Curie Temperature	92
4.4 Concentration of Ferrites	98
4.5 A.F. Demagnetization of Successive TRM's	101
5. Summary	
5.1 Alteration Processes	106
5.2 Self-reversal Mechanisms	110
5.3 Self-reversals in Mid-Atlantic Ridge Samples	117

IV.	BERMUDA SEAMOUNT LAVAS	
1.	Introduction	124
2.	Magnetic Properties of Two Flows	
2.1	Bermuda Flow 38.1, NRM and Saturation Magnetization	125
2.2	Bermuda Flow 122.6, NRM and Saturation Magnetization	128
3.	Viscous Remanent Magnetization	
3.1	Introduction	131
3.2	Procedure	133
3.3	Results	134
4.	NRM Directions	139
5.	Summary	143
V.	REVIEW AND DISCUSSION	
1.	Introduction	145
2.	Effect of Radial Variations within Pillows	146
3.	Effect of Temperature Dependence of Reaction Rate	147
4.	Effect of Possible Self-reversals	157
5.	Summary	159
6.	Future Work	161
	BIBLIOGRAPHY	162
	APPENDIX	173

ABSTRACT

The magnetization of titanomagnetites in pillow basalts is important as the major source for the magnetic anomalies observed over the ocean basins. The magnetization is generally reduced as the titanomagnetites are altered through reaction with sea-water. This alteration and its effects have been studied in three ways: by the examination of young pillow basalts from the Mid-Atlantic Ridge, by laboratory alteration of these pillows and by examination of highly altered lavas from Bermuda.

During alteration at sea-bottom temperatures the titanomagnetites remain single phase and while intensity of NRM is reduced the direction of NRM is preserved. At higher temperatures, 150-200°C, in the laboratory, alteration is much more rapid so that a decrease in NRM which might take a million years at sea-bottom temperatures would need but a few thousand years. After prolonged heating, phase splitting occurs sometimes accompanied by self-reversals.

The accelerated alteration due to even slight heating, the possible self-reversals which may accompany phase splitting, and the scattering of NRM directions as seen in the Bermuda core combine to produce an effective magnetization at depth in layer 2 less than those inferred from dredge haul samples. Because of this lower magnetization it is likely that all of layer 2 will contribute to the magnetic anomalies.

LIST OF FIGURES

1.	A review of mineralogical and magnetic data concerning the system FeO , TiO_2 , Fe_2O_3 (from Grant and West, Interpretation Theory in Applied Geophysics).	6
2.	Sketch map of the Mid-Atlantic Ridge at 45°N , (after Irving <u>et al.</u> 1970) showing the dredge stations.	18
3.	Cross section through a pillow showing how samples were cut.	20
4.	Relations between TRM and grain size.	22
5.	Schematic diagram of apparatus used for obtaining J_s -T curves.	25
6.	Plot of Curie Temperatures of synthetics versus 'X'.	27
7.	Variation of Curie Temperature with distance into the four pillows.	28
8.	Contours of equal Curie Temperature for spinels in $\text{FeO-TiO}_2\text{-Fe}_2\text{O}_3$ system.	30
9.	Contours of equal cell edge for spinels in $\text{FeO-TiO}_2\text{-Fe}_2\text{O}_3$ system.	30
10.	Positions of samples from Pillows a) 197-8, b) 56-3, c) 47A-1 and d) 9-18 plotted on $\text{FeO-TiO}_2\text{-Fe}_2\text{O}_3$ ternary system.	33
11.	Variation of saturation magnetization with distance into the four pillows.	36
12.	Contours of equal saturation magnetization for spinels in $\text{FeO-TiO}_2\text{-Fe}_2\text{O}_3$ system in Bohr magnetons at $T=0^\circ\text{K}$.	37
13.	Evolution of Thermomagnetic curves for $x=0.7$ as degree of oxidation, 'z', increases.	38
14.	Variations of magnetization per gram, I_s , with 'z' for $x=0.6$.	40
15.	Concentration of titanomagnetites by weight as a function of distance into the four pillows.	41

16.	Intensity of NRM as a function of distance into the four pillows.	44
17.	Intensity of NRM divided by intensity of saturation magnetization as a function of distance into the four pillows.	45
18.	A.F. demagnetization of NRM for slices from each pillow.	50
19.	Normalized A.F. demagnetizations for slices from the four pillows.	53
20.	Mean demagnetizing field as a function of distance into the four pillows.	57
21.	Sketch of apparatus used to produce laboratory alterations.	64
22.	Tracings of J_s -T curves.	68
23.	A.F. demagnetization of PTRM's acquired by sample 56-3-35 after cooling from 150°C to room temperature in a 1.00 G field.	71
24.	Normalized A.F. demagnetization of PTRM's acquired by sample 56-3-35.	73
25.	Change in J_s and Curie temperature for five of the samples heated at 210°C as a function of total heating time.	76
26.	Tracing of J_s -T curves for sample 56-3-245.	78
27.	The evolution of the slope of the J_s -T curves for sample 197-8-42.	80
28.	Tracings of J_s -T curves for 73Ma-1-10 showing the evolution from a "paramagnetic" curve to one with multiple Curie points.	82
29.	Variation of PTRM acquired by various slices in cooling from 210°C in a 1.00 G field as a function of total heating time.	84
30.	Normalized A.F. demagnetizations of the samples heated at 210°C for various times.	86
31.	Change in J_s and Curie temperature for five of the samples heated at 150°C as a function of total heating time.	93

32.	Synthesis of J_s -T curves from varying amounts of phases having Curie points of 175°C and 325°C.	95
33.	Evolution of J_s -T curves for sample 56-3-236 before heating and after 990 hours and 1580 hours at 150°C.	97
34.	Variation of PTRM acquired by various slices in cooling from 150°C in a 1.00 G field as a function of total heating time.	100
35.	Normalized A.F. demagnetizations of the samples heated at 150°C for various times.	102
36.	A.F. demagnetization of successive TRM's for 197-8-45.	107
37.	Section of FeO-TiO ₂ -Fe ₂ O ₃ ternary diagram showing self-reversal regions.	111
38.	A model for negative magnetostatic interaction.	115
39.	Analysis of PTRM for sample 197-8-45 after 3023 hours of 150°C into normal and reverse components.	118
40.	A magnetostatic interaction model for self-reversal.	121
41.	Magnetic properties of flow 38.1.	126
42.	Magnetic properties of flow 122.6.	127
43.	Typical J_s -T curves for flows 38.1 and 122.6.	129
44.	Change of direction in two samples from flow 122.6 with A.F. demagnetization.	132
45.	Acquisition of VRM by Bermuda samples.	135
46.	Declination and inclination for flow 38.1.	138
47.	Declination and inclination for flow 122.6.	140
48.	A model showing how the addition of a secondary component to antiparallel vectors could produce the directions measured in flow 122.6.	142

49.	Relation between temperature and time required for maghemitization.	148
50.	A comparison between the PTRM acquired in the laboratory as a function of heating time to the intensity (station average) of dredge haul basalts as a function of age.	150
51.	Contours of constant intensity of magnetization.	152
52.	Profiles across N-S ridge.	154
53.	Profiles across a N15°E trending ridge.	155.
54.	Profiles and their models across several ridges.	156.

LIST OF TABLES

1.	Locations and Ages of Pillows	19
2.	Cell Edges for Mid-Atlantic Ridge Pillows	32
3.	Concentration of Ferrites in Sample 56-3-35	70
4.	Mean Demagnetizing Fields of Sample 73Ma-1-10	89
5.	Variation of Concentration of Ferrites with Heating Time at 150°C	99
6.	Acquisition of VRM's in the Present Epoch	136

TABLE OF SYMBOLS AND ABBREVIATIONS

A.F.	Alternating Field
ARM	Anhyseretic remanent magnetization
CRM	Chemical remanent magnetization
E_s	Activation energy
F	Force
H'	Dipole field
H _c	Coercive force
H _{ex}	External field
I_r	Intensity of isothermal viscous remanent magnetization
I_s	Intensity of saturation magnetization of a mineral, at room temperature
J_s	Intensity of saturation magnetization of a rock, at room temperature
J_{TRM}	Intensity of thermoremanent magnetization
k	Boltzman's constant
M	Magnetic moment
MDF	Mean demagnetizing field
N	Normal polarity
NRM	Natural remanent magnetization
PTRM	Partial thermoremanent magnetization
R	Reversed polarity
S	Viscosity coefficient
t	Time during which field applied in VRM equation
t'	Time required to measure VRM
T	Temperature
TRM	Thermoremanent magnetization

V	Volume of a grain
VRM	Viscous remanent magnetization
x	Fraction of ulvospinel in titanomagnetite
z	A measure of cation deficiency in non-stoichiometric titanomagnetite
λ	Inverse of reaction time
λ_0	An inverse reaction time constant
τ_0	Relaxation time for VRM acquisition

ACKNOWLEDGEMENTS

During the course of this research I have been helped by many people. In particular I would like to thank:

My supervisor, Dr. J. M. Ade-Hall, for his constant guidance, encouragement and support.

The other members of my committee: Drs. E. Irving, M. J. Keen, R. D. Hyndman, and P. H. Reynolds, for their helpful advice and suggestions.

Drs. H. P. Johnson and K. Kitazawa, for many a thought-provoking discussion.

Mr. R. E. Heffler and his staff who made so much of the apparatus without which nothing would have been possible.

My wife, Patricia, who not only typed and retyped the thesis but who also provided the encouragement without which it would never have been finished.

The National Research Council of Canada, for a scholarship which covered the first two and a half years of this work.

The Killam Trust, for an Izaak Walton Killam Memorial Scholarship which covered the final year of this work.

I. INTRODUCTION

1.1 A Brief History

Over the last decade and a half the attention of rock magnetists has been increasingly directed towards the magnetic properties of the rocks which make up the first few kilometres under the ocean floor. This interest first came about with the attempt by Mason and Raff (1961) to interpret the linear magnetic anomalies off the West coast of North America in terms of slabs of rock with a susceptibility different from that of the surrounding rock or sediment. Interest was heightened when Vine and Matthews (1963) suggested that linear magnetic anomalies might be explained by blocks of the crustal layer some 20 km wide being alternately magnetized in the normal and reverse sense; a concept which had also been advanced by Morley and Larochele (1964).

Mapping of the magnetic anomalies over the Atlantic, for example, has revealed not only an exceptionally intense anomaly over the Mid-Atlantic Ridge itself (Keen 1963, Heirtzler et al. 1965), but also that at large distances from the ridge, adjacent to the continental shelves, there are areas in which the anomaly pattern is absent - the magnetic 'smooth zones' (Heirtzler and Hayes 1967). Thus the need has arisen not only to find out the magnetic properties of the basalts for the purpose of constraining magnetic anomaly models, but also to find out how and why

the magnetic properties vary with distance from the ridge axis.

Due to the lack of definitive information regarding the magnetic properties of the ocean crust it has not been possible to interpret the linear magnetic anomalies to give much information about the structure and composition of the crust itself. The difficulty arises because solutions to the magnetic potential problem are not unique; that is the anomaly at the surface from a strongly magnetized thin layer is identical to that due to a weakly magnetized thick layer. Vine and Matthews (1963) original estimate for the thickness of this magnetic layer was 20 km (under most of the ocean but only 11 km under the ridge) using a value for magnetization (J) of 0.005 emu. This value for magnetization corresponds to an effective susceptibility of ± 0.0133 (effective susceptibility = total intensity of magnetization (remanent + induced)/present magnetic field intensity). From that time models have been successively refined as more information became available on the submarine lavas. Loncarevic et al. (1966) used a magnetized layer about 3 km thick, however Irving et al. (1970a) reporting an extensive series of measurements on dredge samples from 45°N found the average sample intensity about twice that of previous model values thereby requiring a magnetic crust substantially thinner than 2 km. Irving et al. (1970b) then developed a model which had a thickness of the magnetized layer of only 200 m for the Median Valley thickening to 1 km for the

Crest Mountains and High Fractured Plateaux. Talwani et al. (1971) used information gained from profiles along anomalies parallel to the ridge crest to obtain values for the intensity of magnetization of 0.03 emu on the ridge and 0.012 emu on either side. Using these values with trial and error fitting they decided on a thickness of 400 m for the magnetized layer which they called layer 2A. More recently, Lowrie et al. (1973) have found basalts with ages of between 21 and 85 million years recovered from DSDP holes in the Atlantic Ocean to have remanent magnetizations half that of dredge samples (about 0.001 emu) due to a lower concentration of opaques than in the dredge haul material, thereby requiring a thickness of around 2.5 km.

Prior to the DSDP and the Deep Drill programmes at Dalhousie University virtually all samples which had been examined to establish rock magnetic properties were pillows or pillow fragments recovered in dredge hauls. Because of this bias towards material recovered from the upper skin of layer 2, material which may have had a very different cooling history compared to the rest of the layer, models based on dredge haul data must be considered open to revision as deeper material becomes available.

Although many different rock types have been recovered from the ocean floor, the most common type encountered is basalt in the form of pillows. The mode of emplacement of these basalts presents a problem. Mathematical models envisage homogeneous rectangular blocks being carried away

from the ridge in a 'conveyor belt' process. Geologically more probable models have been discussed by Watkins and Richardson (1971) and Watkins and Paster (1971). These models involve dyke injection over the space of a few kilometres near the ridge axis with some overlying extrusives. Detailed investigations of the Mid-Atlantic Ridge at 36°30'N by Luyendyk et al. (1974) have shown prominent volcanism within a one kilometre band in the centre of the median valley.

There is considerable evidence that pillows make up a large fraction of basalt. Pillow basalts occur frequently in bottom photographs, Aumento (1968), Moore and Fiske (1969), Luyendyk et al. (1974). Also in the few places where what is thought to be ocean crust outcrops as in Cyprus and Papua pillow layers are of the order of 1 km thick (Gass 1968, Davies 1968). Similar layers of pillows are also found on Newfoundland with thickness up to a few kilometres (Williams 1972). Recent studies from a borehole which has penetrated 800 m into the Bermuda volcano reveal (Aumento and Ade-Hall 1973) an assemblage of pillow basalts with massive interiors and sheets less than 1 m in thickness.

It is not possible at this time to come to a definitive conclusion regarding the nature of the rocks responsible for the magnetic anomalies, nor is it likely to be so until a significant number of deep holes have been drilled into layer 2. Nonetheless, it is useful to study the strongly magnetized pillows, not only because they make up a

considerable fraction of the basalt but also because of their effectiveness as carriers of NRM.

1.2 Relevant Magnetic Mineralogy

The pillows, by the nature of their formation, are rapidly quenched resulting in the formation of predominantly single or pseudo-single domain titanomagnetites (Evans and McElhinny 1969, Dunlop and West 1969, Larson et al. 1969). There are, no doubt, many finer grains smaller than single-domain and perhaps a few multi-domain grains. The magnetic properties of such pillows are quite different from those of thicker subaerial lava flows in which the titanomagnetites are subject to deuteric oxidation (Wilson and Haggerty 1965, Wilson and Watkins 1967, Gromme et al. 1969) and often also to hydrothermal alteration (Ade-Hall et al. 1968, 1971).

The magnetic minerals are the ferrites from the FeO-TiO₂-Fe₂O₃ ternary diagram shown in Figure 1. There are three principal phases.

- 1) Stoichiometric titanomagnetites: Verhoogen (1962) refers to this as the β -phase. A member of this solid solution series is identified by $\beta(x)$ where x is the molecular proportion of ulvöspinel in the molecular formula $x\text{Fe}_2\text{TiO}_4(1-x)\text{Fe}_3\text{O}_4$.
- 2) Stoichiometric ilmenite-hematites: These are normally known as the α -phase. A member of this solid solution series, $y\text{FeTiO}_3(1-y)\text{Fe}_2\text{O}_3$, is denoted by $\alpha(y)$.

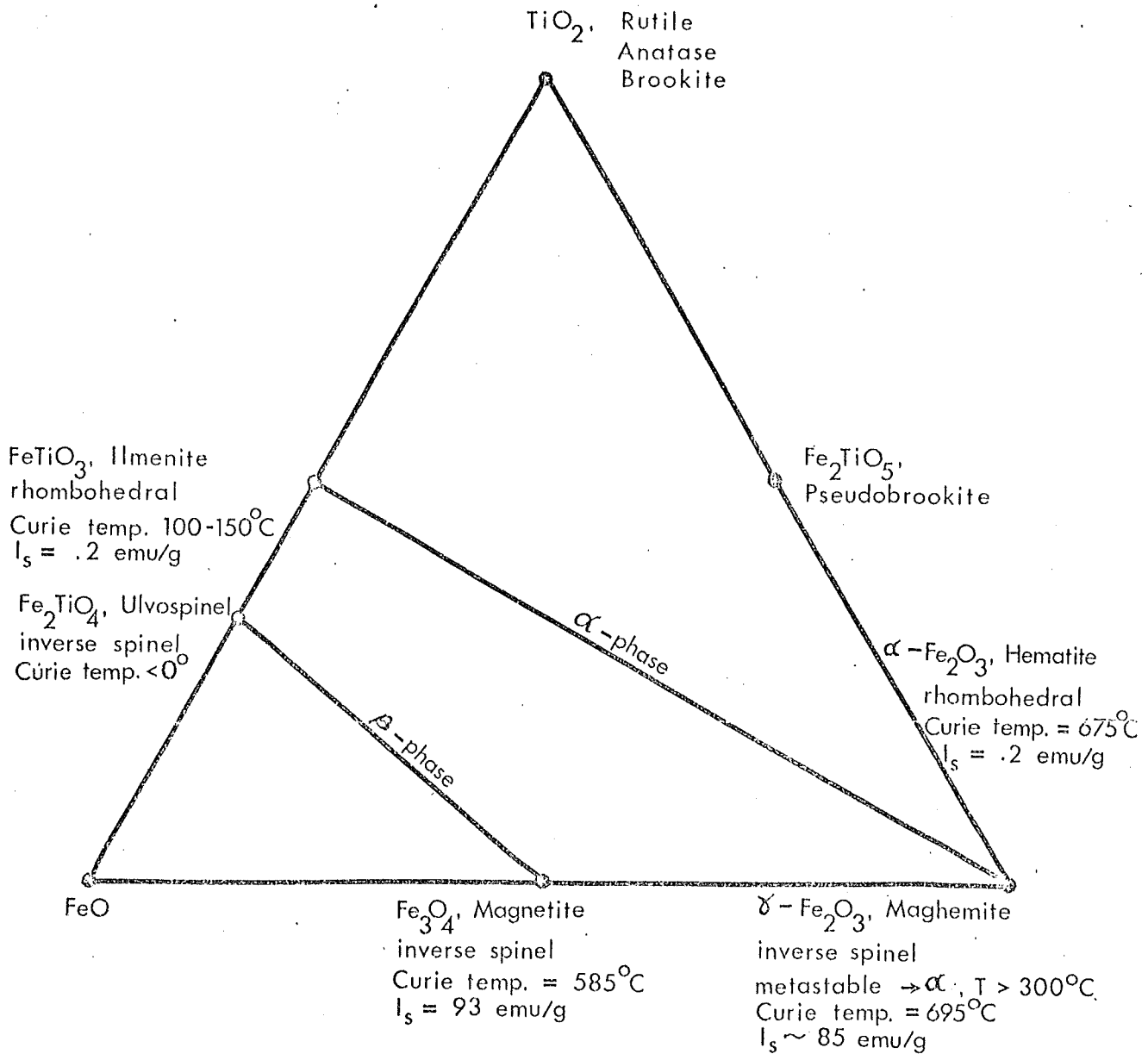
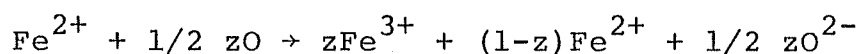


Figure 1. A review of mineralogical and magnetic data concerning the system FeO , TiO_2 , Fe_2O_3 (from Grant and West, Interpretation Theory in Applied Geophysics).

3) Cation-deficient titanomagnetites: All such compositions ($\text{Fe}_a\text{Ti}_b\text{□}_c\text{O}_4$, $a+b+c = 3$, where \square denotes a vacancy), shall be referred to as the γ -phase, to a specific member by the symbol $\gamma(x, z)$. The oxidation parameter, z , is the fraction of total Fe^{2+} ions initially in the sample converted to Fe^{3+} ions, i.e.



A cation-deficient titanomagnetite with the composition of the α -phase but retaining spinel structure is sometimes referred to as titanomaghemite.

The most important magnetic minerals in pillow basalts are titanomagnetites and cation-deficient titanomagnetites.

1.3 Observations from Pillow Lavas

A comprehensive study of the petrology and magnetic properties of dredged pillow lavas from the Mid-Atlantic Ridge has been carried out. The remanent magnetization, susceptibility and iron content was reported (Irving et al. 1970) as was the coercivity, secondary magnetization and thermal stability (Park and Irving 1970). A careful study was made of the relationship between the magnetic properties and the opaque mineralogy as well as determinations of palaeomagnetic field intensity (Carmichael 1970). In addition the thermomagnetic properties were investigated (Schaeffer and Schwarz 1970) in which the Curie temperature of the titanomagnetites was used to help determine the composition of the titanomagnetites. Studies similar to

these were reported (Brooke et al. 1970) on core obtained by a drill rig operating on the sea-floor. The most significant results were summarized in a review paper (Irving 1970):

- a) Grain size up to 1-5 microns although some larger (20 μ) grains were seen.
- b) A scatter of total iron oxide content ($\text{FeO} + \text{Fe}_2\text{O}_3$) of between 7% and 11% but no trend with distance from the ridge.
- c) The oxidation ratio ($\text{FeO}/\text{Fe}_2\text{O}_3$), which is between 5 and 10 at the ridge, falls to unity beyond 20 km from the axis.
- d) The water content increases from 0.5% at the axis to 5% on the high fractured plateaux.
- e) The oxygen isotope ratio ($\text{O}^{18}/\text{O}^{16}$) of the basalt, which is 35 for sea-water, increases from 5 at the axis to 18 at a distance of 150 km from the axis.
- f) The natural remanent magnetization (NRM) decreases rapidly with distance from the ridge axis falling from about 0.1 emu/cm^3 down to about 0.006 emu/cm^3 in the High Fractured Plateaux, the greatest part of the decrease occurring within 10 km from the axis.
- g) Curie temperature increases from 100°C-150°C in the Median Valley to about 350°C in samples from the Crestal Mountains and High Fractured Plateaux.

h) Blocking temperature increases from an average of 230°C in the Median Valley to about 450°C at a distance of 100 km from the axis. The fact that the blocking temperatures measured are higher than the Curie temperatures means that new high blocking temperature material is being formed during the thermal demagnetization.

The conclusion from these observations was that the titanomagnetites were being oxidized by the sea-water at low temperatures. The concept of changes in the basalts with distance from the ridge is not confined to the titanomagnetites. Hart (1970, 1973) has shown systematic chemical trends in major elements with distance from ridge spreading centres.

The model which Irving (1970) put forward to explain these changes in the magnetic properties with distance envisaged the very quick cooling of the lava as it was extruded onto the ocean floor, such as has been observed by Moore et al. (1973). The result would be the rapid crystallization of small titanomagnetite particles which would acquire their remanence by cooling through their initial blocking temperature. Since this is one of the most favourable situations for the formation of thermoremanent magnetization (TRM) it could account for the high axial remanence. Irving (1970) goes on to point out the high ratio of the intensities of NRM to saturation IRM, of the order of 0.1 compared to 0.01 for continental basalts,

means that the natural process of magnetization is an efficient one.

With this very rapid cooling there would be little or no deuteric oxidation. The basalt is dry and begins to absorb oxygen from the sea and the titanomagnetite becomes partially oxidized. Being surrounded by sea-water and with possible mild heating by subsequent flows while near the ridge, oxidation occurs and produces the observed increases in Curie temperatures and the development of a higher blocking temperature remanence of reduced intensity.

1.4 Laboratory Alteration

Alteration of titanomagnetites in submarine basalts occurs during thermal demagnetization of NRM and during measurements of J_s vs. T . Ozima and Larson (1970) have carried out microscopic observations, chemical and X-ray analyses on samples both before and after J_s - T curves had been obtained. By comparing the J_s - T curves obtained in air and in vacuo they are able to distinguish between a titanomagnetite and a titanohematite. They showed that heating of titanomagnetite to several hundred degrees centigrade in air produces a high-temperature oxidation to magnetite and other Ti-Fe phases; not low-temperature oxidation to titanomaghemite.

A typical example of the results of oxidation during thermal demagnetization is seen in the results of Irving et al. (1970) in which they reported blocking temperatures

50°-100°C higher than Curie temperatures of the natural rocks because new magnetic material is being formed during the heating.

The types of alterations just mentioned occur in the course of some thermomagnetic measurement, generally in a few minutes at several hundred degrees Centigrade. Several experiments have been carried out for longer times at lower temperatures in an attempt to reproduce the low temperature oxidation which occurs on the sea-floor.

Park and Irving (1970) in an effort to understand the mechanism of the decrease of NRM with distance from the ridge warmed a series of specimens from basalts of different ages at 100°C for 95 hours. They found that the specimens could be considered in two groups. The first group, consisting of samples distant 10 km or less from the axis, showed a decrease in NRM of 20% or more and an increase in blocking temperature of between 40 and 125°C. The other group, consisting of samples distant more than 20 km from the axis, showed a decrease of about 4% in NRM and little systematic change in blocking temperature. The percentage decrease in NRM is not correlated with the original intensity of NRM, but rather with the blocking temperature. Park and Irving (1970) suggested some unspecified oxidation process as the cause of these and other changes. It is notable that the warming process does not change the original direction of NRM.

Earlier, Ozima and Ozima (1967) had reported the results of an experiment in which they heated in air samples from eight dredged basalts for varying lengths of time at temperatures up to 600°C. Three of the samples showed self-reversal of thermoremanent magnetization when cooled to room temperature in the Earth's field. This self-reversal only occurred when the sample had been heated to between 300°C and 330°C and then only for a short duration of heating. After more than 150 minutes in air at 300°C, it no longer shows self-reversal. They concluded that the self-reversal was due to an interaction between the original titanomagnetite and its oxidation product. They explained the lack of self-reversal in the other samples because they contained highly oxidized titanomaghemite which would unmix directly to magnetite and pseudo-brookite. These conclusions were somewhat speculative since the actual compositions were not directly measured.

Marshall and Cox (1971a) studied the effects of oxidation on the NRM of titanomagnetite in basalt. In their experiment, samples from pillows were heated in air with the samples so aligned that an applied field was perpendicular to the NRM. This arrangement allowed them to monitor the NRM and any CRM independently. Their procedure was to partially demagnetize the sample to 100°C. Next the sample was kept at 250°C for half an hour with NRM and CRM measured every 10 minutes. The temperature was then quickly raised about 50°C and the procedure repeated up to a final

temperature of almost 600°C.

Two cases were considered: the first where oxidation took place at a temperature higher than the Curie temperature, the second at a temperature less than the Curie temperature. In the first case, heating above the Curie temperature simply destroys the original NRM and a CRM was created. On cooling from almost 600°C, the maximum temperature reached, a TRM approximately twice the original NRM was acquired. In the second case, heating below the Curie temperature, which was done by heating a sample with higher initial Curie temperature, the NRM was not destroyed but rather increased with heating. A CRM was produced over about the same temperature range as in the former experiment. In neither of these experiments was the sample kept at any one temperature long enough to come to equilibrium, so it is possible that the results obtained by heating to 580°C would have been obtained had heating at 300°C continued for long enough.

In the first case the original titanomagnetite has been altered to magnetite which has the appropriate Curie temperature and the increased magnetization. In the second case, since the original NRM was not completely destroyed by the heating it was enhanced as more and more material was converted to a titanomagnetite with higher J_s .

While conceding that there were probably differences between the magnetic effect of oxidation at 300°C for a few tens of minutes and oxidation at sea-floor temperatures for

a few million years, they did consider that as long as the heating temperature was below the Curie temperature the processes should be analogous. The most obvious differences between measurements in pillows and Marshall and Cox's results is that in pillows NRM decreases with oxidation while in Marshall and Cox's experiment it increases. Therefore the same mechanism cannot be at work. It is possible that at the temperatures they used the original titanomagnetite is unmixing to produce some magnetite which would account for the higher magnetization. When they studied heating at lower than Curie temperature, they did not heat at a lower temperature but rather used a sample with a higher Curie temperature, that is, a sample which had been oxidized.

Marshall and Cox have chosen to consider their heating experiments in two categories, those below and those above the Curie temperature. This would seem to be the important division as far as effect on NRM is concerned. From the mineralogical standpoint there is another dividing point, some temperature below which there is homogeneous oxidation and above which the original titanomagnetite unmixes. Because of the increase in J_s in their measurement most of Marshall and Cox's heatings will have been above this temperature while in nature J_s decreases as the γ -phase becomes more highly cation-deficient.

1.5 This Study

The work described in this thesis is an attempt to duplicate in the laboratory the changes in magnetic properties found in nature. In order to reproduce natural conditions as closely as possible, the chemical alteration was carried out in water at pressures approximately those on the sea-floor. While the aim was to keep heating temperatures as low as possible, it would be necessary to use temperatures higher than sea-floor temperature in order to bring reaction times within the life-time of the experimenter. The intention was to monitor the composition of the titanomagnetites during the heating so that their evolution could be compared with natural processes - something which had not been done in previous work. It was hoped that a self-reversal such as reported by Ozima et al. (1967) might occur and that it would be possible to determine if such a self-reversal was due to the titanomagnetite splitting into two phases, or oxidation into the possible self-reversal region in the $\text{FeO-TiO}_2\text{-Fe}_2\text{O}_3$ ternary diagram suggested by Verhoogen (1962) and later refined by O'Reilly and Banerjee (1966).

Because of the sparseness of published information, it was necessary to establish a datum against which laboratory alteration could be judged. For this reason it was decided to carry out a systematic study on four pillow basalts of different ages to establish the relationships between the magnetic properties, alteration, ages and distance from the

Median Valley.

As this work progressed, material from Bermuda at least 90 million years old became available. These lavas were examined as a possible end product of the chemical alteration process first seen in the young pillows and then produced in the laboratory.

Thus, chemical alteration of the magnetic minerals of pillow basalts is being investigated in the following manner. First, an examination of young basalts to establish a starting point for the titanomagnetites and to establish how they vary radially and with age. Second, an attempt to reproduce and possibly extend these alterations in the laboratory and finally a check with the older Bermuda material to find if it is an end member consistent with the processes observed in the young pillows and in the laboratory.

Since the study of the young pillows is necessary as a basis against which everything else will be judged, it will be dealt with first.

If the alteration processes produced in the laboratory prove to be comparable to those observed in nature, then it may be possible to establish the reaction rates for the processes observed in nature from laboratory data. From this reaction rate it may be possible to construct a model for alteration of the titanomagnetites as a function of temperature and distance from a spreading ridge.

II. STUDY OF PILLOW LAVAS

1. Introduction

The general pattern of the alteration of the magnetic properties in pillows with distance from the Mid-Atlantic Ridge has been compiled by Irving (1970). These measurements were based on cores taken from what was judged to be the fresh material from the interior of the pillows. Marshall and Cox (1971b), on the other hand, clearly showed variations in magnetic properties within different pillows from the Juan de Fuca Rise. It was necessary to make a detailed study of the pillows to be used in the alteration experiments so that any laboratory induced changes could be compared with natural ones. In addition such a study would permit a direct comparison of natural changes within each pillow with changes between pillows of different ages.

Four pillows dredged from the Mid-Atlantic Ridge were investigated. The locations and ages of these pillows is given in Figure 2 and Table 1. Ages for all except 197-8 were obtained by Aumento (1969). No age is available for 197-8 but it is thought to be less than a few thousand years old because it was recovered from the ridge axis, and in light of the alteration of magnetic properties with time, probably younger than 56-3.

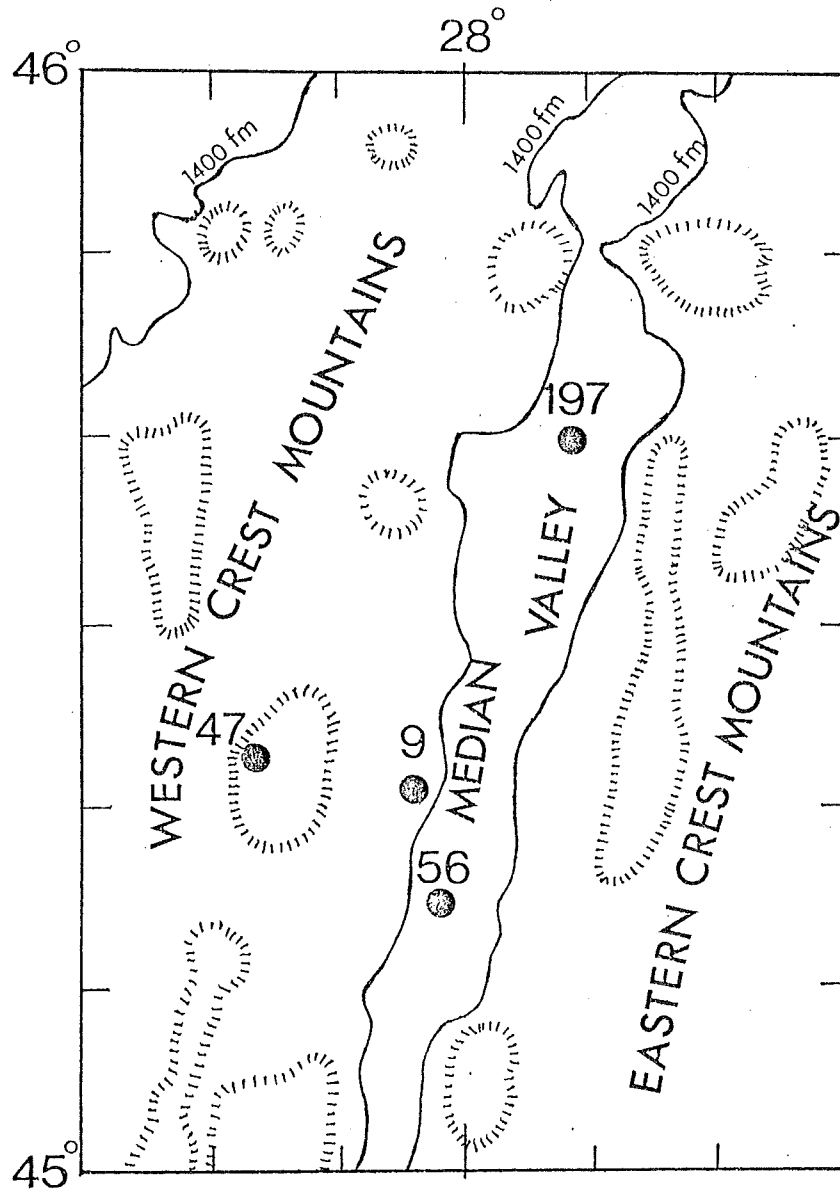


Figure 2. Sketch map of the Mid-Atlantic Ridge at 45°N, (after Irving et al. 1970) showing the dredge stations.

TABLE 1.
LOCATIONS AND AGES OF PILLOWS

Pillow	Distance from Ridge	Age (thousand years)	Polarity Zone
Hu 197-8	0 km		N
Hu 56-3	0 km	12 ± 18	N
Hu 9-18	10 km	286 ± 74	N
Hu 47A-1	25 km	740 ± 370	R

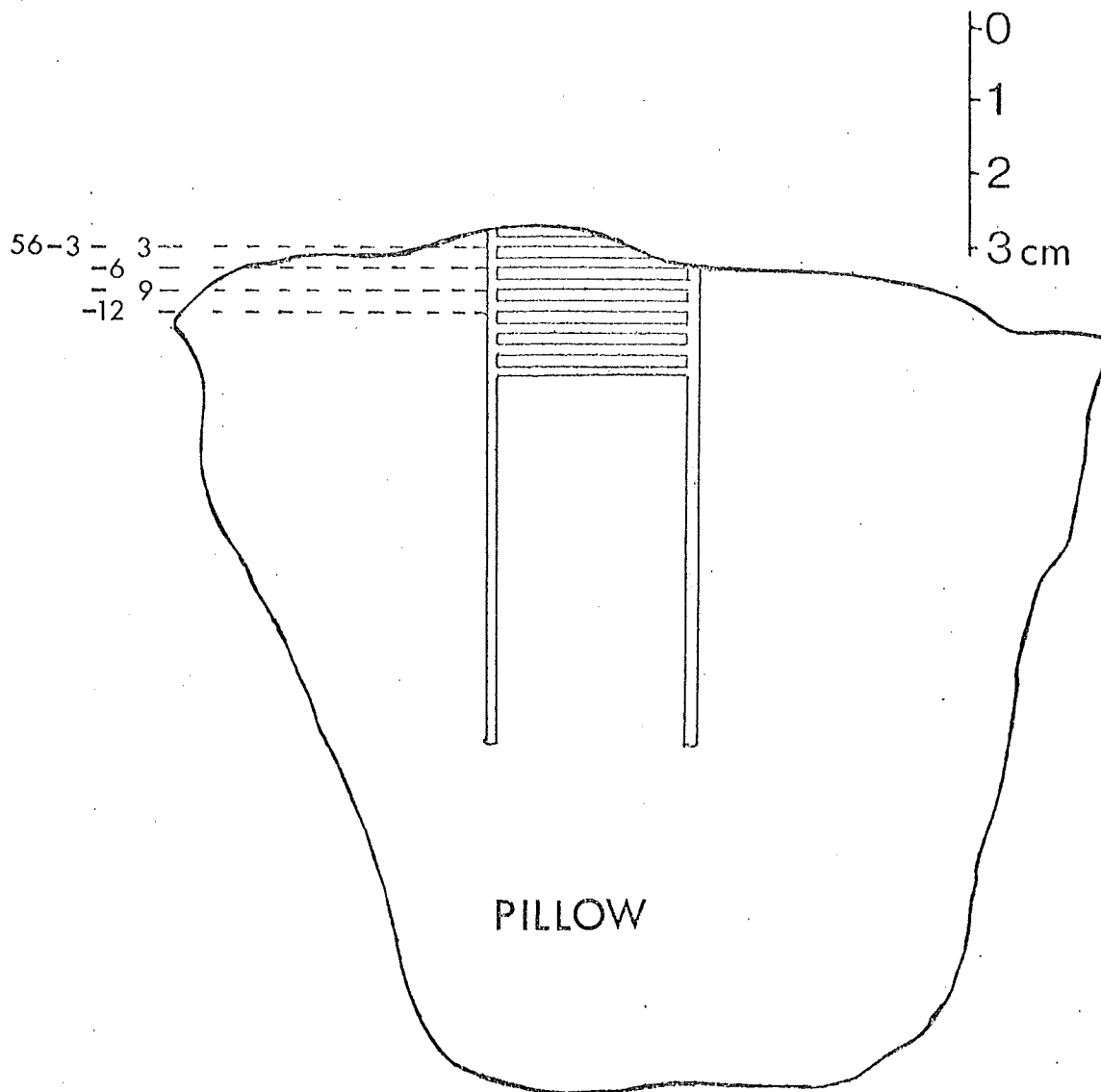
2. Sampling Techniques

A one inch diameter core was drilled from each pillow along a radius. Slices were cut off every 3 millimetres and each slice numbered according to its distance in millimetres from the outside of the pillow. Later a second core was drilled from 56-3 when more material was needed. Figure 3 illustrates the sampling technique. The shaded areas in the figure represent material lost in the cutting operation. The numbers indicating the distance of the sample into the pillow were appended to the pillow number, thus 56-3-48 would indicate a slice 48 mm from the outside of pillow 56-3.

3. Characteristics of Pillows

3.1 Grain Size

Four polished sections from each pillow were examined at a magnification of 1200 using oil immersion. All the pillows have a radial variation in grain size. Pillows



SAMPLING TECHNIQUE

Figure 3. Cross section through a pillow showing how samples were cut.

56-3 and 9-18 are very similar. In neither of them were the grains in the outer regions large enough to be visible. At a depth of about one and a half centimetres grains as large as $2\mu \times 3\mu$ could be seen although the majority of grains are smaller. With greater depth into the pillow larger and larger grains are encountered finally reaching about $10\mu \times 3\mu$. Grain growth seems to occur only in one direction, that is the larger grains are not equidimensional but have a minimum dimension about 2μ or 3μ .

Pillow 47A-1 has slightly less radial variation. Grains of just over a micron are visible in the outer slice with a growth of up to $5\mu \times 6\mu$ in the interior, six centimetres into the pillow. These grains were of skeletal form.

Grains in 197-8 were generally larger than in the other pillows. The slice from half a centimetre from the outside had some grains as large as $4\mu \times 1/2\mu$, although these grains look more like chains of smaller grains than single homogeneous grains. Once again grain size increases with distance into the pillow, although the impression is more one of a sharp increase in size somewhere around the 3 cm mark rather than a gradual increase. At depths of 4 cm and 5 cm there are some grains as large as $20\mu \times 6\mu$ although once again these grains are skeletal.

All the sizes mentioned are maximum sizes. Grains are present down to the limit of visibility, so there are probably many smaller grains which cannot be seen.

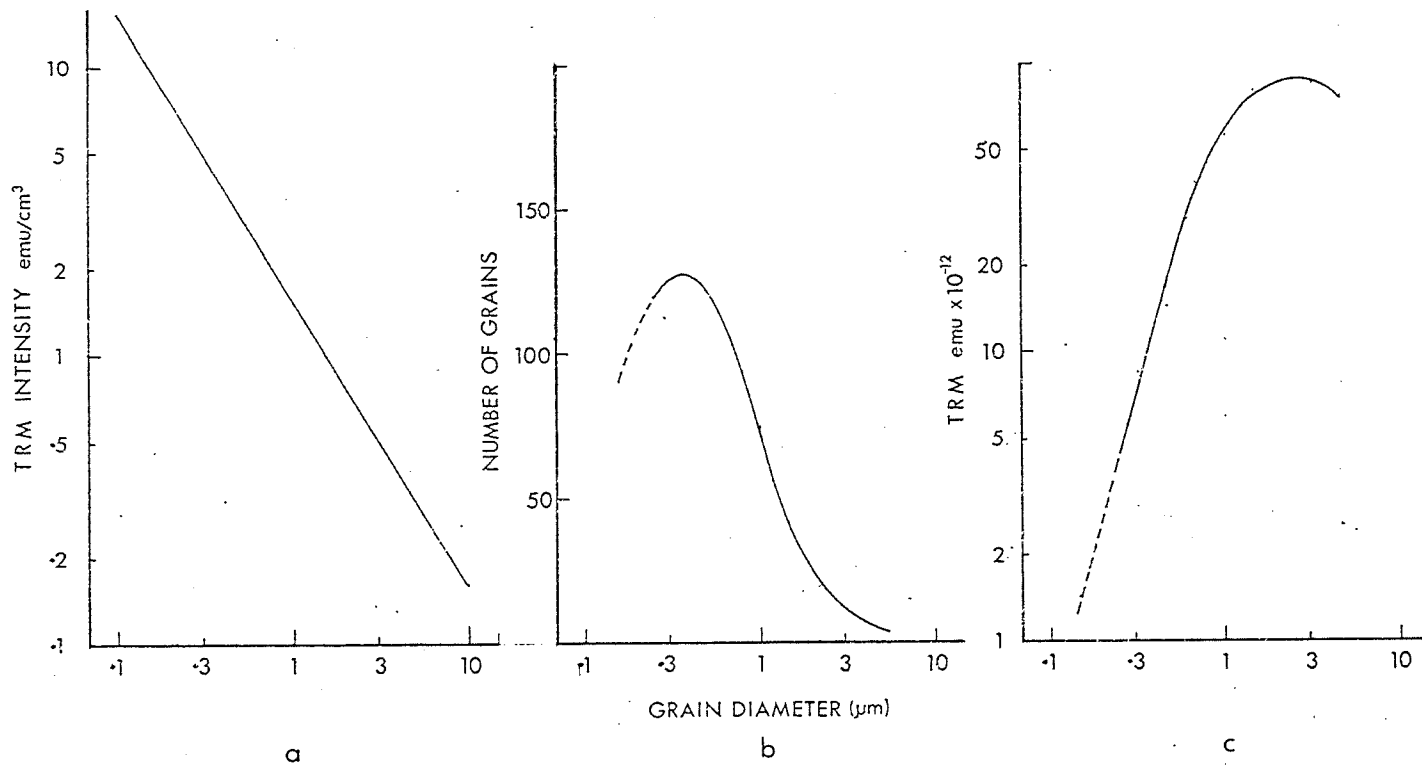


Figure 4. Relations between TRM and grain size.

- a) Intensity of TRM (emu/cm^3) as a function of grain diameter. Dunlop (1973) Fig. 7.
- b) Number of grains of titanomagnetite as a function of diameter in an area examined by Evans and Wayman (1970) Fig. 5.
- c) Intensity of TRM as a function of grain size calculated for an area examined by Evans and Wayman. This shows how grains a few microns dominate TRM. The integral of this curve could be total TRM of this sample.

Recently considerable attention has been paid to the role of very small grains in carrying the NRM. Using photomicrographs Evans et al. (1968) and Evans and McElhinny (1969) extrapolated from visible grains to establish a peak of grain size between 0.5μ and 0.25μ . Later Evans and Weyman (1970), using electron microscopy, found a peak in the grain size distribution of a Mid-Atlantic Ridge basalt of about 0.25μ . Similarly Larson et al. (1969) have postulated a peak in grain size distribution around 0.5μ . Generally these peaks were obtained on one or more sections from a pillow. There would be some variation in the peak with distance into the pillow but considering that the maximum grain sizes observed in the pillows of this study are not much different from those of Evans, then it is reasonable to expect a similar peak in size.

Since grains less than a few microns will be single or pseudo-single domain, then the intensity of the TRM is dependent on the inverse of grain size in a manner as shown in Figure 4a (which is Dunlop's (1973) Figure 7). If this relation is combined with a grain size distribution such as Figure 4b (which is Evans and Weyman's (1970) Figure 5), then relative TRM versus grain size relationship shown in Figure 4c is representative of such a basalt. This diagram shows that the most significant grains magnetically are those from 0.5 microns up to about 5 microns, the maximum size generally observed.

3.2 Saturation Magnetization and Curie Temperature

3.2.1 Equipment

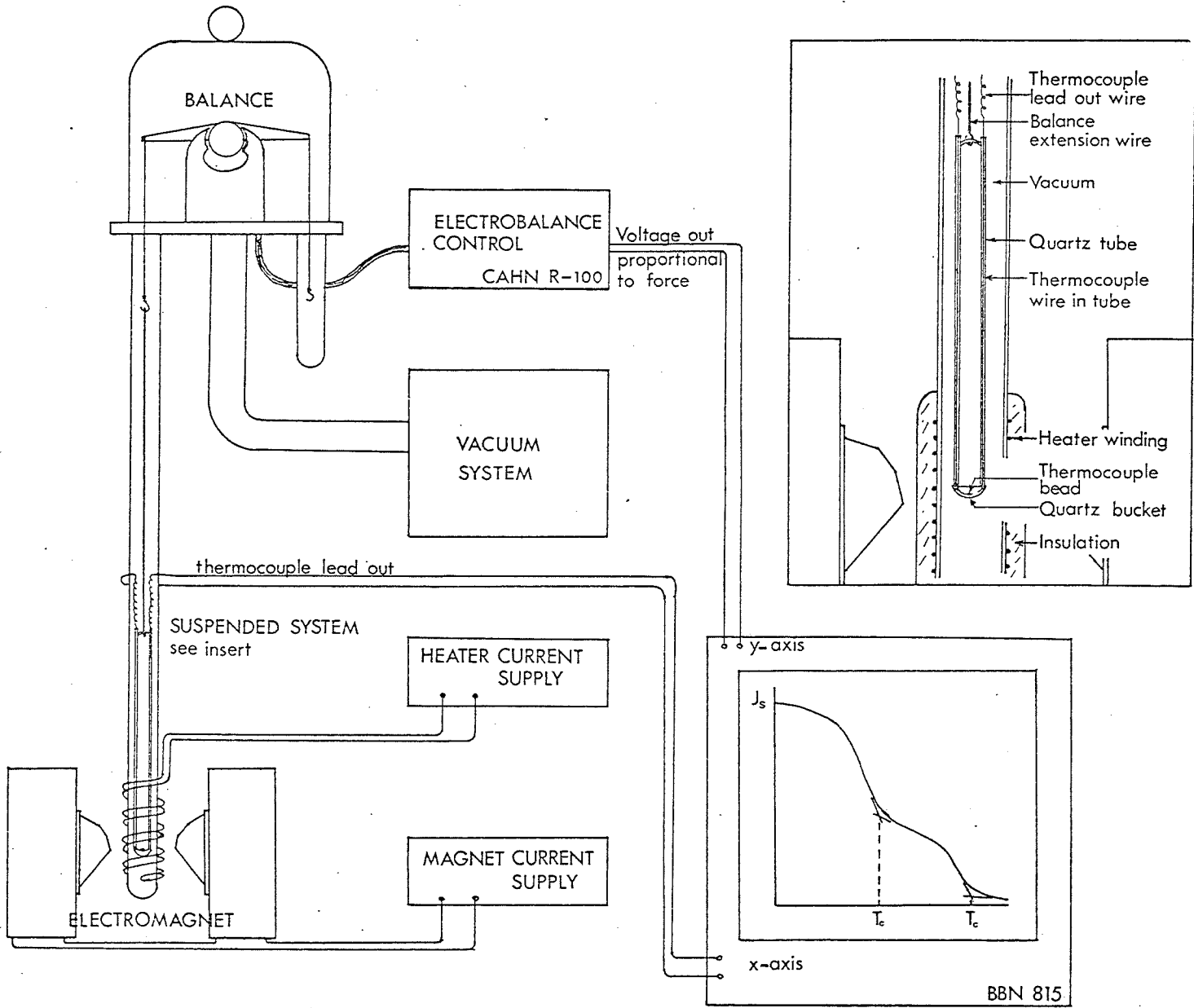
Saturation magnetization was used as a means of obtaining information about the concentration of the titanomagnetites. Since saturation magnetization was measured as a function of temperature it was possible to determine the Curie temperature and hence the composition. Saturation magnetization was measured using small (10-30 mg) chips broken from the slices.

A block diagram of the apparatus is given in Figure 5. In these measurements the samples were placed in a quartz bucket suspended between the pole pieces of a 7 kiloGauss electromagnet. The bucket was suspended from one arm of a Cahn R-100 electrobalance. The mass of the bucket and sample were counterbalanced so that the force measured by the balance was the magnetic force of the magnetic field acting on the sample. The force on the sample is simply related to the magnetization by the equation:

$$F = J \left(\frac{dH}{dz} \right)$$

where F is the force, J is the saturation magnetization for the sample and $\frac{dH}{dz}$ is the field gradient. Since the current in the electromagnet is kept constant and since the electrobalance measures the force about an equilibrium position, then $\frac{dH}{dz}$ is constant. Thus F is proportional to J . Since J for the rock sample is equal to I_{sat} for the magnetic mineral times the concentration of the magnetic mineral,

Figure 5. Schematic diagram of apparatus used for obtaining J_s - T curves.



then if the composition of the titanomagnetite and hence I_{sat} is known it is possible to determine the concentration.

The output of the balance, i.e. the magnetic force which is proportional to J , was displayed on the y-axis of a BBN 815M x-y plotter. A platinum/platinum+13% rhodium thermocouple was mounted in the quartz bucket with its output used to drive the x-axis of the plotter. Thus when the sample was heated a J_s versus T curve was drawn. The entire system was evacuated to a pressure of about 1×10^{-5} torr for all measurements. This proved a sufficiently low pressure to prevent significant oxidation of both rock samples and synthetic titanomagnetite powders in the time required to determine the Curie point.

The output of the Cahn balance was in milligrams. The balance was calibrated in emu by measuring the force on a known mass of Nickel. With magnet current at 10 amps, equivalent to 7 kiloGauss used throughout, the calibration was conveniently 1.0 emu/gram.

The system was calibrated for temperature using synthetic titanomagnetites prepared by Jensen (1973) by the method of Barth and Posnjak (1932). Curie temperatures were determined by drawing two straight lines as tangents to the J_s - T curve above and below the estimated Curie point and then projecting the intersection to the temperature axis as described by Gromme et al. (1969). An example of this procedure can be seen on the J_s - T curve on the plotter in Figure 5.

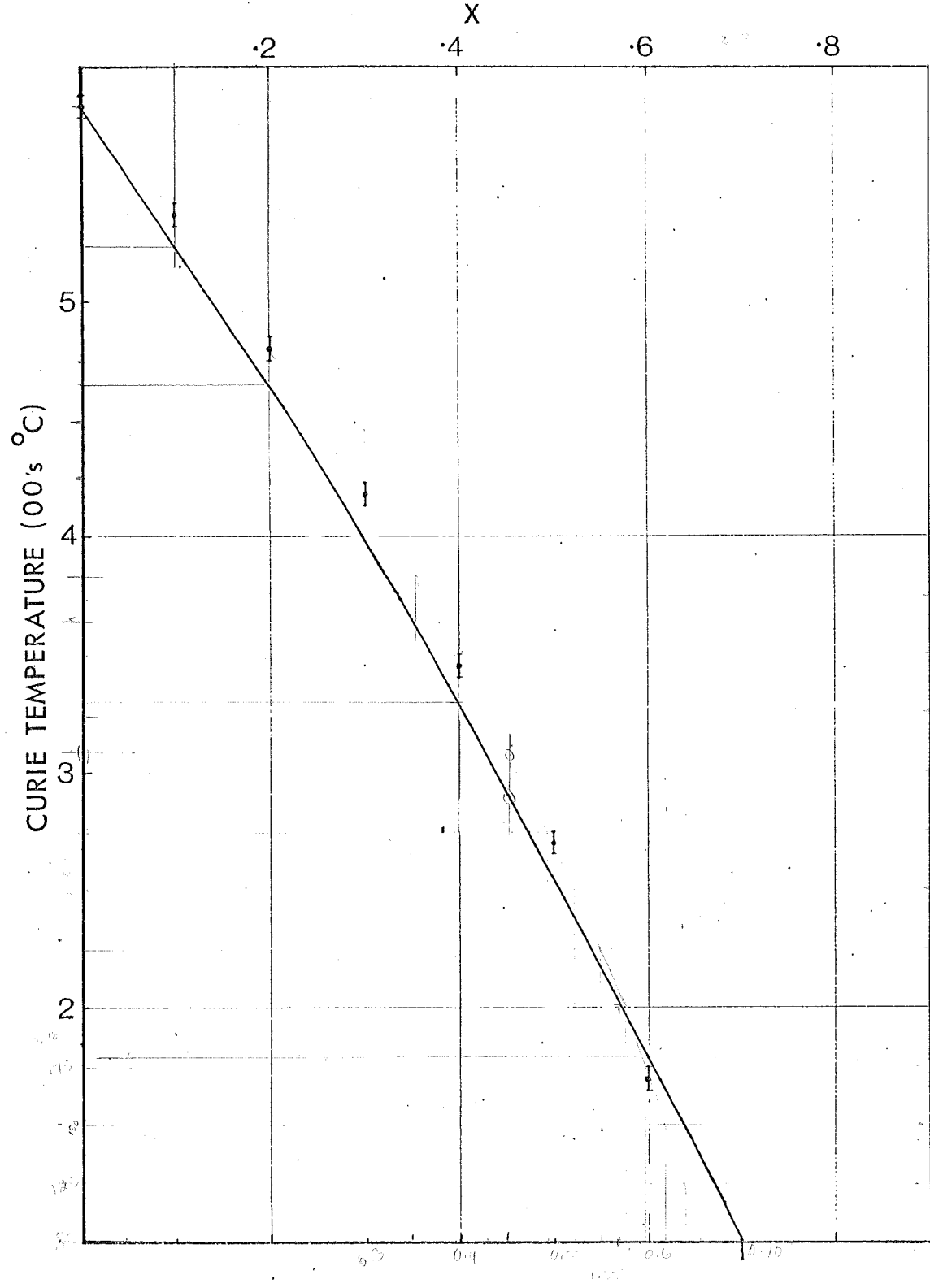
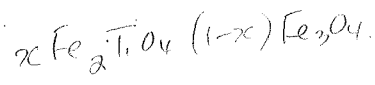


Figure 6. Plot of Curie Temperatures of synthetics versus 'X'. Line represents values from Akimoto et al. (1958). Dots are results obtained in present work.

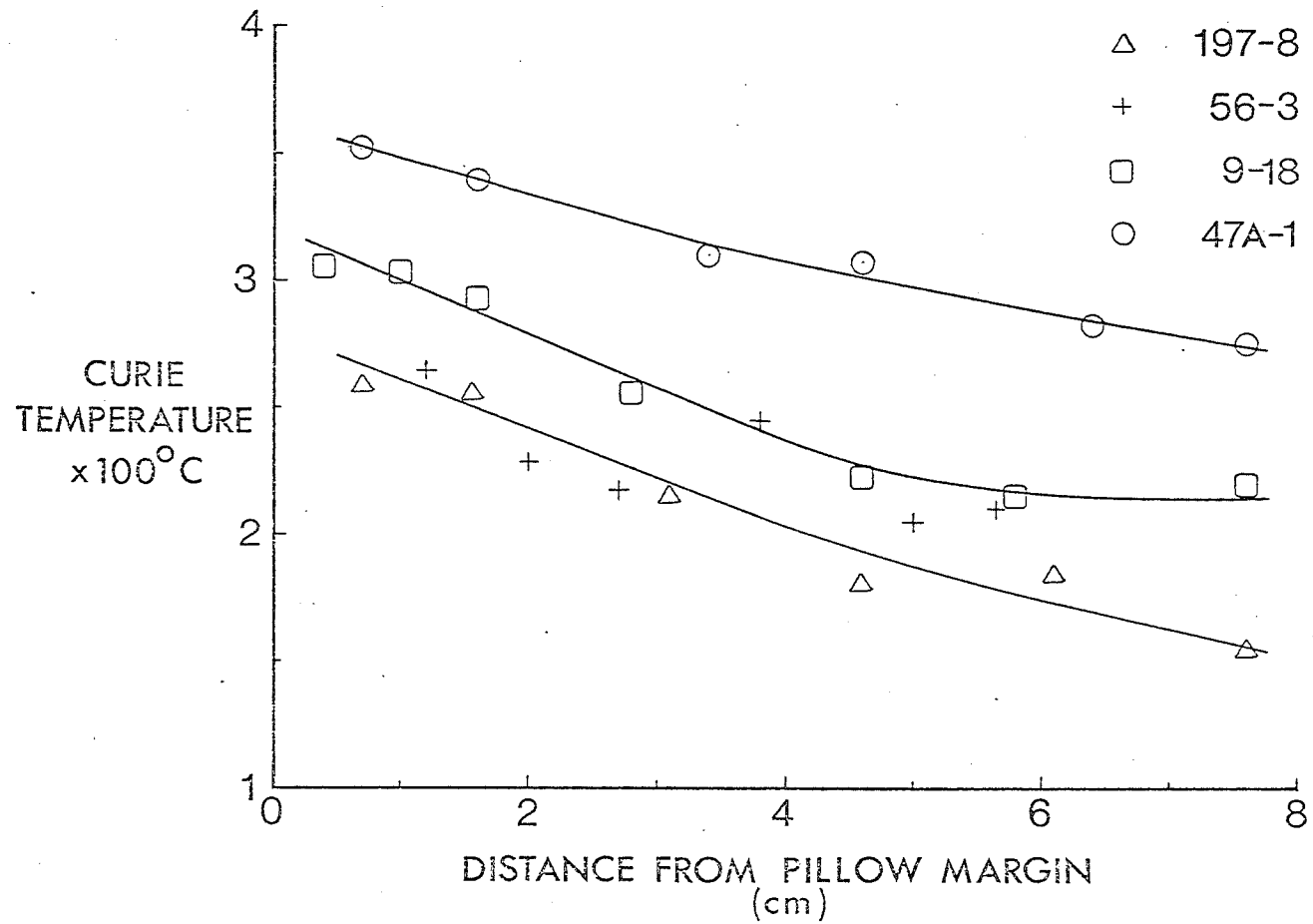


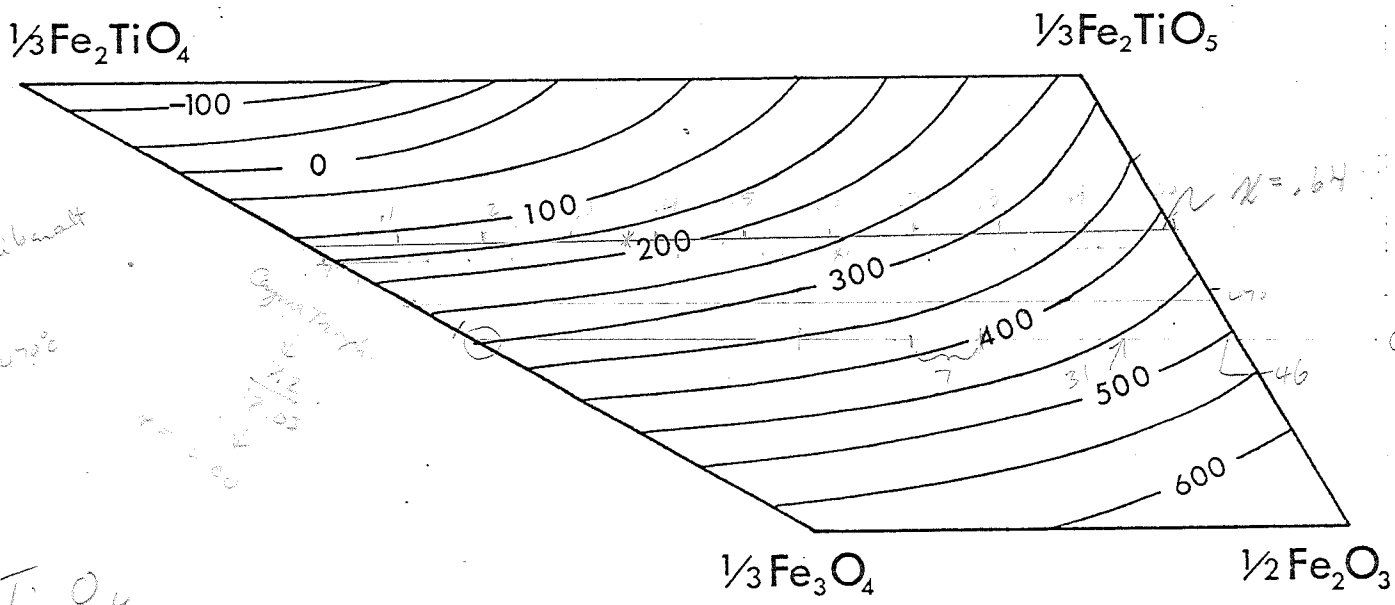
Figure 7. Variation of Curie Temperature with distance into the four pillows.

The Curie temperatures obtained with the synthetics are shown in Figure 6 along with the results of Akimoto et al. (1958). It can be seen that the system used here gives Curie temperatures up to 20° higher than accepted values, possibly because of some different rate of heating between the thermocouple and synthetic sample. From this figure a calibration between measured temperatures and accepted values was worked out and applied to all measured temperatures of the samples. This calibration was confirmed using pure (99.99%) Nickel which showed a Curie temperature of 356°C after applying the correction. This is in good agreement with the accepted Curie temperature of Nickel of 358° (Chikazumi 1964).

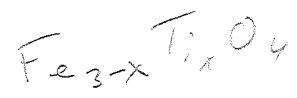
3.2.2 Results: Curie Temperature

The corrected Curie temperatures are plotted in Figure 7 for slices from each pillow. Since the Curie temperature depends solely on the composition of the titanomagnetite it should be possible to use it to determine the oxidation state. Contours of equal Curie temperature for spinels in the $\text{FeO-TiO}_2\text{-Fe}_2\text{O}_3$ system are given in Figure 8 as established by Readman and O'Reilly (1972, their Figure 7b). If one assumes that the interior of 197-8, the youngest pillow, is unaltered and therefore that 'z' is equal to 0, then one obtains $x = 0.6$. If the oxidation process is one of the development of an increasingly cation-deficient spinel, then the oxidation path would be a horizontal line through $x = 0.6$ on the ternary

6.7 0.55
12.13



Paterson say 0.52
Arzoo's method alkalibasalt
 $T_c = 2700^\circ\text{C}$
 $x = \frac{6.1}{12.02} = 0.51$
 $Z = 1.0, T_c = 4700^\circ\text{C}$



typical basalt
 $x \approx 0.6$

CONTOURS OF EQUAL CURIE TEMPERATURE

Figure 8. Contours of equal Curie Temperature for spinels in FeO-TiO₂-Fe₂O₃ system.

101
5.7-6.7 : 0.57
8.4 : 0.31
9.9 : 0.21
30.
Z
0.56-0.66
0.83
0.98

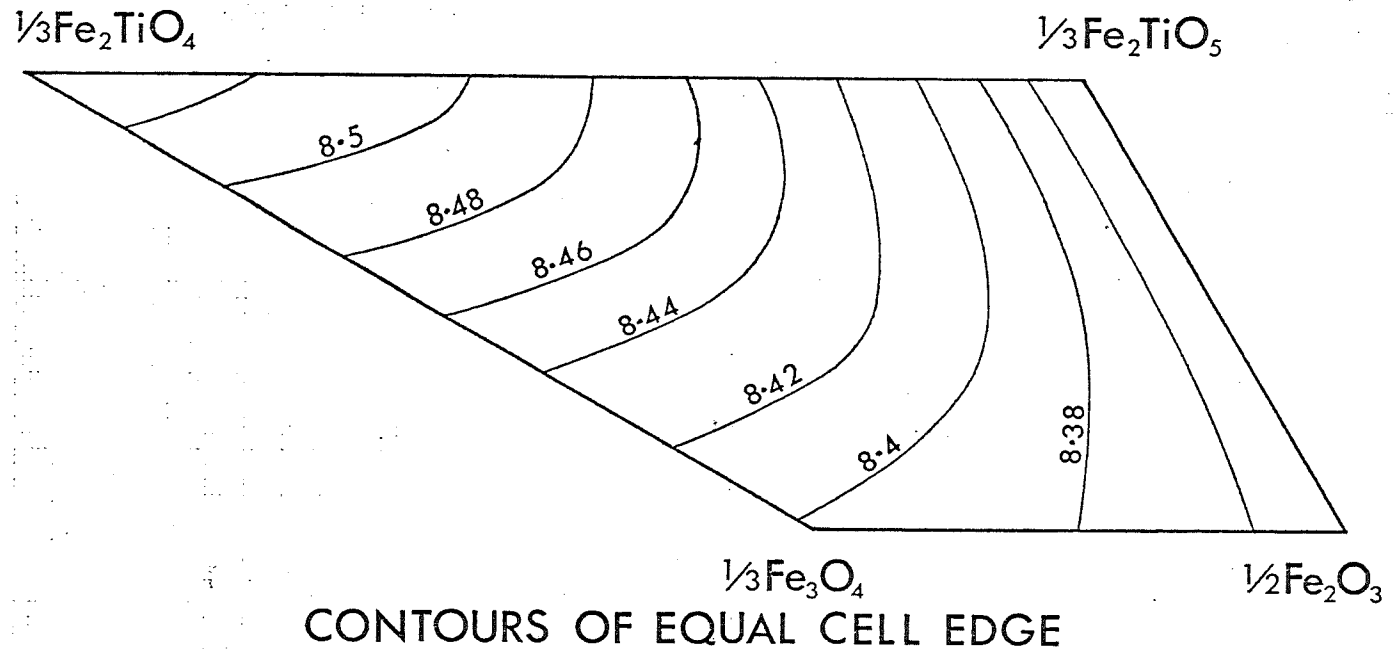


Figure 9. Contours of equal cell edge for spinels in FeO-TiO₂-Fe₂O₃ system.

diagram as seen in Figure 8.

However in some cases of low temperature hydrothermal alteration, such as the Mull lavas reported by Ade-Hall et al. (1971), splitting of the titanomagnetite into two phases has been observed. This splitting involves the exsolution of a Ti-rich component leaving a Ti-poor residuum which causes a rapid rise in Curie temperature. Although there is no evidence of such splitting in the grains of titanomagnetite examined in this study, since some of the grains are at the limit of visibility it was thought useful to examine the grains by another method.

3.2.3 Results: Cell Edges

The cation-deficient titanomagnetites, or γ -phase, are of spinel structure. Variations in the lattice parameter of a unit cell, the cell edge, have been measured for different compositions in the γ -phase and are given in Figure 9, taken from Readman and O'Reilly (1972, their Figure 7a). It will be noted that these contours intersect those of Curie temperature. Thus, if it were possible to measure both Curie temperature and cell edge the points could be plotted on the ternary diagram without making any assumptions about 'x' or 'z'.

X-ray measurements were made using a Debye-Scherrer powder camera. For this purpose about a gram of each sample was ground under acetone. The ground up material was sieved through a 44 μ sieve. The sieved material was made into a slurry with acetone and the magnetic particles extracted

with a hand magnet. With the very small grain size of the titanomagnetites it was not possible to get pure magnetic extract.

It was not possible to obtain very accurate x-ray determinations because of the rather broad lines. There are two principal causes for this line broadening. One is the fact that there is probably a distribution of oxidation states within one gram of sample material, the other is that the very small particles in these pillow basalts, some less than a micron, will also cause line broadening. For this reason the error on cell edge determinations is probably $\pm 0.02 \text{ \AA}$.

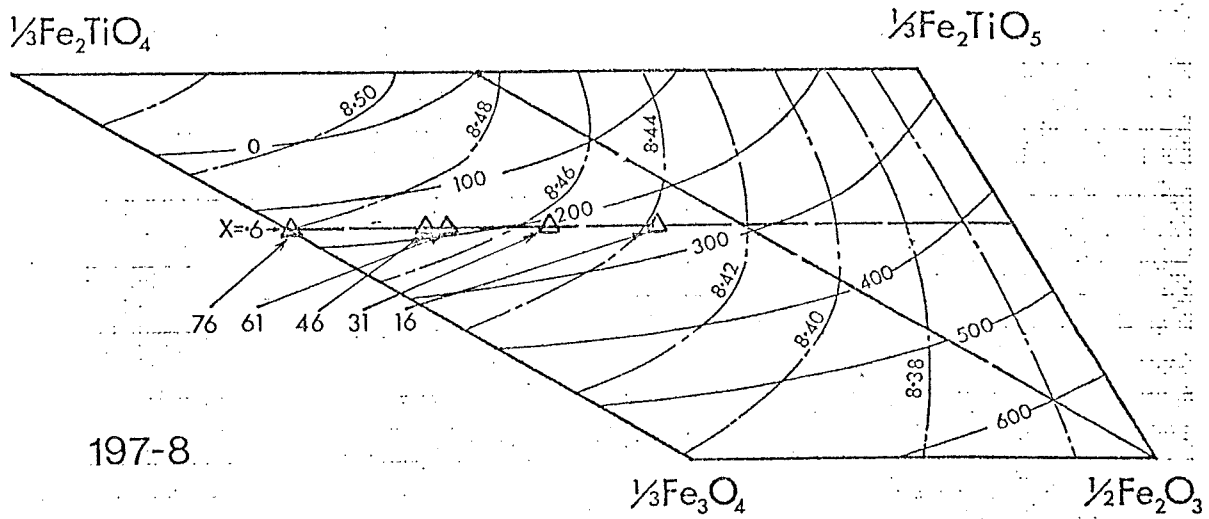
TABLE 2.
CELL EDGES

Sample	Cell Edge	Sample	Cell Edge	Sample	Cell Edge
197-8-10	8.45	9-18-		47A-1-10	8.38
-55	8.45	-40	8.43	-44	8.40
-79	8.45	-76	8.43	-76	8.41

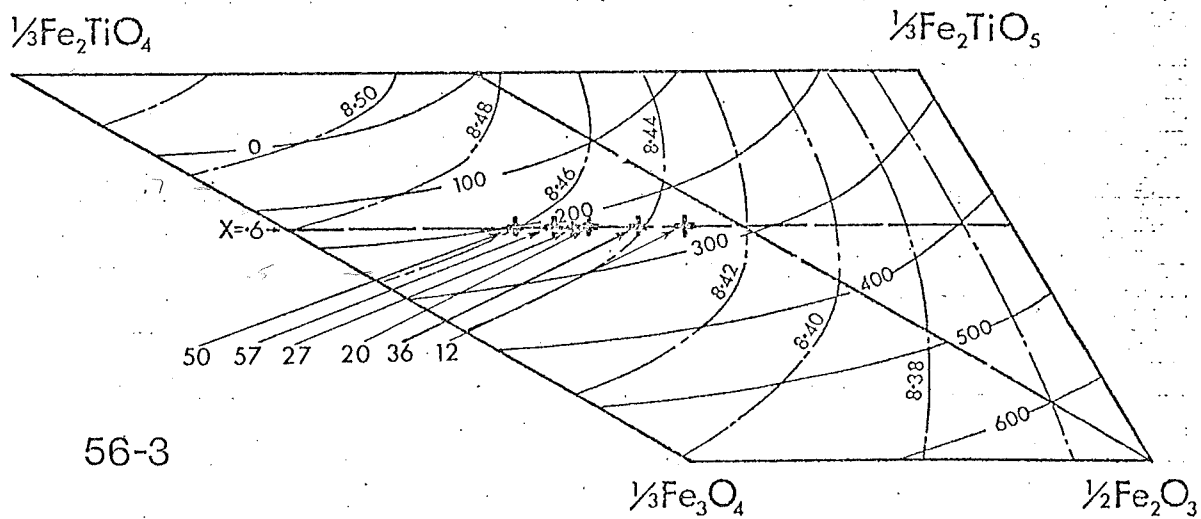
Note: All cell edges $\pm 0.02 \text{ \AA}$.

The results as presented in Table 2 do show a decrease in the cell edge and hence an increase in oxidation state with the age of the pillows and 47A-1 shows an increase in oxidation state towards the outside of the pillow.

Due to the large errors in the cell edges it is not practical to try to plot the positions of various slices on



a



b

Figure 10. Positions of samples from Pillows a) 197-8, b) 56-3, c) 47A-1 and d) 9-18 plotted on $\text{FeO-TiO}_2\text{-Fe}_2\text{O}_3$ ternary system. Solid lines are Curie temperatures, dashed lines are cell edges.

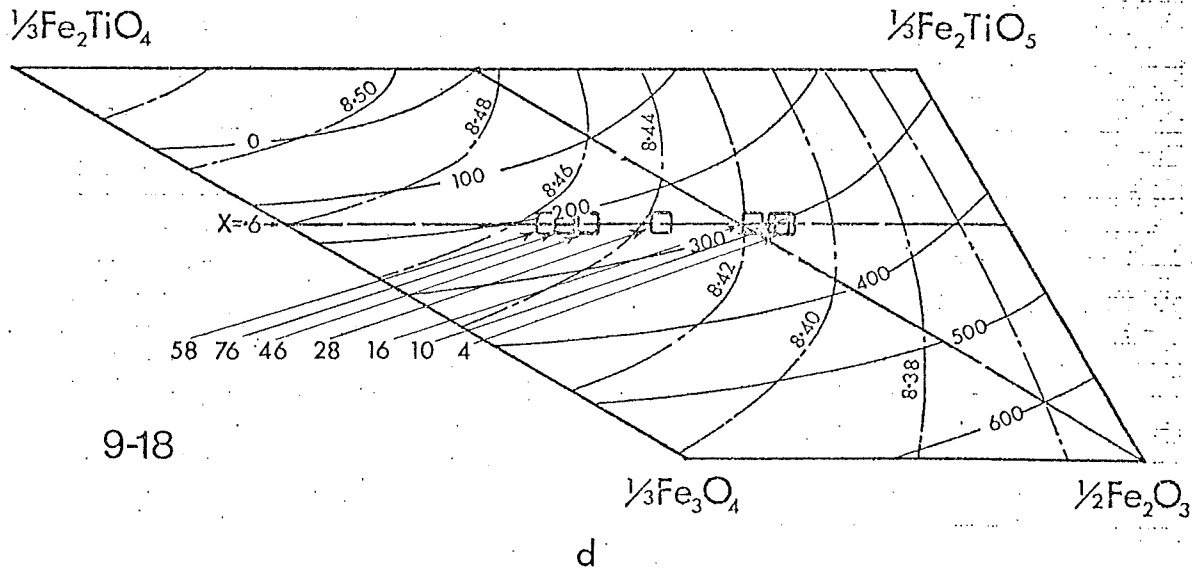
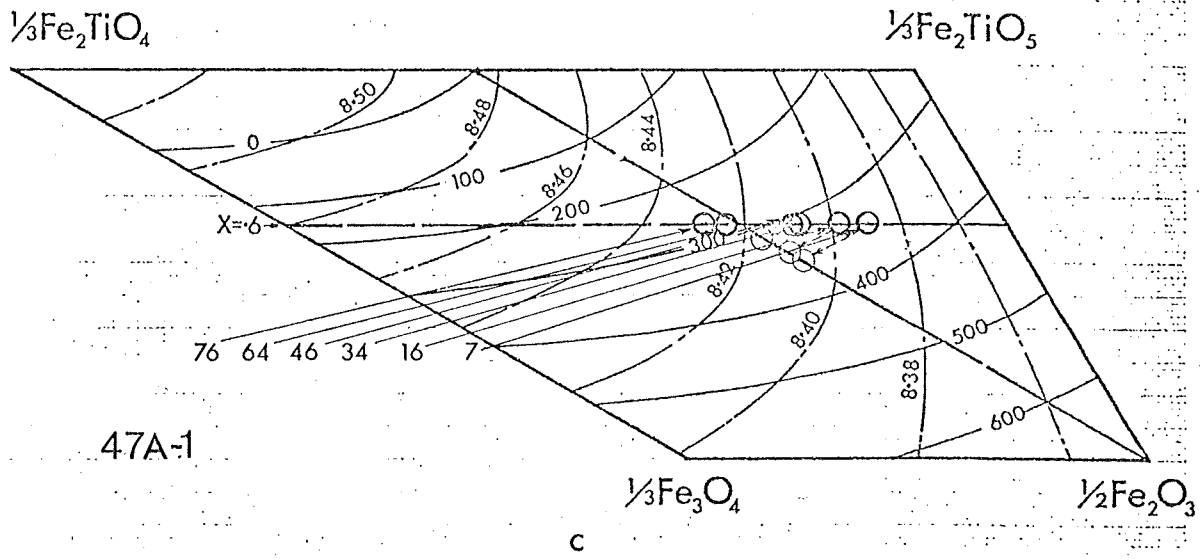


Figure 10 (continued).

contours of cell edge and Curie temperature. However, it is possible to plot the slices on the line of constant Fe/Ti through $x = 0.6$ as described in the previous section and check if the cell edges are consistent with such a procedure.

The Curie temperatures for the various slices are plotted on the ternary diagram in Figure 10a-d. It can be seen that the cell edges are consistent with such a mechanism of oxidation to an homogeneous cation-deficient titanomagnetite.

3.2.4 Results: Saturation Magnetization and Concentration

The saturation magnetization (J_s) in emu/g of rock for some slices from the pillows is plotted in Figure 11. Pillows 197-8 and 9-18 show a smooth trend as indicated by the lines. Pillows 47A-1 and 56-3 show considerable scatter. There are two possible causes of this scatter; one is that it might reflect an irregular variation of concentration throughout the pillows, the other is that the measuring chips used are so small that the scatter is a reflection of the titanomagnetites not being uniformly distributed on this scale.

In order to estimate the scatter due to the small size of the chips compared to the sample five adjacent chips were broken off slice 56-3-30 from the second core drilled from pillow 56-3. All the values from these chips fell within the range 0.26 ± 0.02 emu/g, so any variation greater than

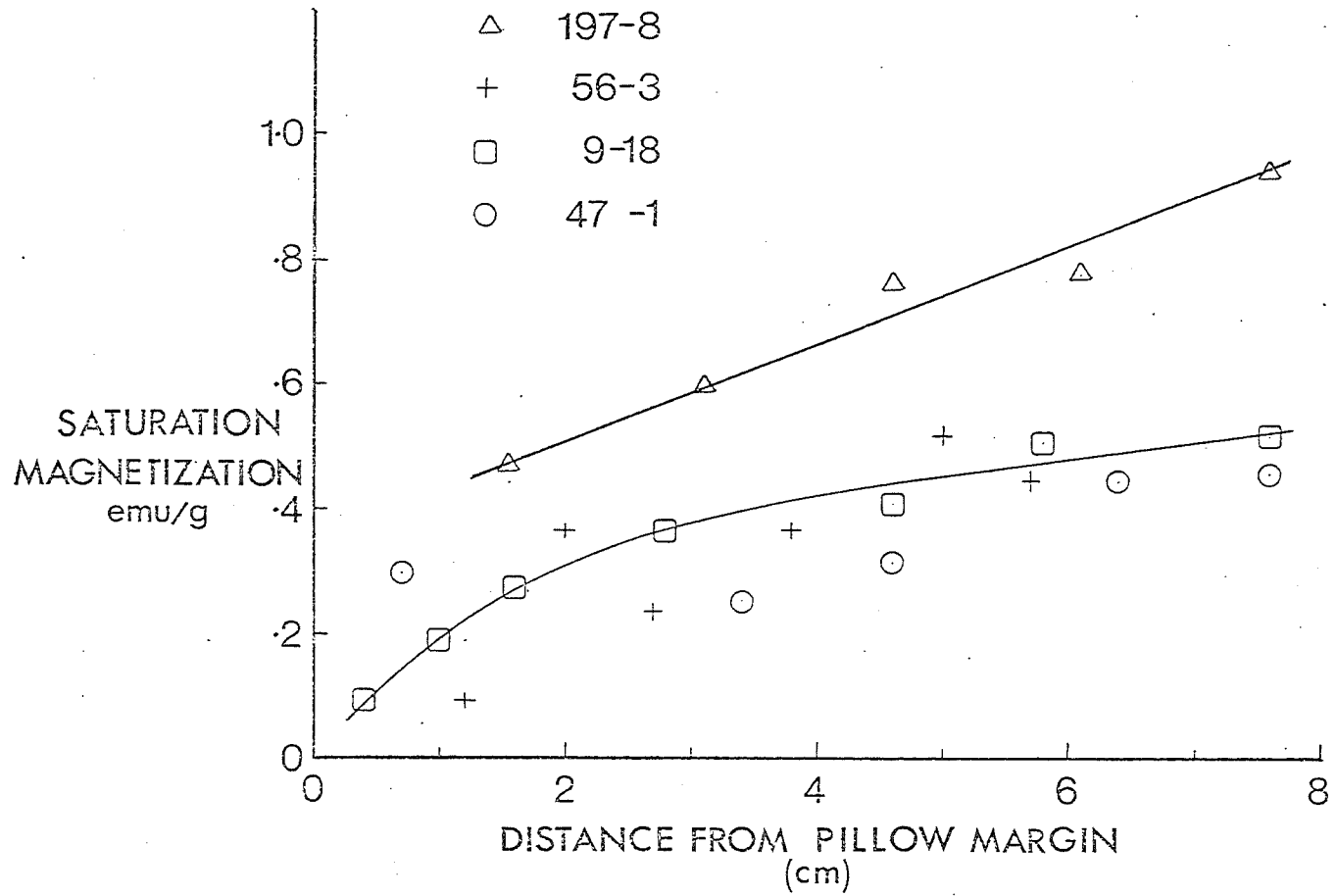
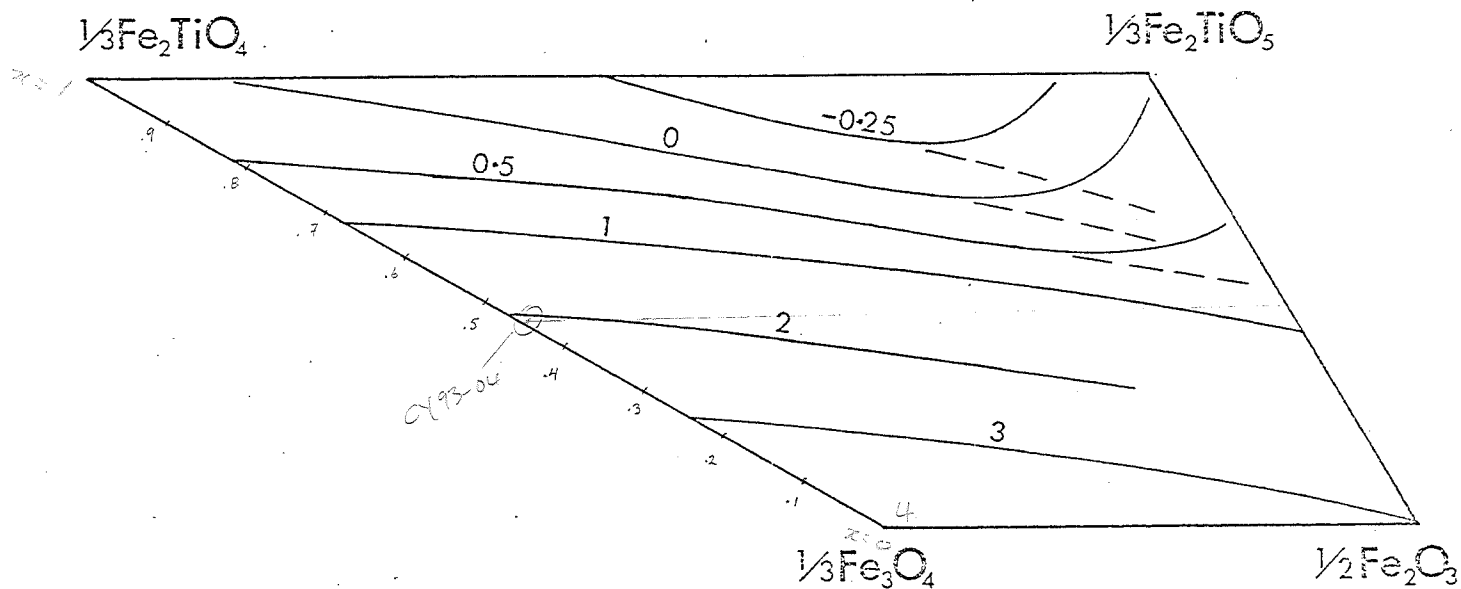


Figure 11. Variation of saturation magnetization with distance into the four pillows.



CONTOURS OF EQUAL SATURATION MAGNETIZATION
IN BOHR MAGNETONS AT $T=0^\circ\text{K}$

Figure 12. Contours of equal saturation magnetization for spinels in $\text{FeO-TiO}_2\text{-Fe}_2\text{O}_3$ system in Bohr magnetons at $T=0^\circ\text{K}$.

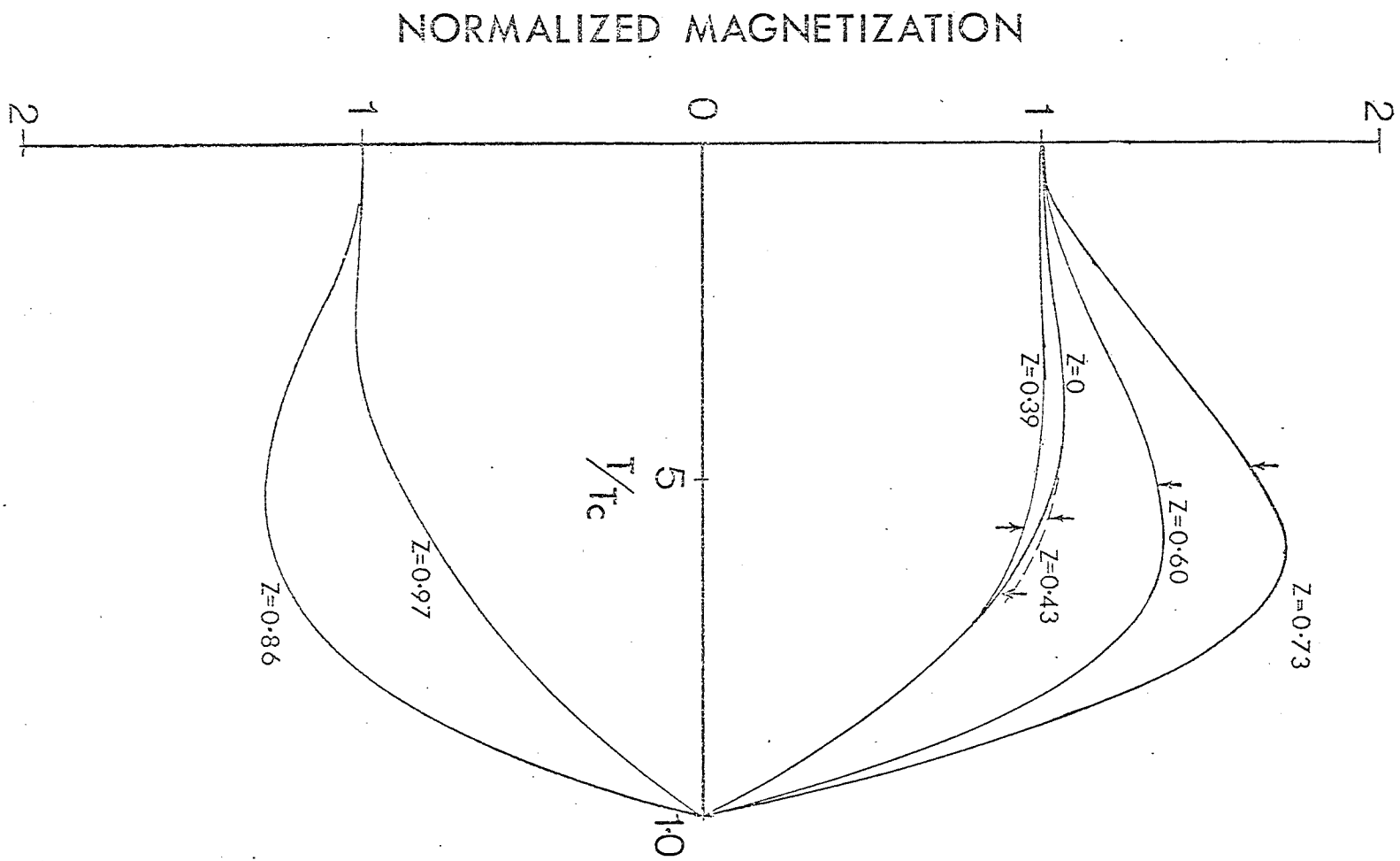


Figure 13. Evolution of Thermomagnetic curves for $x=0.7$ as degree of oxidation, 'z', increases.

about 10% may be interpreted as a real variation in the pillow and not due to the small size of the chips. The percent titanomagnetite can be calculated using a value for J_s depending on 'x' and the oxidation state of 'z'.

Values of J_s as a function of 'x' and 'z' at 0°K, Figure 12 (Readman, 1974, pers. comm.) are used as a starting point. The variation of J_s with temperature for different values of 'z' is given in Figure 13 for $x = 0.7$ (Readman and O'Reilly, 1972, their Figure 5). It will be assumed that this Figure is valid at $x = 0.6$. By using Figures 12 and 13 it is possible to obtain J_s as a function of 'z' at room temperature for $x = 0.6$, shown in Figure 14. Using the Curie points of samples as plotted on Figure 8, it is possible to determine their 'z' and then from Figure 14 the appropriate J_s . These values of J_s are used to convert from Figure 11 into the concentrations of titanomagnetite given in Figure 15.

The shape of the curves of Figure 13 provides a check on 'z'. The arrows against the curves show the position of room temperature. For cation-deficient titanomagnetites in the range $0.6 < z < 0.9$ these should be a hump in the J_s -T curves starting at room temperature. For sample 47A-1-34 with a Curie temperature of 310°C and hence $z \sim 0.65$ there is indeed a slight hump. Samples 47A-1-16 and -7 while initially flat do not show any hump and 9-18-10 and -4 are not even flat.

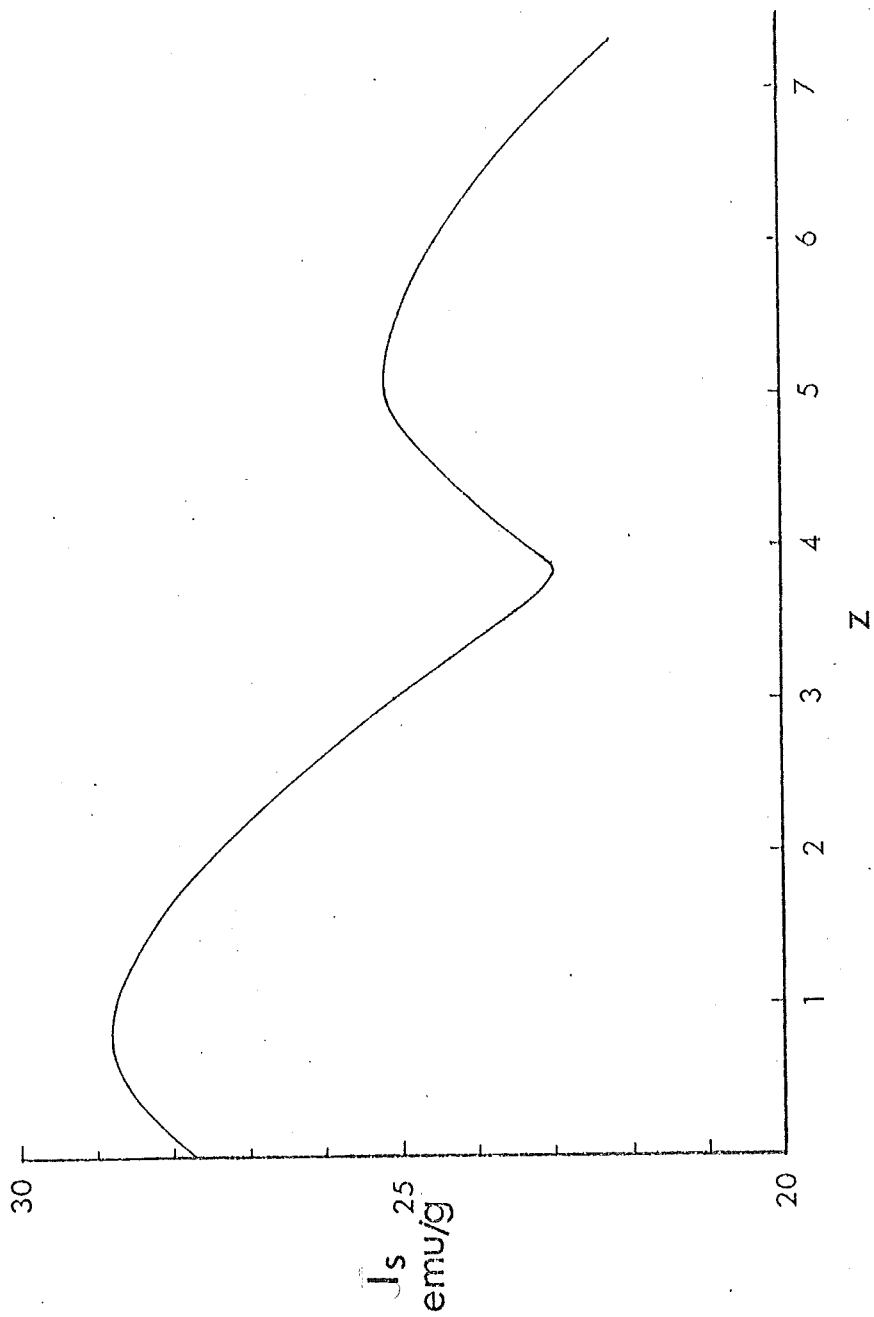


Figure 14. Variations of magnetization per gram, I_s , with 'z' for $x=0.6$.

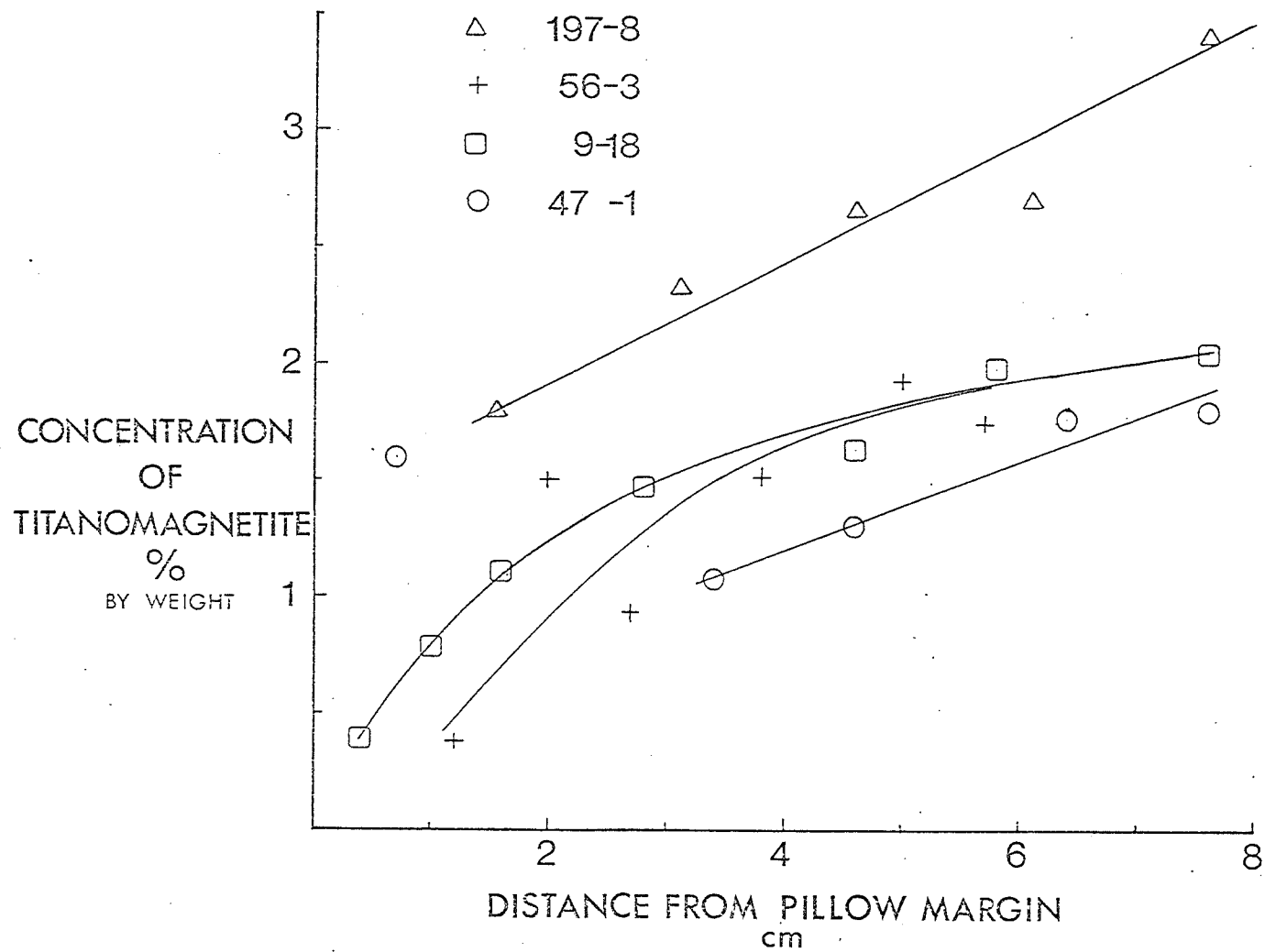


Figure 15. Concentration of titanomagnetites by weight as a function of distance into the four pillows.

There are two possible reasons for this: one is that the γ -phase does not proceed to higher 'z' but rather exsolves along the ilmenite-hematite join. The other is the competing effect of a larger percentage contribution to J_s from paramagnetic material because the concentration of titanomagnetites near the exterior is less.

Considering the results from 47A-1, the Curie temperatures and cell edge measurements indicate an homogeneous oxidation while the lack of hump in the J_s -T curve may indicate exsolution along the ilmenite-hematite join as suggested by Creer (1971). If such exsolution takes place then the concentrations obtained by assuming homogeneous oxidation will be too large since J_s will actually be higher than the values used from Figure 14.

A caution should be added about Figure 14. Some points for this could be read directly off the curves in Figure 13, others required interpolation. The points for $z = 0.1, 0.2, 0.3$ are based on interpolating between the curves for $z = 0$ and $z = 0.39$, since these are close little error will be introduced. The point for $z = 0.5$ is based on interpolation between $z = 0.43$ and $z = 0.63$ which may be a cause of some error. The most critical factor in determining the accuracy of Figure 14 is the accuracy of Readman and O'Reilly's published curves. No information is available on this.

The four pillows show a radial variation in concentration, Figure 15. Pillow 197-8 has a considerably greater concentration than the others suggesting that a more complete

crystallization of the titanomagnetites has occurred. This concentration ranges from about 2% at a depth of 2 centimetres up to about 3 1/2% at 8 centimetres. This compares closely with Marshall and Cox's (1971b) type H pillows: (1 1/2% at 2 cm - 3 1/2% at 6 cm). Their concentrations were determined by microscopic examination. The other three pillow concentrations group together ranging from about 1% at 1 cm to 2% at 8 cm compared to Marshall and Cox's (1971b) type L pillows: (0.3% at 1 cm - 0.7% at 6 cm). Since the type L pillows are fine grained it is possible that Marshall and Cox did not see some of the very fine grains which make up much of the titanomagnetite. The range of typical concentrations for DSDP basalts reported by Lowrie et al. (1973) is from less than 1% to about 3%, so it can be seen that the concentrations in the four pillows of this study are typical of pillow basalts.

3.3 Results: Natural Remanence

3.3.1 Variation with Distance into the Pillows

The NRM for each slice was measured using a Schonstedt SSM 1A Spinner Magnetometer. The results are plotted against distance in Figure 16. The three youngest pillows show an increase in intensity of NRM (J_{NRM}) from a value of virtually zero at the outside to about 70×10^{-4} emu/g of rock for 9-18, 130×10^{-4} emu/g for 56-3 and 310×10^{-4} emu/g for 197-8. The plot of 47A-1 is relatively level at around $7-10 \times 10^{-4}$ emu/g. The variations in these plots show

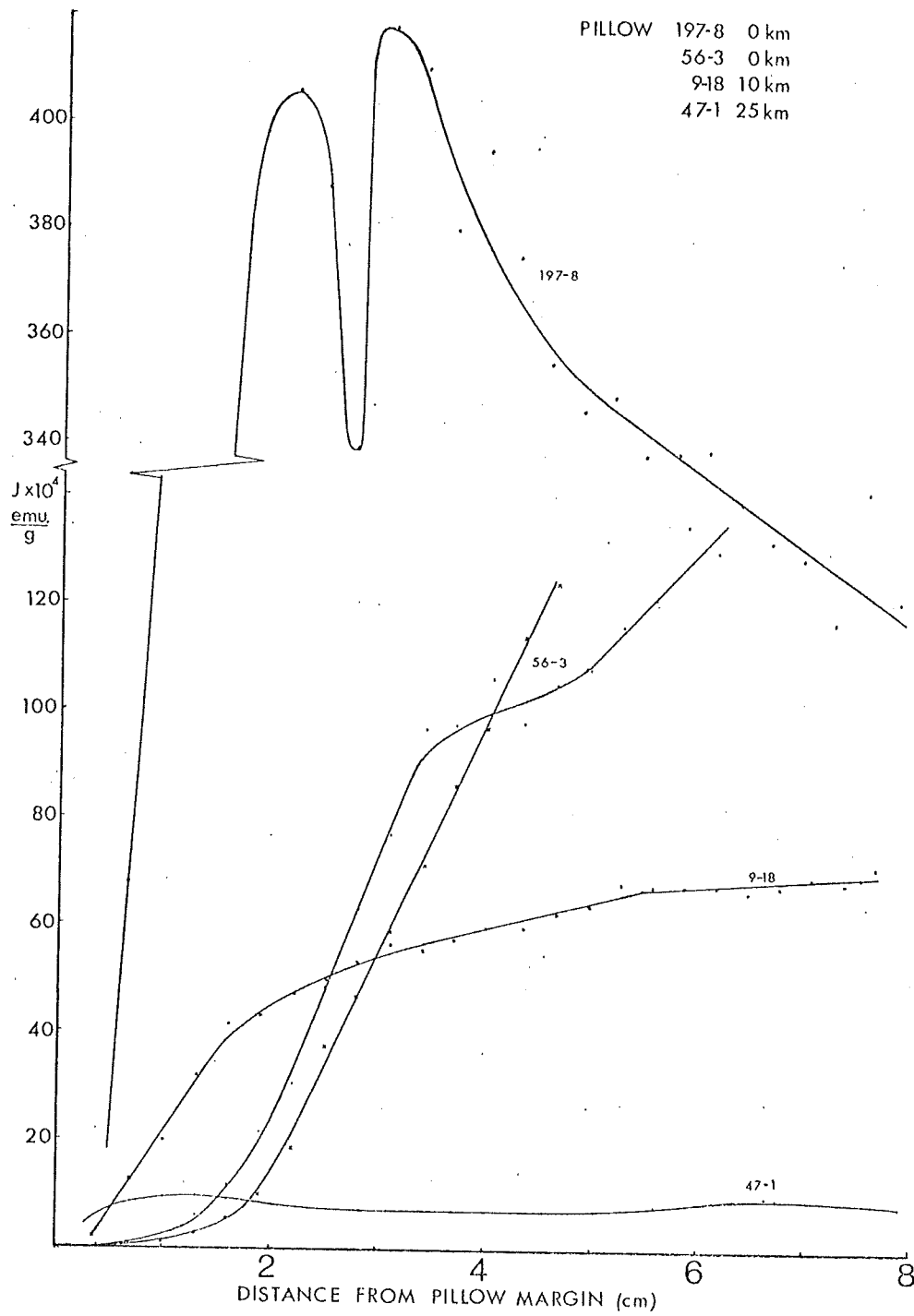


Figure 16. Intensity of NRM as a function of distance into the four pillows.

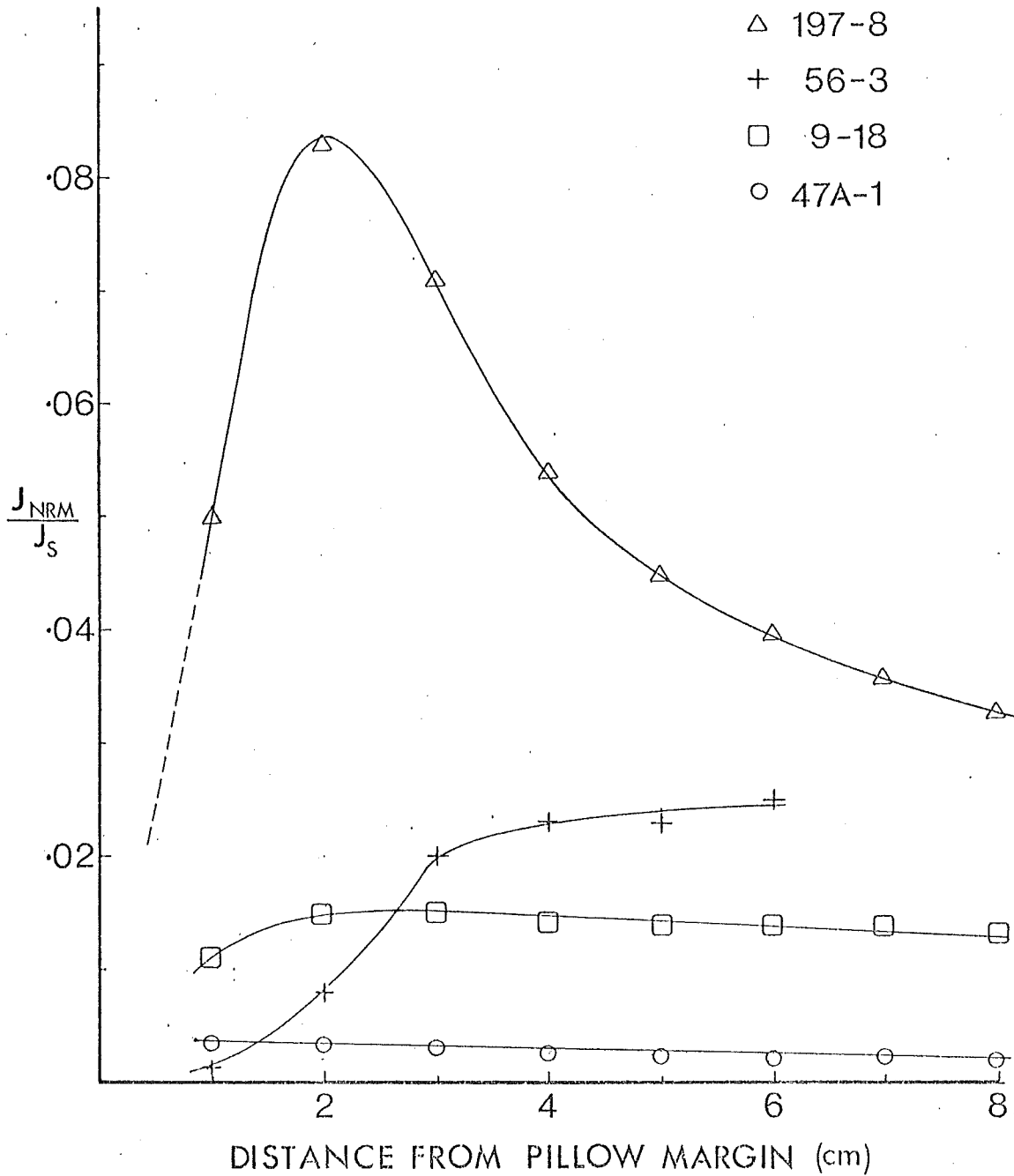


Figure 17. Intensity of NRM divided by intensity of saturation magnetization as a function of distance into the four pillows. This plot was prepared using smoothed curves from figures 11 and 16. The main factor affecting J_{NRM}/J_s is the grain size.

dramatically the difficulty of assigning an average J_{NRM} for young pillow basalts. Once the basalts have become weathered throughout as in 47A-1, then an average J_{NRM} becomes meaningful.

The intensity of NRM of 197-8 quickly reaches a peak of 400×10^{-4} emu/g at a distance of two centimetres from the outside and then falls off to three-quarters of its peak value. J_{NRM} of a grain depends both on J_{S} of the titanomagnetite and the size of the grain. For a rock, J_{NRM} depends on the concentration of the titanomagnetite as well as its composition and the average grain size. The variations in Figure 16 are due to all three factors. The product of two of these variables, concentration and composition of the titanomagnetites, have been measured and shown in Figure 11. By using values taken from the smoothed curves of Figure 16 and 11 and dividing the one by the other one obtains a plot of $J_{\text{NRM}}/J_{\text{S}}$ against distance into the pillow, Figure 17. This operation removes the effect of concentration and composition from J_{NRM} , leaving a plot which gives an idea of the effectiveness of parts of the pillow as carriers of NRM, a plot which is primarily a function of grain size.

The removal of the effect of concentration and composition still leaves a large variation between the pillows. Pillow 197-8 is still the most effective carrier of NRM and still shows a peak two centimetres from the outside. Similar behaviour has been observed before by Marshall and

Cox (1971b) and it is attributed to the cooling history of the pillow which is controlled by the pillow radius. Their conclusion is that in igneous bodies with chilled margins, the intensity of remanence reveals a maximum level where crystallization is nearly complete. In an igneous body, perhaps a few tens of centimetres across, with slow enough cooling rates there should be a maximum towards the outside and then a decrease towards the centre as the magnetic grain sizes become larger, hence reducing J_{TRM} . If the pillows are small, a radius of about 10 centimetres, then they cool so quickly that crystallization cannot become sufficiently advanced to produce such an intensity maximum.

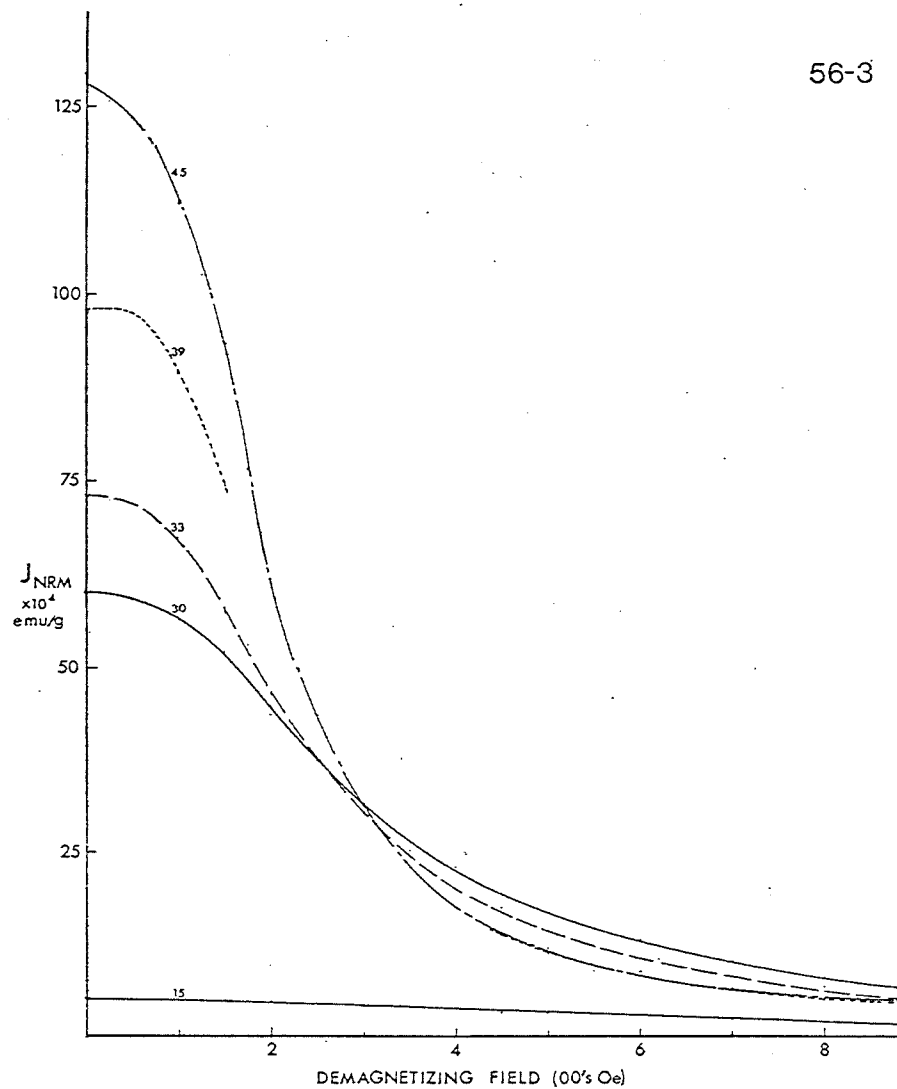
Since the cores for 56-3 and 197-8 were obtained from pillow fragments rather than complete pillows it is not possible to accurately assign a radius to them. It does seem that the outer surface of 197-8 has a larger radius of curvature than 56-3. Considering that 197-8 does have considerably larger grains than 56-3, see section 3.1, then 197-8 has experienced slower cooling and probably did have a larger radius. Grains from the interior of 56-3 are about the same size as those from the outer half centimetre of 197-8 and J_{NRM}/J_S for these regions is comparable at about 0.025. Thus one may consider the curve for 56-3 to be equivalent to the first half centimetre or so of the curve for 197-8, with a ten times expansion in the horizontal scale brought about by the different cooling rate.

In the process of explaining the differences between pillows 197-8 and 56-3 it has become necessary to introduce another variable affecting the NRM - the radius of the pillow. Figure 7 shows that the Curie temperatures of 56-3 are scattered around those of 197-8, so compositionally their titanomagnetites are not much different. They are both very young, being from the Median Valley, so not much difference would be expected. Pillow 197-8 does not evolve into 56-3, but rather both pillows develop in parallel, the difference in their J_{NRM} is caused by the different radii and hence different cooling rates and resulting grain sizes.

3.3.2 Alternating Field Demagnetization

Representative samples from each core were chosen and partly demagnetized in an alternating field up to 1000 Oersteds. Demagnetization was carried out in steps of 25 Oe. up to 200 Oe., then in steps of 50 Oe. up to 500 Oe. and finally in steps of 100 Oe. up to 1000 Oe. Figure 18a-e shows the remaining NRM for different slices from each pillow plotted against demagnetization field. For the three youngest pillows, while the NRM at low demagnetizing fields is greater for the interior than for the exterior, at high demagnetizing fields the situation is reversed. For pillow 47A-1 the demagnetization curves are too interwoven to permit any such simple observation. The NRM of all slices from 47A-1 does increase by up to 5% in the first 150 Oe. of demagnetization indicating the removal of a small secondary component. This is consistent with 47A-1 having been

56-3



56-3

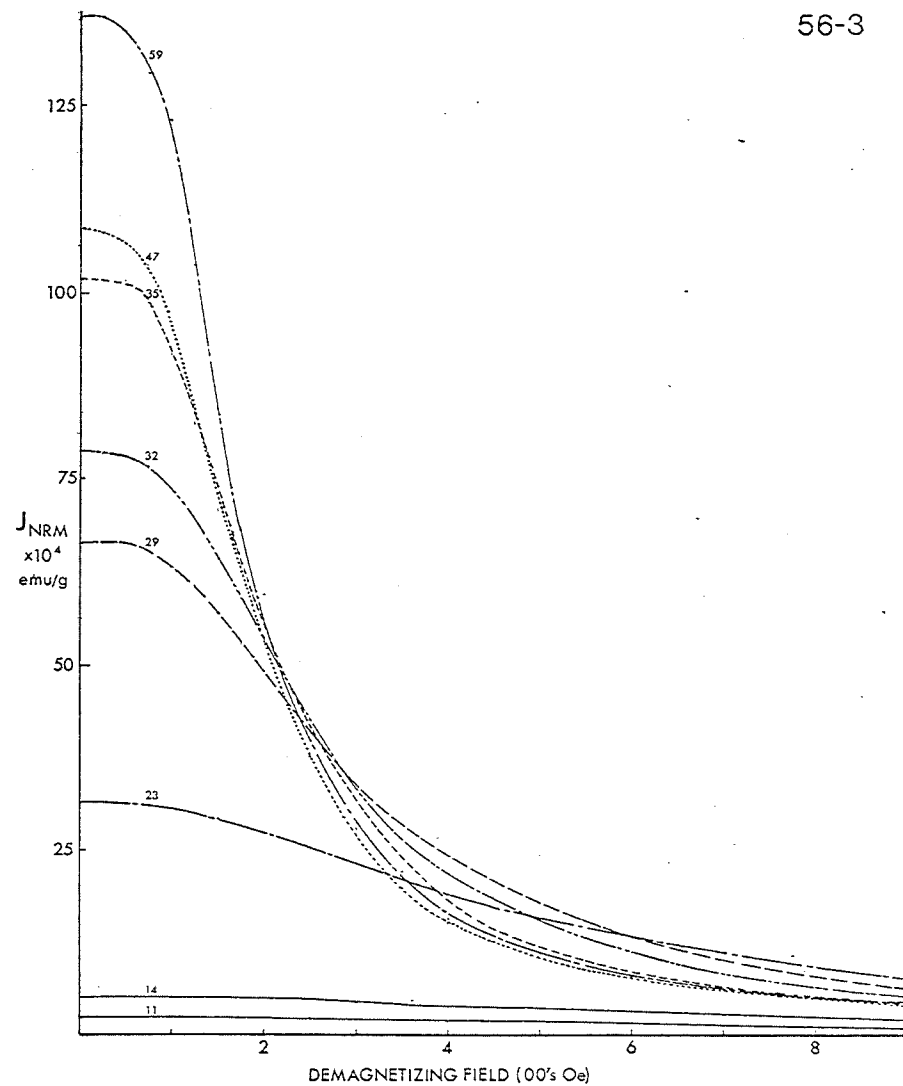
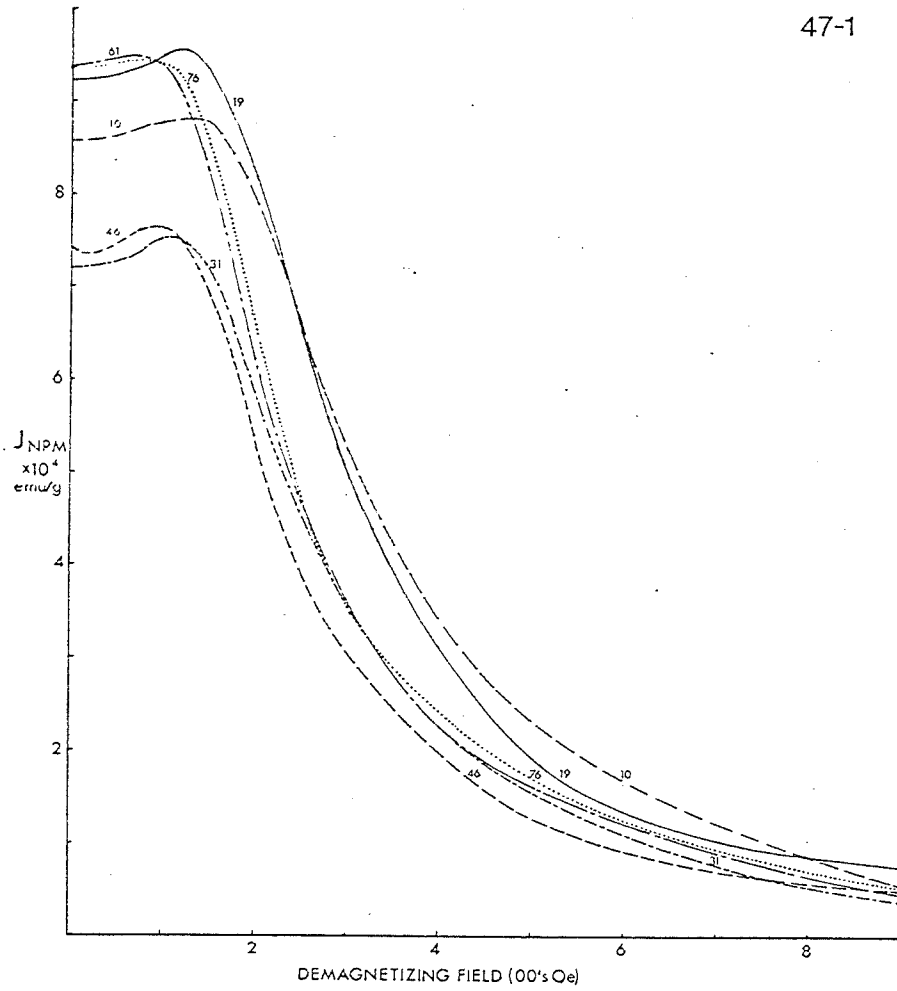


Figure 18. A.F. demagnetization of NRM for slices from each pillow. The small numbers against each line is the distance in millimetres from the outside of the pillow.
 a) 56-3, b) 56-3(2), c) 47-1, d) 9-18, e) 197-8.

47-1



9-18

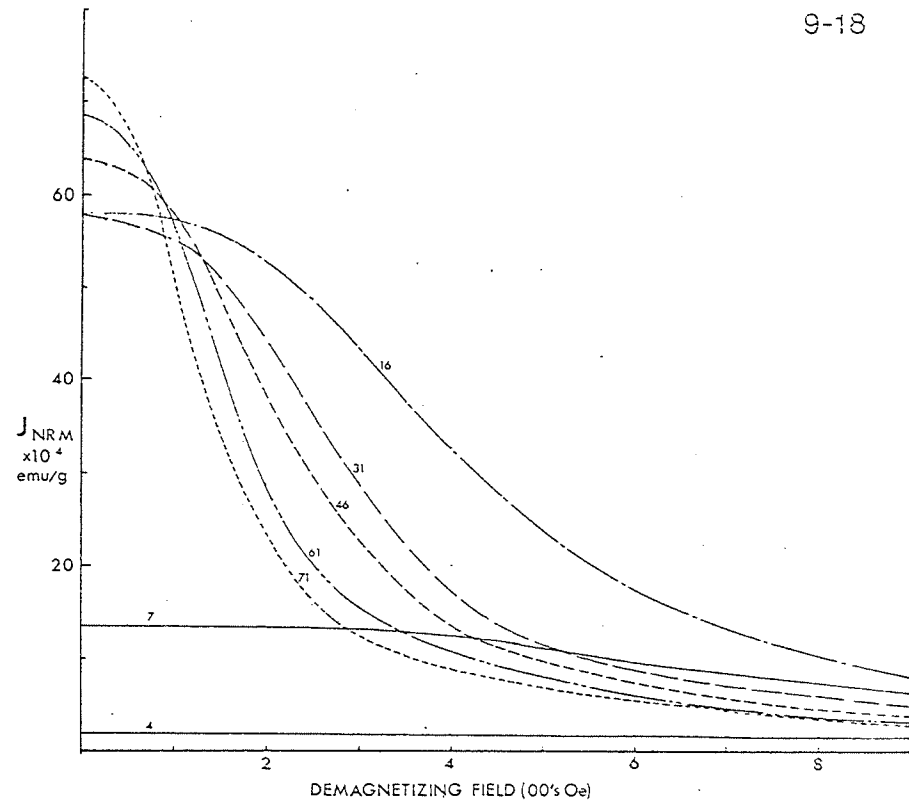
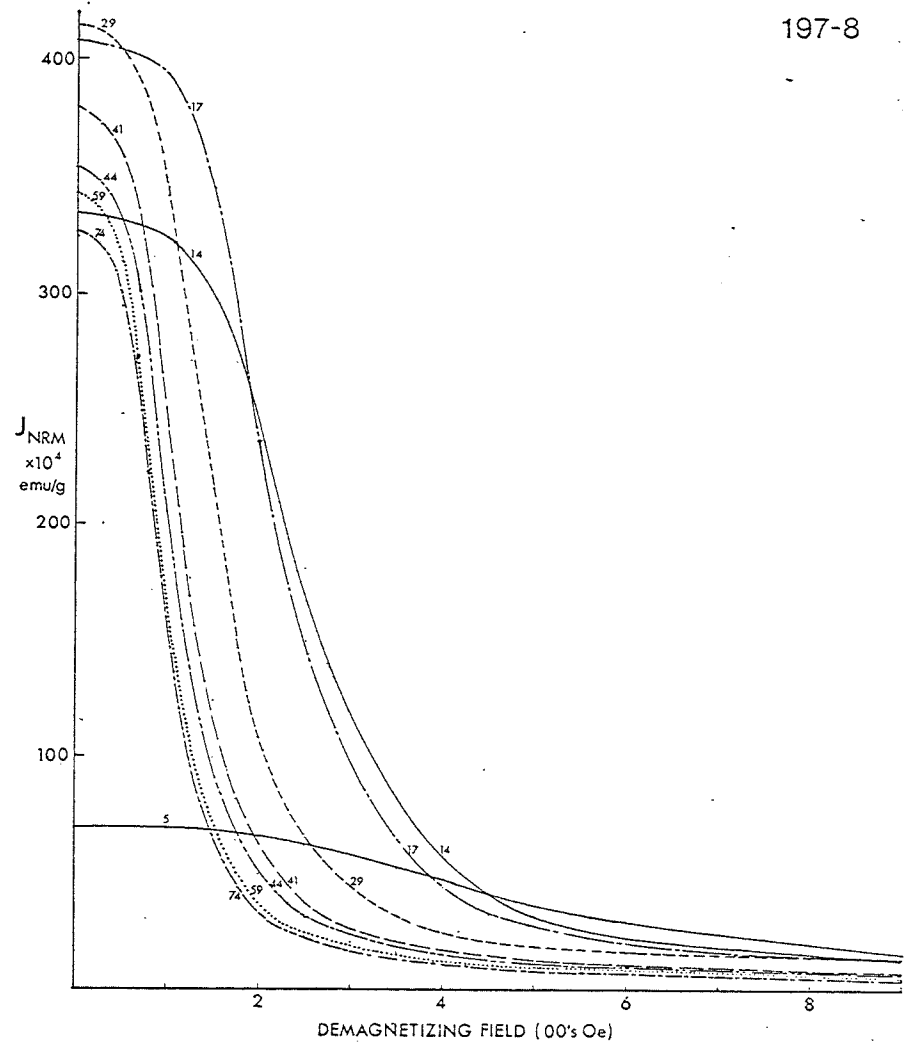


Figure 18 (continued).

Figure 18 (continued).



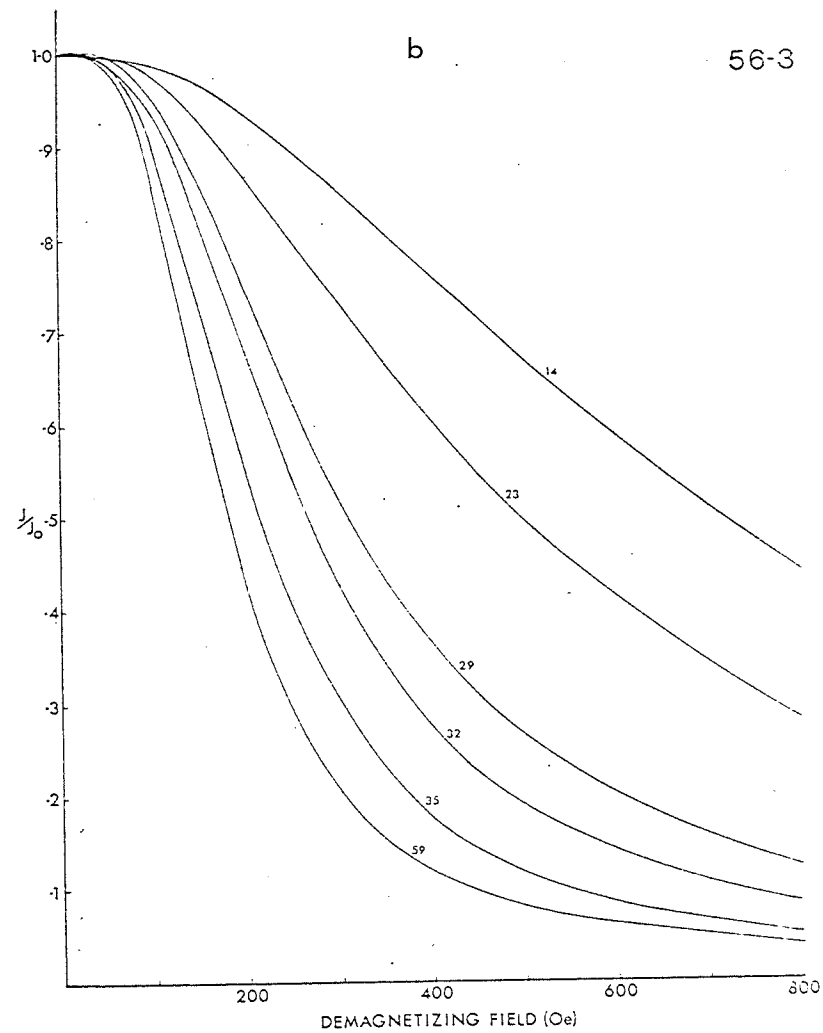
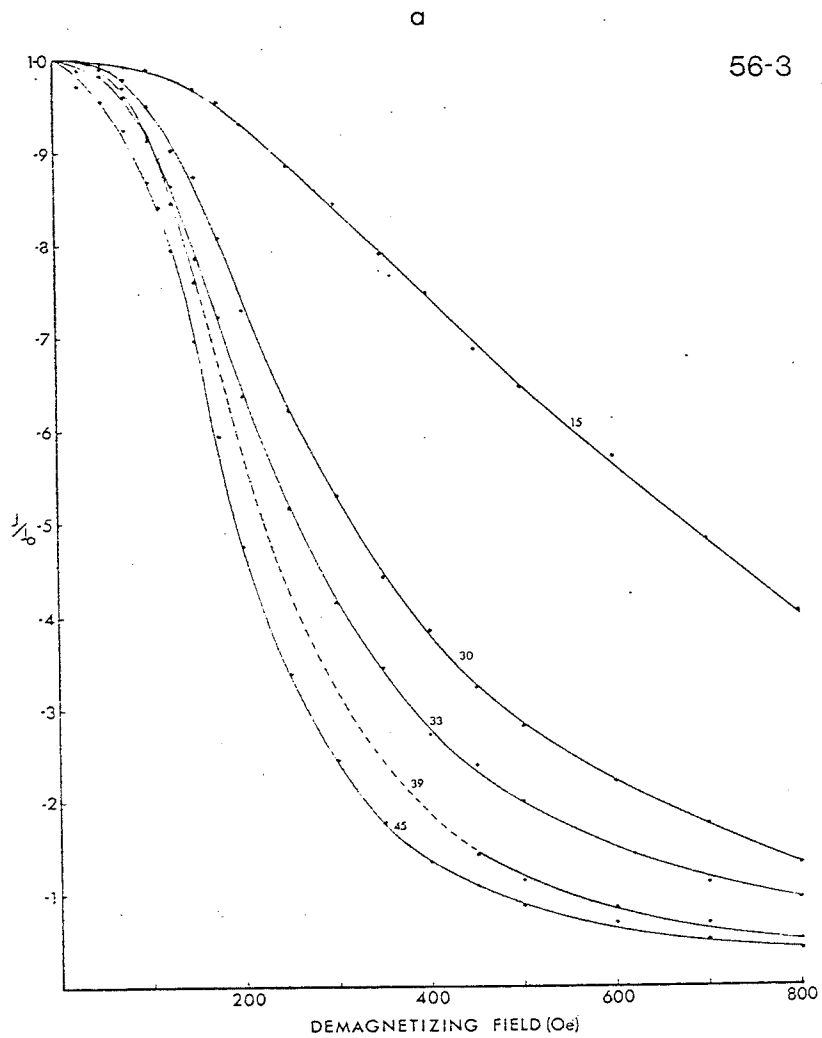


Figure 19. Normalized A.F. demagnetizations for slices from the four pillows. The small numbers have the same meaning as in Figure 18. This figure better shows the increasing hardness of NRM close to the outside of the pillow.

a) 56-3, b) 56-3(2), c) 47A-1, d) 9-18, e) 197-8.

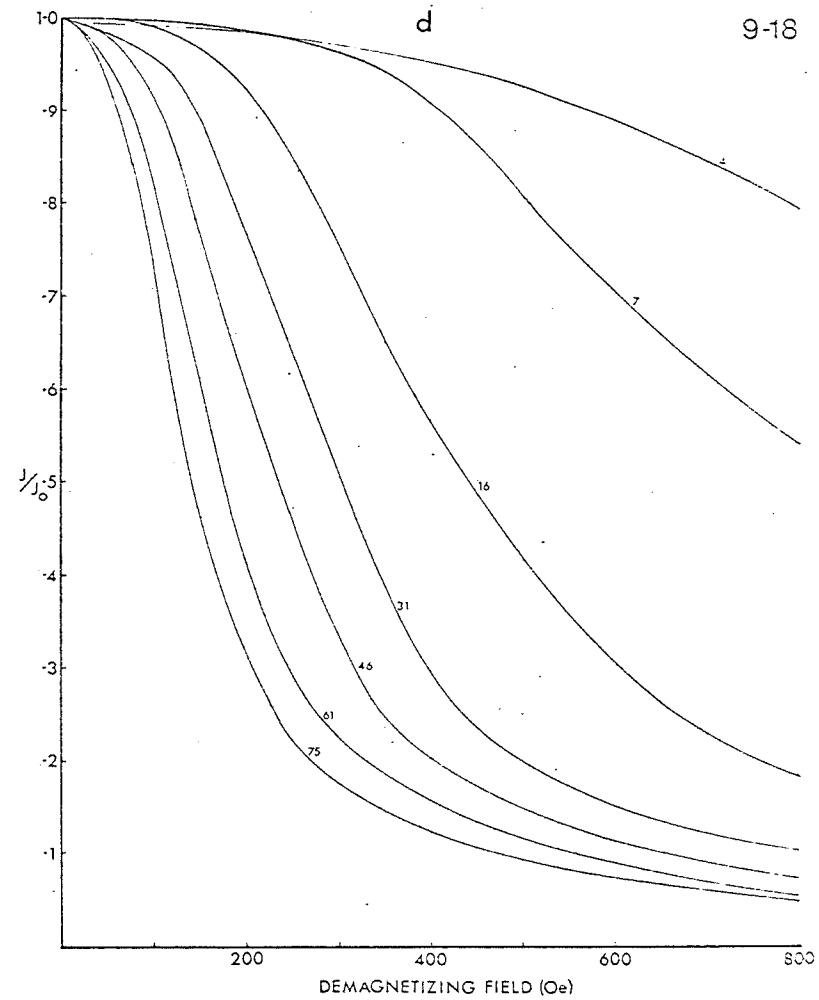
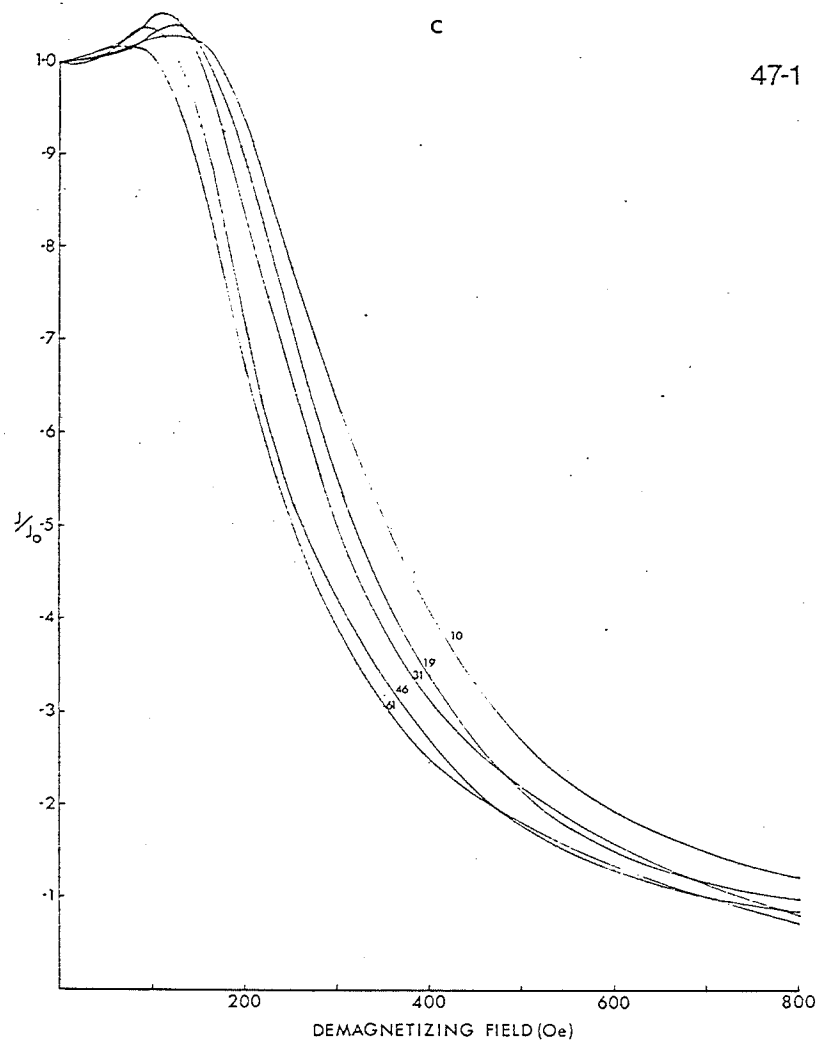


Figure 19 (continued).

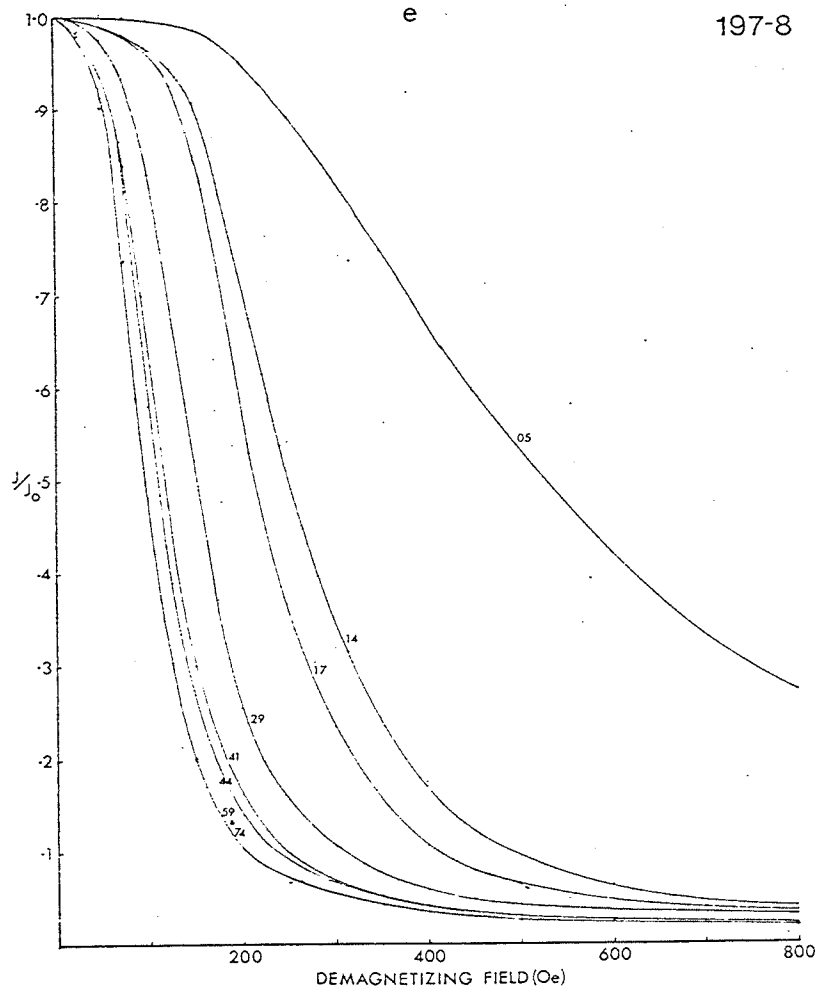


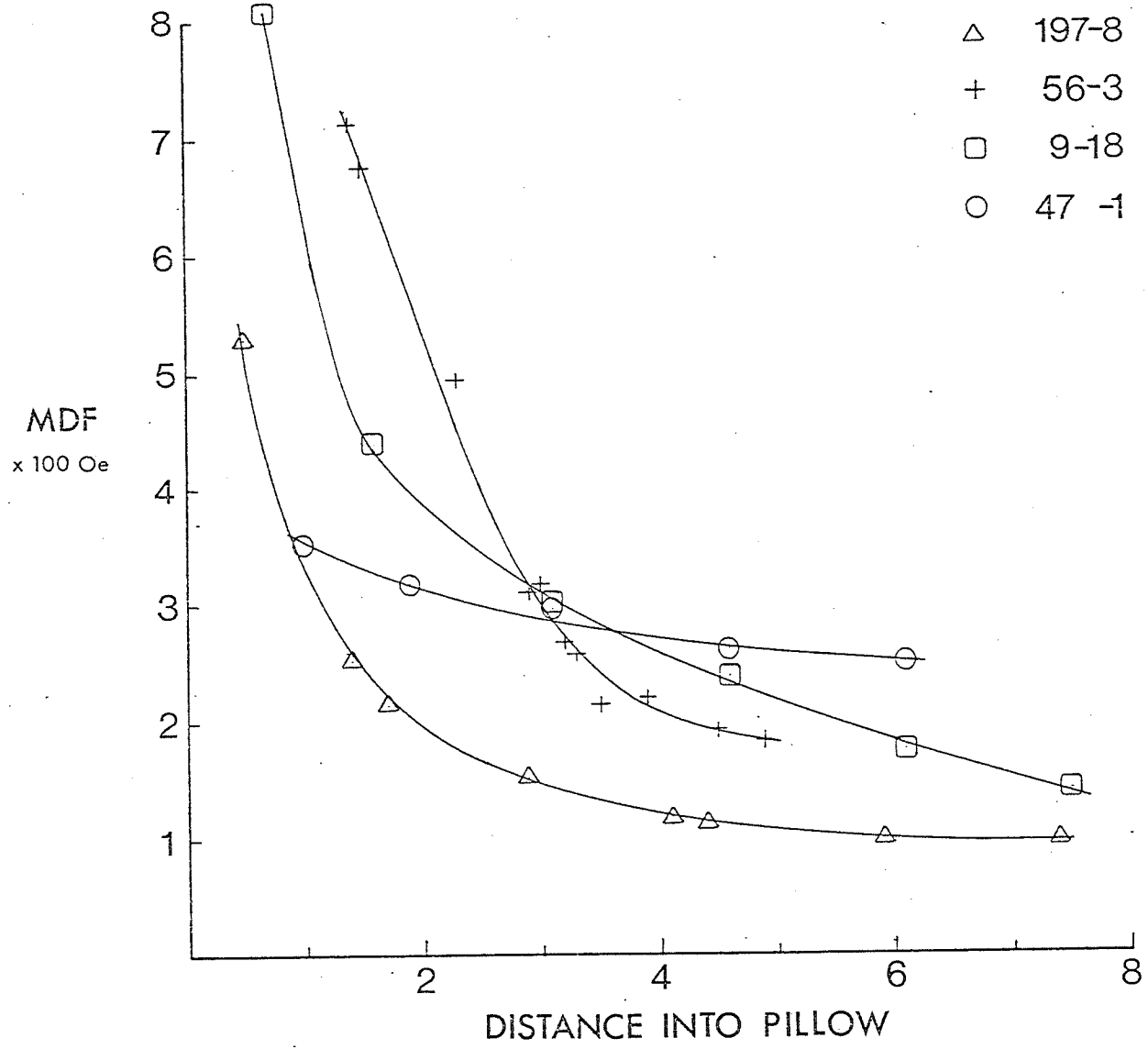
Figure 19 (continued).

recovered from a reversed polarity zone.

The alternating field (AF) demagnetization data is normalized by dividing the NRM intensity at each demagnetization step by J_{NRM} at zero field. The normalized curves plotted in Figure 19a-e show clearly the increase in coercivity of remanence from the interior to the exterior. The mean demagnetizing field (MDF), the field required to reduce the remanence to 50%, is plotted against distance into the pillow in Figure 20. There is a rise in MDF towards the outside, particularly in the outer two centimetres or so.

Since the four pillows have about the same grain shapes, generally highly irregular skeletal shapes, the two factors to be considered influencing the MDF are the grain size and the oxidation state. Consider pillow 197-8 compared to the other pillows. It has by far the lowest MDF's, the largest grains and the lowest oxidation state. According to Ince quoted by Readman and O'Reilly (1972) there is a linear decrease of coercive force with 'z', that is the greater 'z', the lower the coercive force and hence the lower MDF. Pillow 197-8 has the lowest 'z' and the lowest MDF so the oxidation state cannot be controlling the MDF. On the other hand Parry (1965) and Dunlop (1973) have shown an increase in coercive force with decreasing grain size. On this basis 197-8 with the largest grains should have the lowest MDF; as is observed. Within any one pillow exactly the same arguments may be applied. The outer regions have the

Figure 20. Mean demagnetizing Field as a function of distance into the four pillows.



smallest grain sizes and the highest MDF's. The outer regions of pillows 56-3 and 9-10 have the highest MDF's and in these regions the grains are so small that they cannot be seen under the microscope. Pillow 47A-1, which has the least radial variation in grain size, has the least radial variation in MDF. From this evidence the main factor controlling MDF is the grain size.

3.3.3 Direction of NRM

The direction of NRM is stable with demagnetization. The declination and inclination remain constant within plus or minus one and one-half degrees from 0 to 1000 Oe. in the case of pillows 56-3 and 197-8 but only to 500 Oe. in the case of pillow 47A-1. At higher fields 47A-1 begins to acquire anhysteretic remanent magnetization (ARM).

Most important for palaeomagnetic purposes, the direction is constant throughout the pillows. There is less than plus or minus two degrees variation between all the slices from one pillow and part of this variation may be due to aligning successive samples in the holder. This constancy is clear evidence that the alteration process that has occurred has not affected the direction of NRM.

4. Summary

While undertaken largely to establish a basis against which to judge laboratory alteration, this study of four pillows from the Mid-Atlantic Ridge has produced some interesting results. The mechanism of alteration of the

pillow basalts on the sea-floor has been established by Curie temperature and x-ray measurements. The progressive oxidation of the titanomagnetite to increasingly cation-deficient titanomagnetite has been measured not only progressing into each pillow but also progressing with age among the four pillows. The oxidation is homogeneous up to the ilmenite-hematite join. To the right of the join the process is less clearly defined. Some criteria, e.g. Curie points and cell edges suggest continuing homogeneous oxidation while the shape of the J_s -T curve may require unmixing along the join. The older the pillow, the more advanced the oxidation. That is the composition of the titanomagnetite in the interior of an old pillow resembles that of the exterior of a young pillow.

Within each pillow there are radial variations in concentration of titanomagnetite. Even after allowing for the variation in concentration there is still a variation in intensity of NRM. To a large extent the intensity of NRM is controlled by the grain size which in turn depends on the initial cooling of the pillow and hence its radius. There is a peak in J_{NRM} with grain size about $2\mu \times 5\mu$. Much work has been devoted (Dunlop, Evans etc.) to the importance of sub-micron grains as carriers of NRM. Some of these experiments (Dunlop 1973) have been carried out on magnetite powders in which the single-domain - paramagnetic boundary is a few hundred angstroms. For titanomagnetites the boundary size is much greater (Soffel 1971). Theories

of single-domain grains usually consider spherical grains while titanomagnetite grains in rocks are highly irregular in shape and would be single domain to somewhat larger sizes.

In light of this study, particularly the intensity of NRM from pillows 197-8 and 56-3, it would seem that grains of a few microns are the most important for palaeomagnetic purposes.

III LABORATORY ALTERATION OF VERY YOUNG

SUBMARINE BASALTS

1. Introduction

One of the principal aims of this study was to produce in the laboratory the same weathering changes as were observed in submarine basalts. In order to give as great a chance as possible of duplicating natural alteration processes, every effort was made to duplicate natural conditions. The basalt pillows examined in Section II had been recovered from depths ranging from 3600 metres for pillow 197-8 to about 1000 metres for pillow 47A-1. These depths correspond to pressures of about 80 bars (1200 psi) and 360 bars (5100 psi) respectively. In nature the pillows would be surrounded by sea water which under these pressures would be forced into the pores of the rock. Therefore these experiments were carried out in water in a pressure vessel which would allow sea-floor pressures to be reached. The use of sea-floor pressure also ensured that no unknown effects of pressure would cause a different result in the laboratory than that encountered in nature.

The alteration in nature would be occurring at between 0 and 6°C over tens and hundreds of thousands of years, although some material whose magnetization contributes towards the magnetic anomalies may be heated, for a short time at least, to higher temperatures as a result of burial by subsequent flows. Because of the very long times

involved, it was necessary to use experimental temperatures higher than that of the sea-floor. The temperatures finally used were a compromise between the need to raise temperature to speed the reactions and the need to keep temperature as low as possible to duplicate natural conditions. For example, Ade-Hall et al. (1971) have reported granulation (i.e. phase splitting) of titanomagnetites which have been heated to about 200°C in regional hydrothermal alteration, while pillows on the sea-floor whose titanomagnetites remain homogeneous have presumably not been heated much above 4°C. By heating to too high a temperature one would be modelling low-temperature regional hydrothermal alteration rather than the halmyrolysis (alteration at bottom water temperature) of the pillow lavas. Three distinct sets of experiments were carried out. After a description of the apparatus and experimental procedures, results from the experiments will be given. The significance of these results will be considered in a concluding section.

1.2 Apparatus

The pressure vessel in which all experiments were carried out was a cylinder with an inside diameter of one inch and a length of eight inches made of 316 stainless steel by the American Instrument Company (their Preliminary Test Vessel 41-19230). The pressure vessel was placed inside a stainless steel sleeve around which were wrapped the wires of a non-inductively wound furnace. These wires were

in turn surrounded by a coil of copper tube for cooling water. The whole assembly was surrounded by alumina insulation and placed inside an aluminum cylinder. This system, which is illustrated by Figure 21, was capable of pressures up to 700 bars (10,000 psi) and temperatures in excess of 400°C. For the experiments about to be described operating pressure was generally about 400 bars (6000 psi) and temperatures were 150°C and 210°C. The system required approximately an hour to attain working temperature and also an hour to cool to room temperature. All experimental times given are exclusive of these heating and cooling periods.

In the first experiment at 150°C temperature control was very crude. It had been hoped that by setting a constant power, that temperature would remain constant. In practice this did not work very satisfactorily. The temperature drifted on a 24-hour cycle with other long term variations. The longer term variations were probably caused by changes in room temperature, and hence heat loss, with the weather; while the 24-hour variation was primarily due to supply voltage drifting. As a result the temperature has a large uncertainty at any instant, although 150°C is probably a good long-term average. The temperature at any instant was within the range of $150 \pm 8^\circ\text{C}$. For all later experiments, the temperature was controlled by an RFL zero firing temperature controller, model 7872. With this controller, temperature variation was less than $\pm 2^\circ\text{C}$.

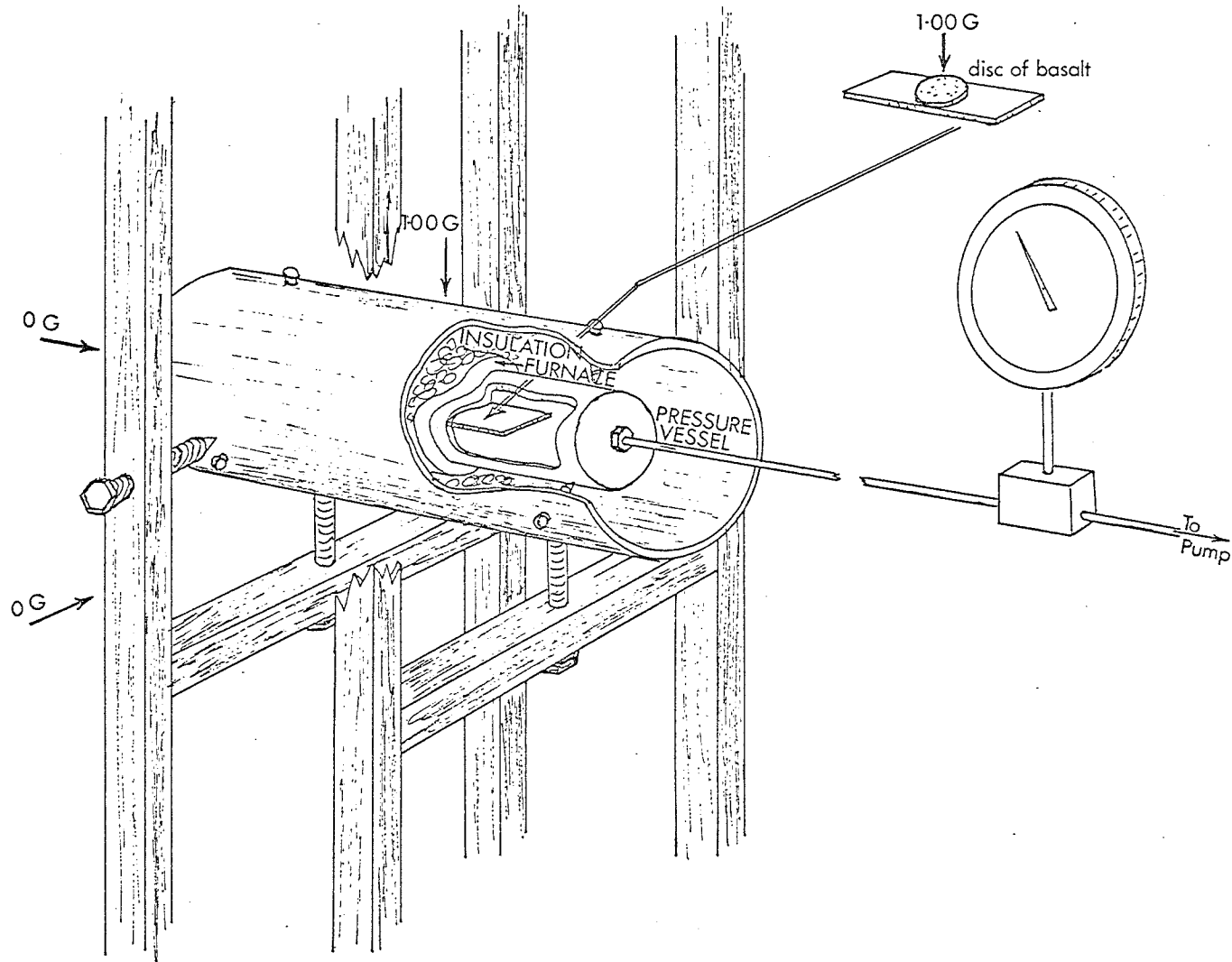


Figure 21. Sketch of apparatus used to produce laboratory alterations. The three orthogonal pairs of Helmholtz coils are omitted for the sake of clarity.

The water used for the first 150°C experiment and for the 210°C experiment was Halifax city tap water, while the second 150°C experiment used sea-water from the North West Arm. The compositions of these waters is given in an appendix.

The furnace was placed in the centre of three orthogonal pairs of Helmholtz coils, each coil approximately two feet in diameter. The current through the coils was adjusted to produce a field less than 2 m Gauss along each of the horizontal axes and 1.00 Gauss vertically. The drift of the fields during the duration of the experiments was less than 0.005 Gauss.

The samples used were some of the discs which had been used in the pillow studies, that is discs 2.5 cm diameter and about 1 1/2 mm thick. The slices were mounted on a tray in the pressure vessel as shown in Figure 21.

1.3 Experimental Procedure

In all the experiments about to be described the same procedure was followed.

- 1) The NRM of the sample was A.F. demagnetized in the same way as in the pillow studies up to 1000 Oersteds.
- 2) The fields in the Helmholtz coils were checked to be zero, i.e. less than 2 m G, horizontally and 1.00 G vertically.
- 3) The samples were mounted on the tray and slid into the pressure vessel. The pressure vessel was pumped full of water up to about 400 bars (6000 psi).

- 4) The heater was turned on and the furnace brought to the desired temperature either by manual control for the first experiment or by the RFL controller in later experiments. In all cases the temperature was monitored by a thermocouple in the pressure vessel whose output was displayed either on a chart recorder or a Digital Voltmeter. This was done as a precaution against overshoot on the heating and to monitor long-term stability.
- 5) The samples were heated under these conditions for the desired time which ranged from zero time (i.e. the cooling was started immediately the operating temperature was reached) to over 2000 hours (90 days).
- 6) At the end of the desired period the heater would be turned off and the cooling water turned on to cool the samples to room temperature in the 1.00 Gauss field.
- 7) After the samples had cooled they were removed and A.F. demagnetized to 1000 Oersteds as in step 1. This demagnetization was carried out so that the effects of changing oxidation state on the coercivity could be followed. Since A.F. demagnetization is a standard palaeomagnetic procedure it would be potentially useful if the shape of the A.F. demagnetization curves were found to be diagnostic of the samples' history.
- 8) A small chip was broken off each slice for J_s -T measurements, usually after every second heating. This step was not followed in the first 150°C heating experiment.
- 9) The procedure was repeated from step 2.

2. Initial Experiment at 150°C

2.1 Sample

This initial experiment was undertaken as much as a test of the practicality of the whole system as an attempt to produce well documented alteration. For this experiment sample 35 from pillow 56-3 was chosen because it seemed a 'typical' slice since it falls in the middle of the range of Curie temperatures for the younger pillows.

2.2 Saturation Magnetization and Curie Temperature

Unfortunately when this experiment was started the J_s -T apparatus had not been assembled and the precaution of preserving chips as the experiment progressed was not taken. From Figure 7, the plot of Curie temperatures into the pillows, a Curie temperature of $230 \pm 10^\circ\text{C}$ has been estimated for the slice as it was cut from the pillow. After 3540 hours at 150°C the Curie temperature had risen to 354°C . While a J_s -T curve had not been obtained for sample 56-3-35 prior to heating in the laboratory one was later obtained for sample 56-3-38. Since slices 35 and 38 would not be greatly different, the curve for slice 38 will be used as a type curve for slice 35.

The J_s -T curve for slice 38, Figure 22, shows a single Curie temperature on heating of 256°C , a somewhat higher temperature than the surrounding slices of pillow 56-3. Nonetheless this J_s -T curve prior to laboratory alteration is a simple curve indicative of a single Curie temperature homogeneous phase. With allowance for some temperature

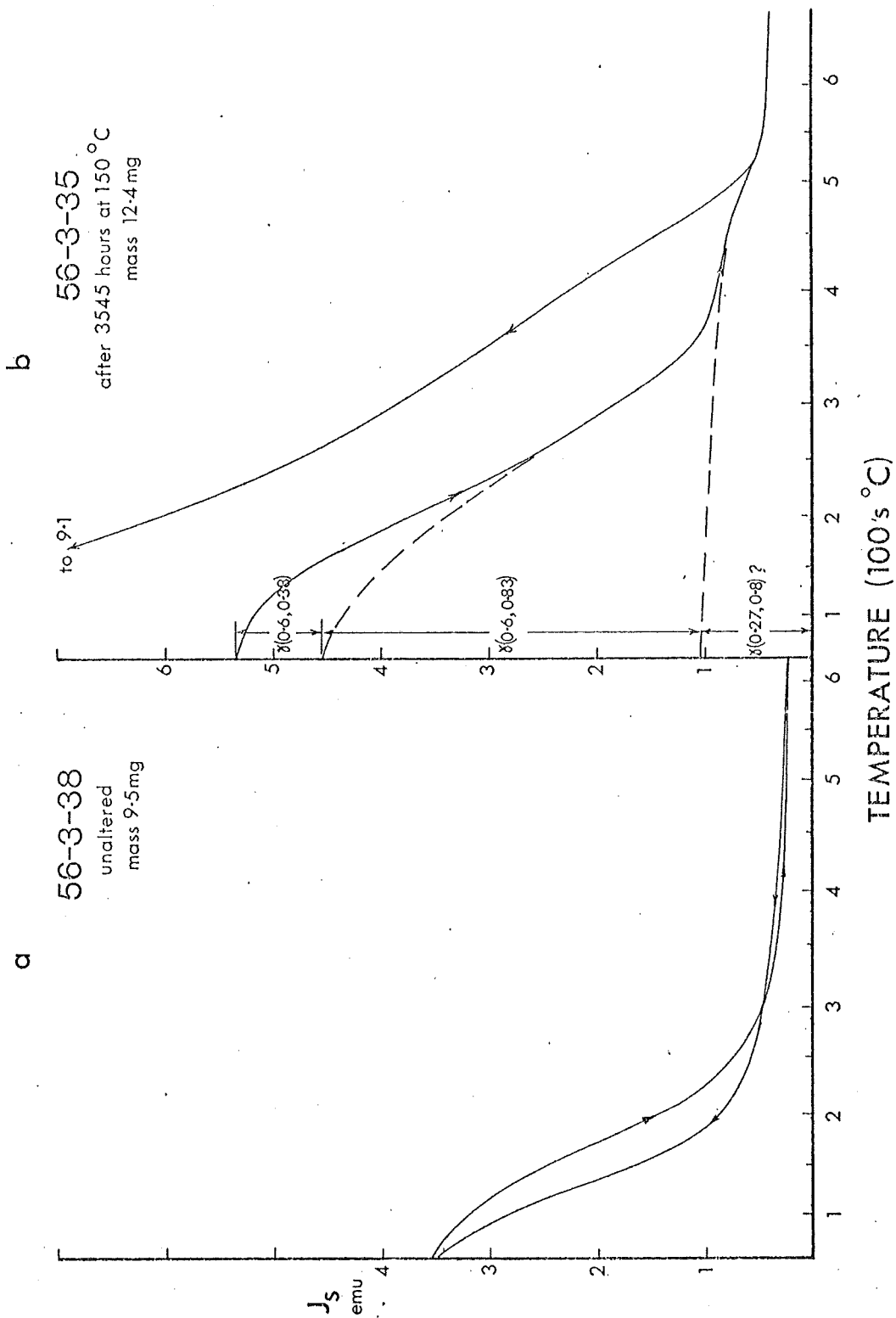


Figure 22. Tracings of J_s -T curves.

- For 9.5 mg of sample 56-3-38 in its natural state.
- For 12.4 mg of sample 56-3-35 after 3545 hours at 150°C in water. The dotted lines are projections intended to show the contributions of the various components.

hysteresis, partly caused by the apparatus, the curve is reversible.

The shape of the J_s -T curve after laboratory alteration is very different. Not only is the Curie temperature much higher at 354°C, but the curve no longer has the same simple form. There is a definite high temperature Curie point at 520±10°C; there is also a faint suggestion of a Curie point at about 250°C - this is slightly more apparent on the original curve.

This J_s -T may be made up from the superposition of three J_s -T curves as shown in Figure 22b. While it is realized that there are potentially large errors associated with the projections involved here it is still a useful process in order to put some limits on possible oxidation mechanisms. If one takes the contribution to J_s from each of the phases and divides by I_s from each phase, then the concentration of each phase may be obtained. The only information available to determine I_s is the Curie point. Knowing the initial composition of the γ -phase, $\gamma(0.6, 0.38)$, and assuming oxidation along the $x=0.6$ line, then the second phase with a Curie point of 354°C is $\gamma(0.6, 0.83)$. I_s for these phases may be obtained from Figure 14. It is more difficult to establish I_s for the phase with the 520°C Curie point. If it were a titanomagnetite, then I_s would be about 80 emu/g. If however it is a titanomaghemite, then I_s would be slightly less. Using these values the following table is obtained:

TABLE 3
 CONCENTRATIONS OF FERRITES IN 56-3-35

Phase	J_s (emu/g rock)	I_s (emu/g ferrite)	% ferrite
$\gamma(0.6, 0.38)$	0.064	24	0.27
$\gamma(0.6, 0.83)$	0.276	18	1.55
$\gamma(0.27, 0.8)?$	0.060	75	0.08
Total	0.40		1.9

This concentration of 1.9% is somewhat larger than the initial concentration of 1.58% obtained from Figure 22a. The difference is even greater if the Ti-rich component formed by the unmixing which produced the 520°C Curie point component is considered. This would bring the total concentration to slightly more than 2.0%. The difference between 1.6% and 2.0% is larger than could be easily explained by the scatter between chips, so probably one of the initial assumptions is incorrect. The most likely cause is that homogeneous oxidation does not proceed to the right of the ilmenite-hematite(maghemite) join but rather unmixing occurs when the γ -phase reaches the join with a Curie point around 300°C. This would mean that the 354°C Curie point phase is an unmixing product towards the maghemite end of the join which would have a higher I_s and therefore could account for the observed J_s with the original concentration of 1.6%.

56-3-35

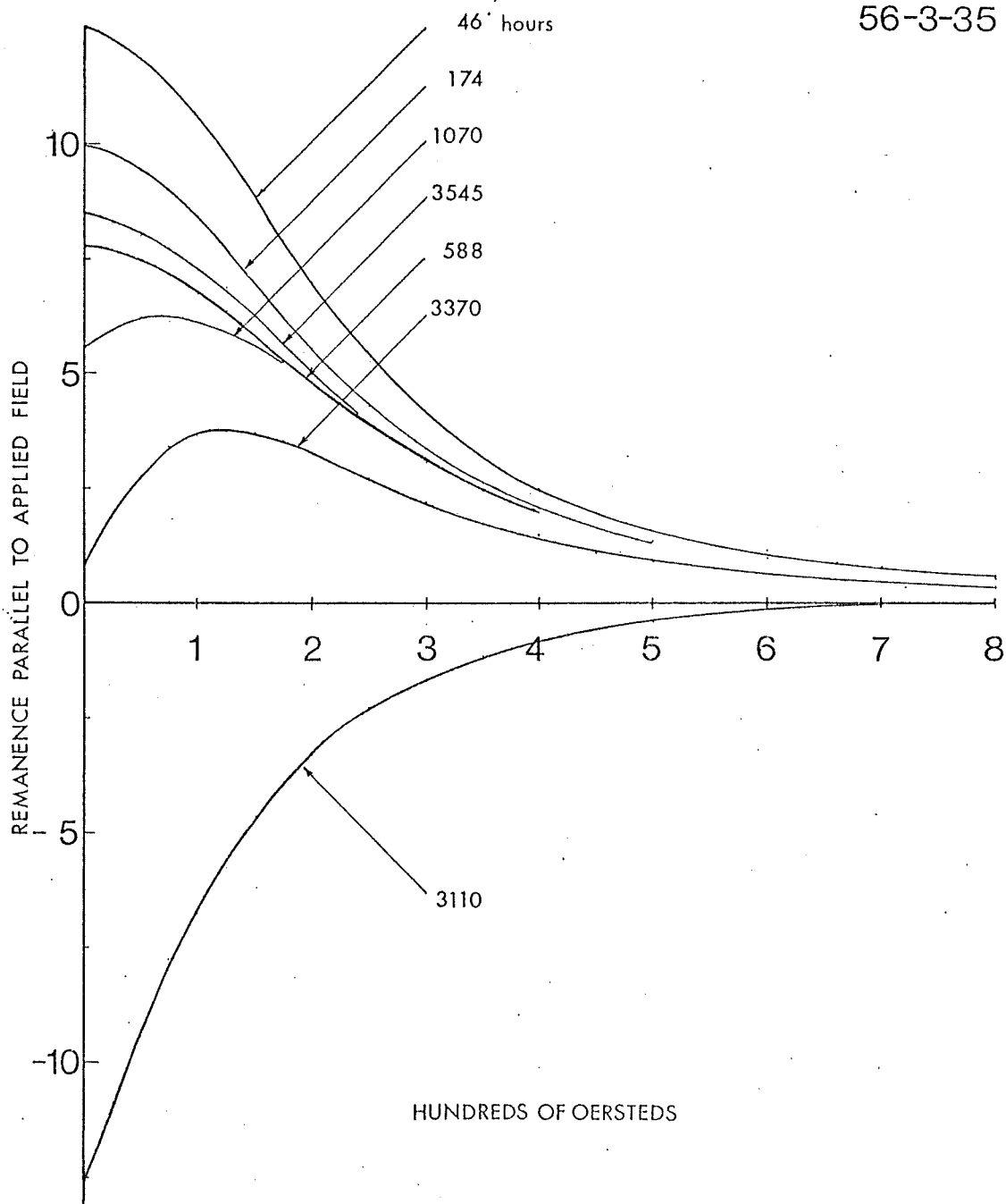


Figure 23. A.F. demagnetization of PTRM's acquired by sample 56-3-35 after cooling from 150°C to room temperature in a 1.00 G field. The numbers against each line give the number of hours the sample had spent at 150°C.

2.3 A.F. Demagnetization of Successive TRM's

After each period of heating the sample was cooled in the 1.00 G field, removed, and A.F. demagnetized as outlined in the procedure. The results are given in Figure 23 which shows the A.F. demagnetization of that component of the TRM parallel to the applied field in absolute terms while Figure 24 shows the same results normalized. For the first six hundred hours or so, the TRM becomes gradually weaker but, as can be seen in Figure 24, somewhat 'harder', that is the MDF increases slightly. Looking at the normalized curves there is considerable resemblance between the change over this first six hundred hours and the progression in the pillow from slice 35 to slice 32.

After a thousand hours heating the demagnetization characteristics begin to change drastically. The TRM increases with the first 75 Oe. A.F. demagnetization. This increase indicates the removal of a small reverse component of magnetization. Due to troubles with both the spinner magnetometer and the fluxgate used to check the Helmholtz coils the next period of heating was very long, 2000 hours. After a total of 3110 hours the TRM was completely reversed with about the same intensity as the initial TRM but with a lower MDF, 110 Oe. compared to 225 Oe. With subsequent heating the reversed component decreased until after 3545 hours the TRM was completely normal, identical to that at 304 hours.

56-3-35

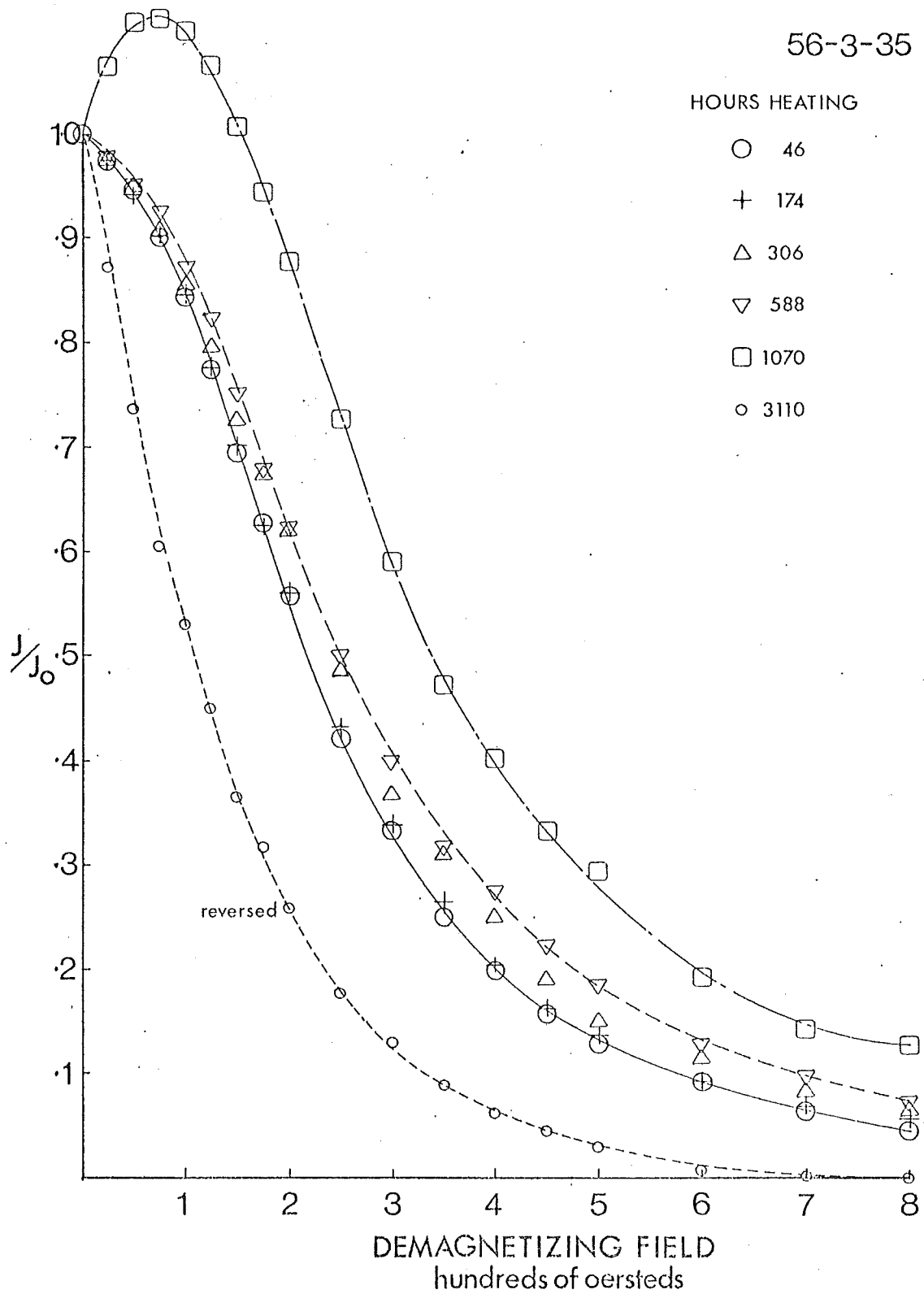


Figure 24. Normalized A.F. demagnetization of PTRM's acquired by sample 56-3-35.

What has occurred is the growth and then decay of a self-reversed TRM. A similar transient self-reversal has been observed by Ozima and Ozima (1967) who encountered such a phenomenon while heating in air a submarine basalt to 300°C.

Because of this very intriguing self-reversal produced it was decided to repeat the experiment with a group of samples in an effort to reproduce this phenomenon. This time chips would be kept from the different slices after successive heatings and used for J_s -T measurements so that the changes in composition of the titanomagnetites could be followed throughout the alteration process. In order to reduce the time required for self-reversal the temperature was increased to 210°C.

3. Experiment at 210°C

3.1 Samples

In order both to give a good chance of reproducing the self-reversal and to discover if the self-reversal phenomenon was peculiar to sample 56-3-35 or if it could be produced in other samples, this experiment was carried out with six samples. Two of the samples were very close in composition to 56-3-35, namely 56-3-233 and -239 (the 2 indicating they were cut from a second core drilled from pillow 56-3). Of the other four discs, one, 56-3-245, was a fresher sample from pillow 56-3; two, 197-8-18 and -42, were from the more intensely magnetized pillow 197-8; while the fourth sample

was from a piece of basaltic glass. This basaltic glass had been recovered by Dr. J. Moore in 1973 at a depth of 25 feet, a half mile west of Apua Point on the south side of Hawaii. This sample (73Ma-1-10) had been recovered immediately after extrusion onto the sea-floor, in fact it was still warm when broken off the lava tube.

3.2 Saturation Magnetization and Curie Temperature

The behaviour of saturation magnetization and Curie temperature with duration of heating has some parallels with the natural progression from the core to the rim in basalt pillows but also some differences. The Curie temperature, as shown in Figure 25, increases with increased heating time. This increase is not linear but rather a very rapid increase from 200°C to 360°C in the first 100 hours followed by a much slower increase to about 420°C after 1000 hours. The change in Curie temperature in the first 100 hours is comparable to the change in ridge basalts over several hundred thousand years.

However the differences between the characteristics of natural and laboratory alteration as revealed in this experiment are important. With the increase of cation-deficiency, that is of 'z', in the pillows the saturation magnetization decreases, however in this experiment J_s increases with increased laboratory heating time. Since the samples from the various pillows have somewhat different behaviour they will be considered separately.

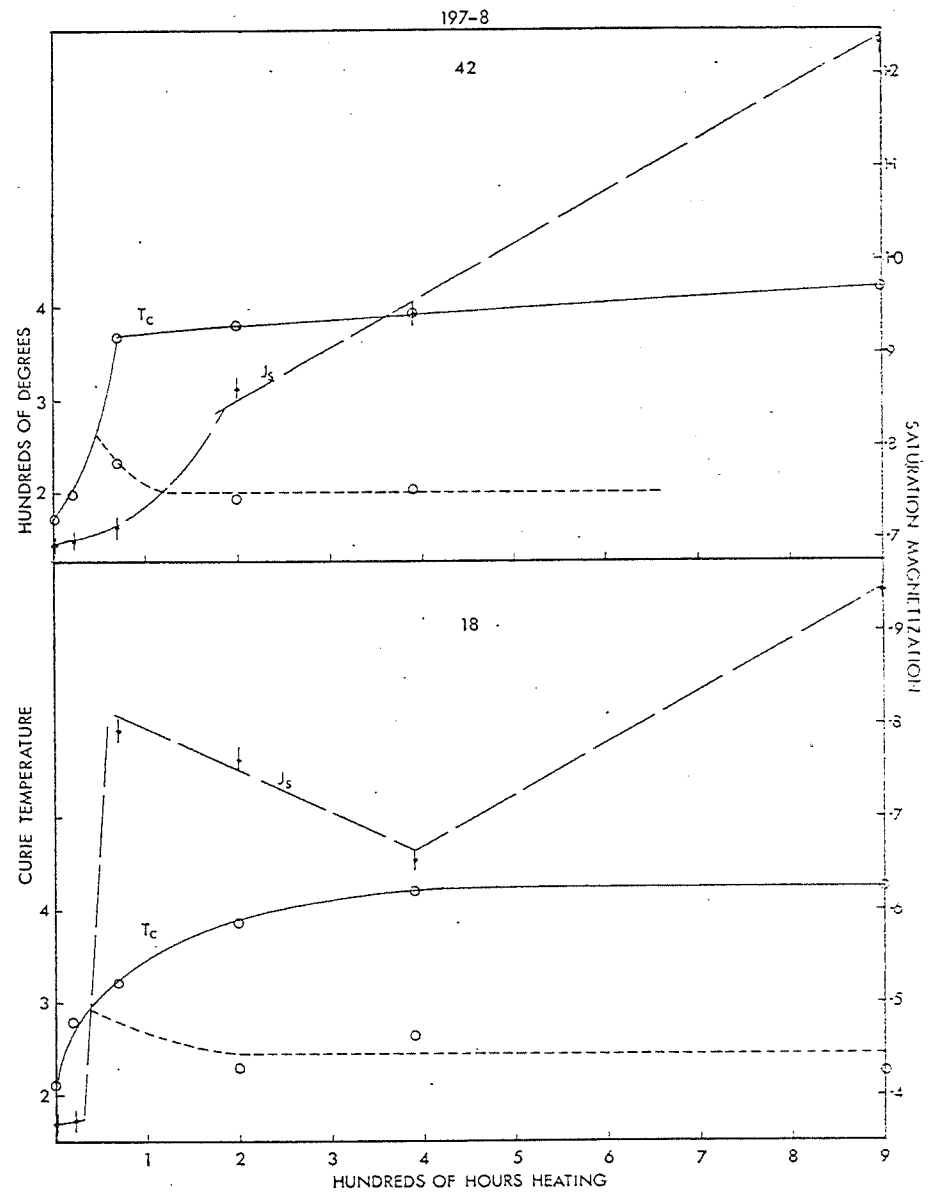
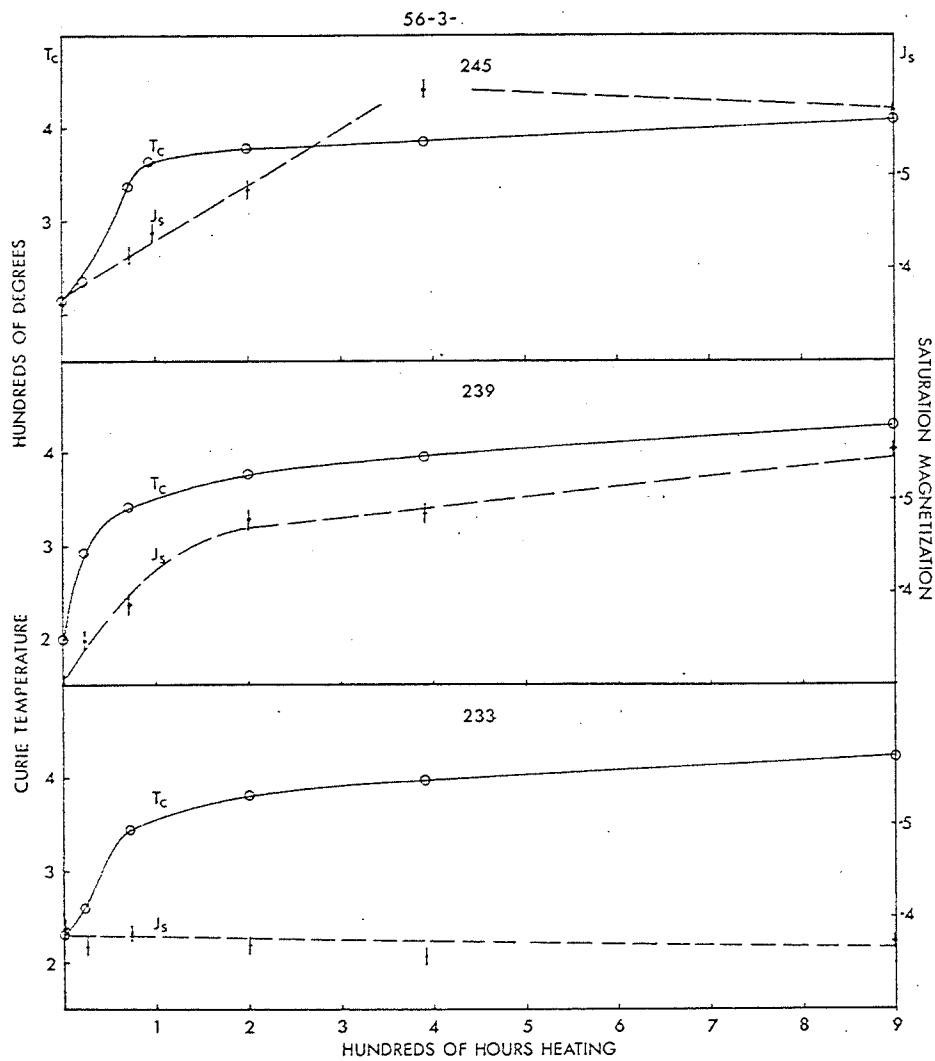


Figure 25. Change in J_s and Curie temperature for five of the samples heated at 210°C as a function of total heating time. Saturation Magnetization is in emu/g.

Pillow 56-3: Of the three samples -233, -239 and -245 the latter two are very similar while -233 is different in that for it alone J_s slowly decreases with heating time while for all the others it increases. In sample -233 the Curie temperature increases rapidly in the first 100 hours. The heating curves of the J_s -T measurements reveal a hint of a higher Curie temperature at about 550°C in all the later runs. This is a very weak indication so the amount of titanomagnetite with this Curie temperature must be very small. On cooling the sample reverted to a Curie temperature of 217±15°C. It would seem that the effect of alteration in the water had been to produce a cation-deficient titanomagnetite of high 'z' which had been reduced on heating in vacuum.

Sample -239 and sample -245 from pillow 56-3 differ from -233 in that their J_s increase with heating time from initial values of 0.30 and 0.37 emu/g respectively to 0.55 and 0.56 emu/g, while Curie temperature rises from about 200°C to 425±10°C. Up to about a hundred hours heating the J_s -T curves are typical of an homogeneous cation-deficient titanomagnetite in the heating cycle, but indicate two Curie temperatures, one higher and one lower than the heating Curie temperature, in the cooling part of the J_s -T curve. After more than a hundred hours heating at 210°C, for example at about 400 hours, two Curie temperatures are apparent both in the heating and cooling curves. The lower Curie temperature is approximately the Curie temperature of the

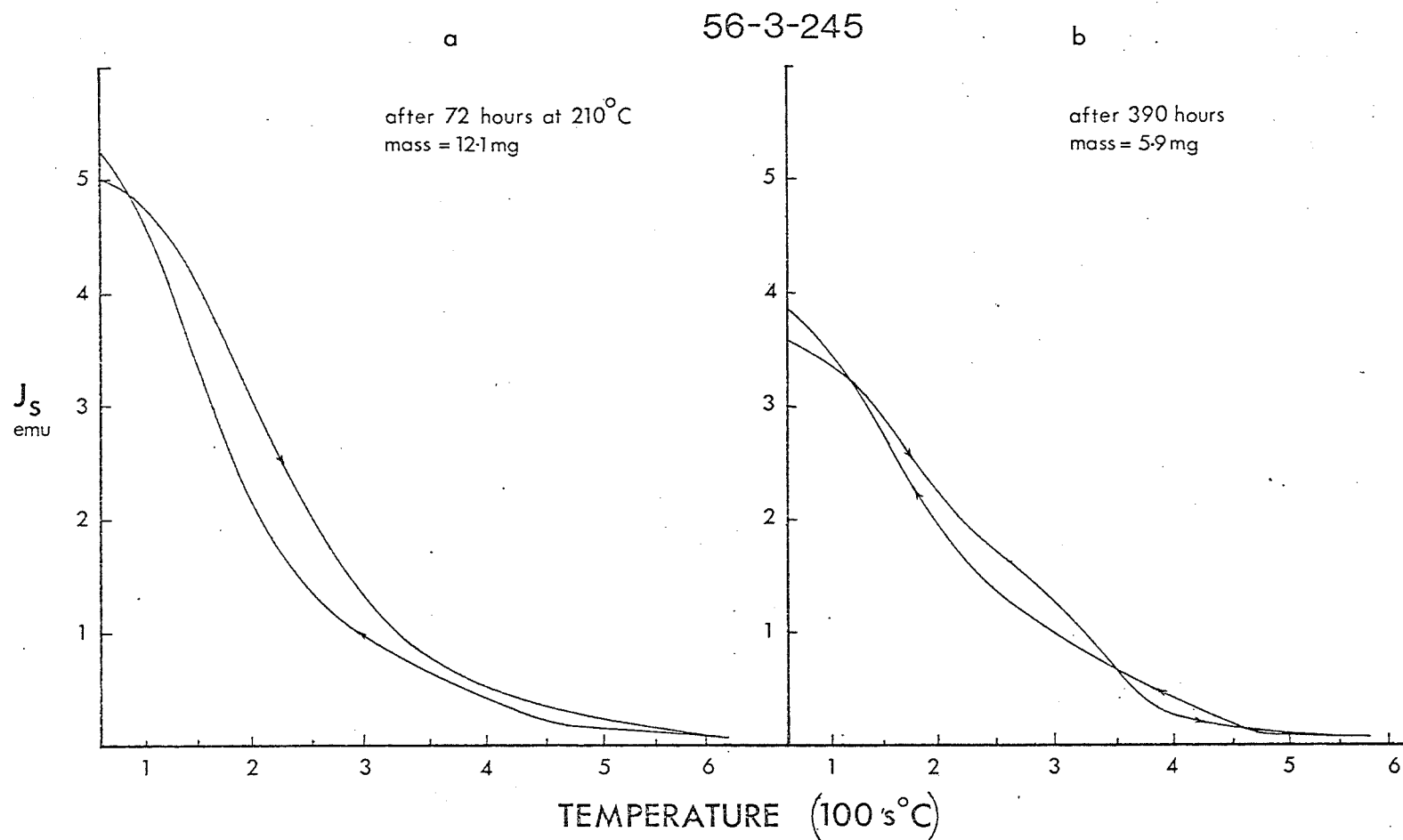


Figure 26. Tracing of J_s -T curves for sample 56-3-245.
a) for 12.1 mg after 72 hours at 210°C.
b) for 5.9 mg after 390 hours at 210°C.

titanomagnetite prior to laboratory alteration while the upper one is about 400°C. Figure 26 shows the different curves for 56-3-245 at 72 hours and 390 hours.

Pillow 197-8: The two samples -18 and -42 show much the same behaviour as 56-3-239 and -245, except that the onset of two Curie temperatures on heating occurs earlier, at about 72 hours. With these two samples there is a great increase in J_s from 0.4 emu/g to 0.95 emu/g for -18 and from 0.7 emu/g to 1.24 emu/g for -42. As in pillow 56-3, the onset of two Curie temperatures coincides with the increase in J_s . Now J_s decreases with increasing 'z' but increases with decreasing 'x'. The evidence of two Curie temperatures and increasing J_s means that the higher 'z' homogeneous cation-deficient titanomagnetite, which is formed in the initial heating, is being broken down in further heating. One of the products of this unmixing is a Ti-poor phase with a composition approaching maghemite and a higher J_s . The lower of the two Curie temperatures measured is close to the original Curie temperature of the sample.

In looking at the J_s -T plots of sample 197-8-42 after successive heatings shown in Figure 27, the increasing amount of the high Curie point material becomes apparent while the low Curie point material becomes less noticeable. Because each of these curves is for a different mass of rock, they can only be used to realize the changing importance of the two phases as heating time increases.

197-8-42

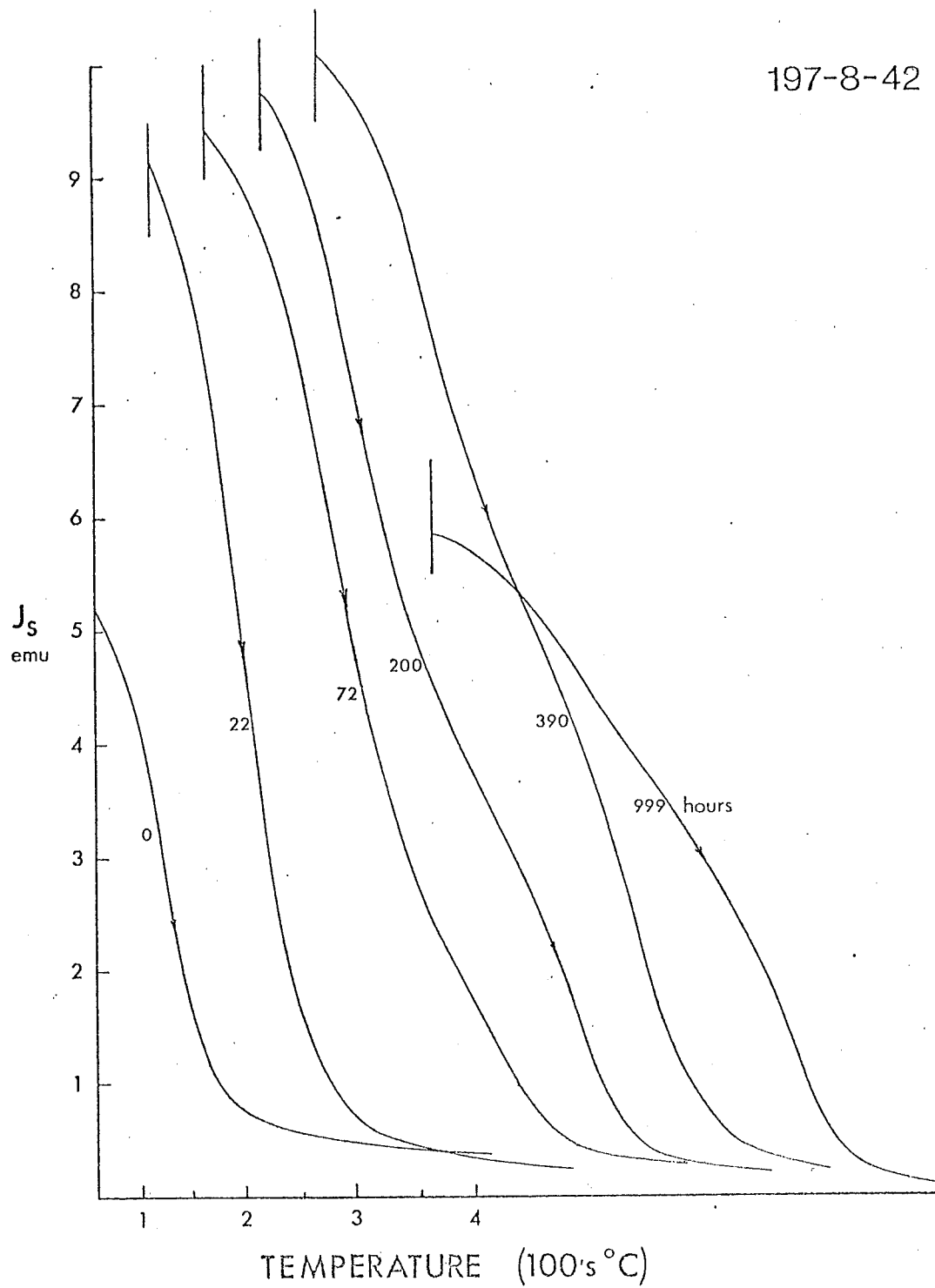


Figure 27. The evolution of the slope of the J_s -T curves for sample 197-8-42. The small numbers against each curve are the number of hours heating at 210°C. Each curve is for a different mass of sample.

It would seem that the initial heating had altered some of the original cation-deficient titanomagnetite to a higher oxidation state. After less than a hundred hours heating in the case of pillow 197-8, or four hundred hours in the case of 56-3, this high 'z' titanomagnetite with a Curie point at about 320°C breaks down. The break-down products are an Fe-rich phase with a composition approaching magnetite or maghemite, responsible for the high Curie temperature and high J_s and a Ti-rich phase whose Curie temperature is probably less than room temperature and so will not be seen on the J_s -T plot.

The lower of the two Curie points is about that of the starting material in the sample. Probably some of the original phase is present throughout the oxidation process but its Curie point and that of the higher 'z' phase cannot be distinguished separately until they are several tens of degrees apart.

Pillow 73Ma-1: The behaviour of the Hawaiian sample is completely different from the Mid-Atlantic Ridge samples. The development of the J_s -T curves for this sample is shown in Figure 28. Initially the material has no single Curie temperature and appears to be paramagnetic. Since it does acquire a small TRM there must be at least some ferrimagnetic material. Probably there are γ -phases with a wide range of Curie points. The first sign of discernible Curie points occurs after 344 hours heating, one at 100°C, the other at

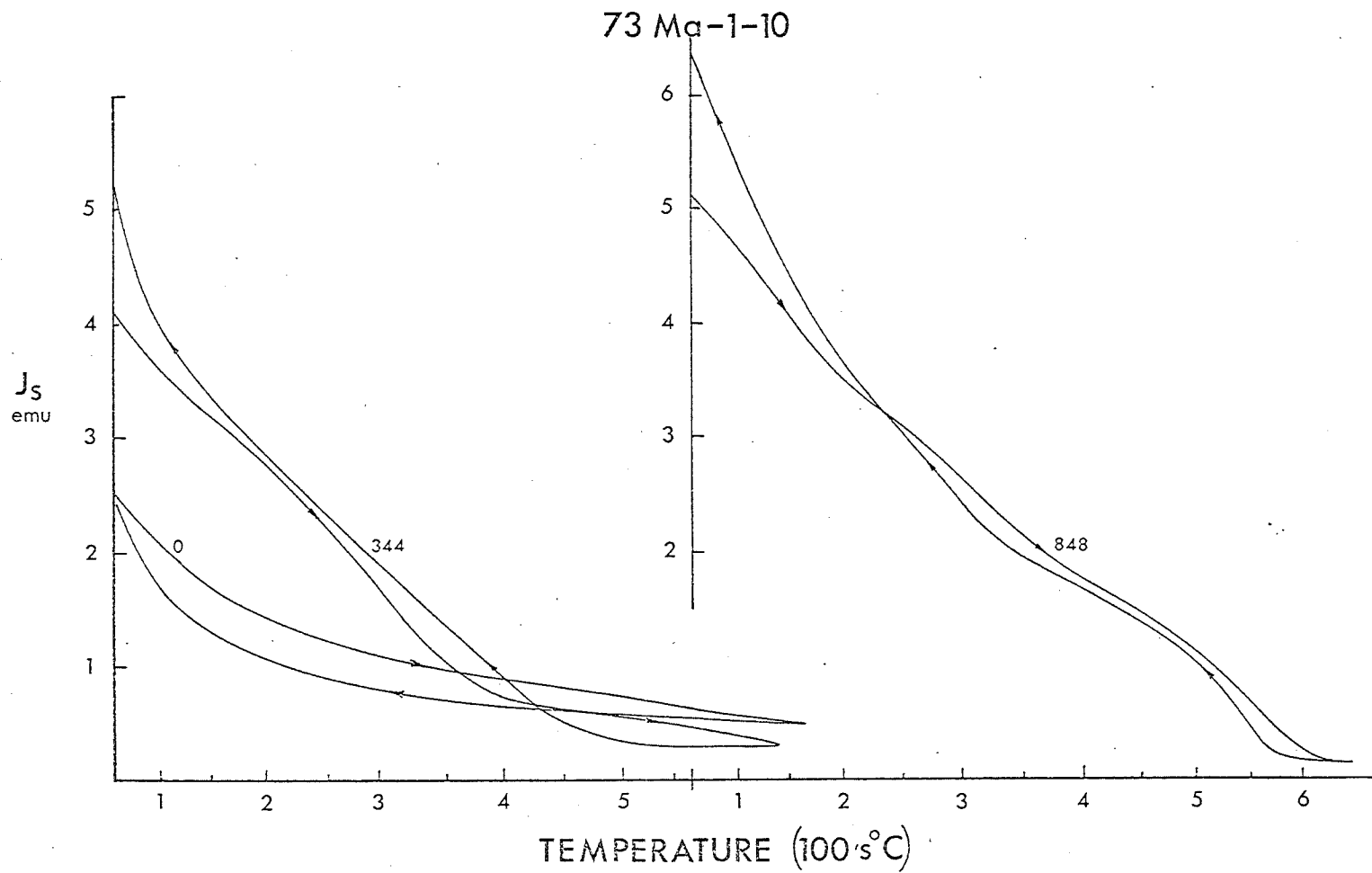


Figure 28. Tracings of J_S -T curves for 73Ma-1-10 showing the evolution from a "paramagnetic" curve to one with multiple Curie points.

about 360°C. After 852 hours, the J_s -T curve is more complicated with Curie points at about 180°C, 360°C and 600°C.

This sample had been cut from the glassy outer centimetre of the pillow in which very fine grains of a wide range of compositions may have been formed in the initial cooling of the lava. With heating in the laboratory it appears that there has been some concentration into γ -phase of two or three compositions. Due to the increase in J_s it may also be that there has been formation of titanomagnetite from some silicate minerals.

3.3 A.F. Demagnetization of Successive TRM's

The intensity of the remanence acquired in cooling from 210°C in a 1.00 G field after successive heatings is shown for the six samples in Figure 29. For the samples from the Mid-Atlantic Ridge pillows the TRM acquired decreases with heating time. This decrease occurs in at least two steps. There is a very rapid decrease to about half the initial value in the first one hundred hours at 210°C. The remanence then decreases by about a third of its value at a hundred hours in the next four hundred hours while after that the decrease is very slow. There is a marked similarity between the shape of these curves and the shape of the decrease in NRM of Mid-Atlantic Ridge pillows with distance from the ridge as given by Irving et al. (1970). This similarity will be further considered in the summary. Sample 73Ma-1-10 is contrary to this trend because its TRM increases with

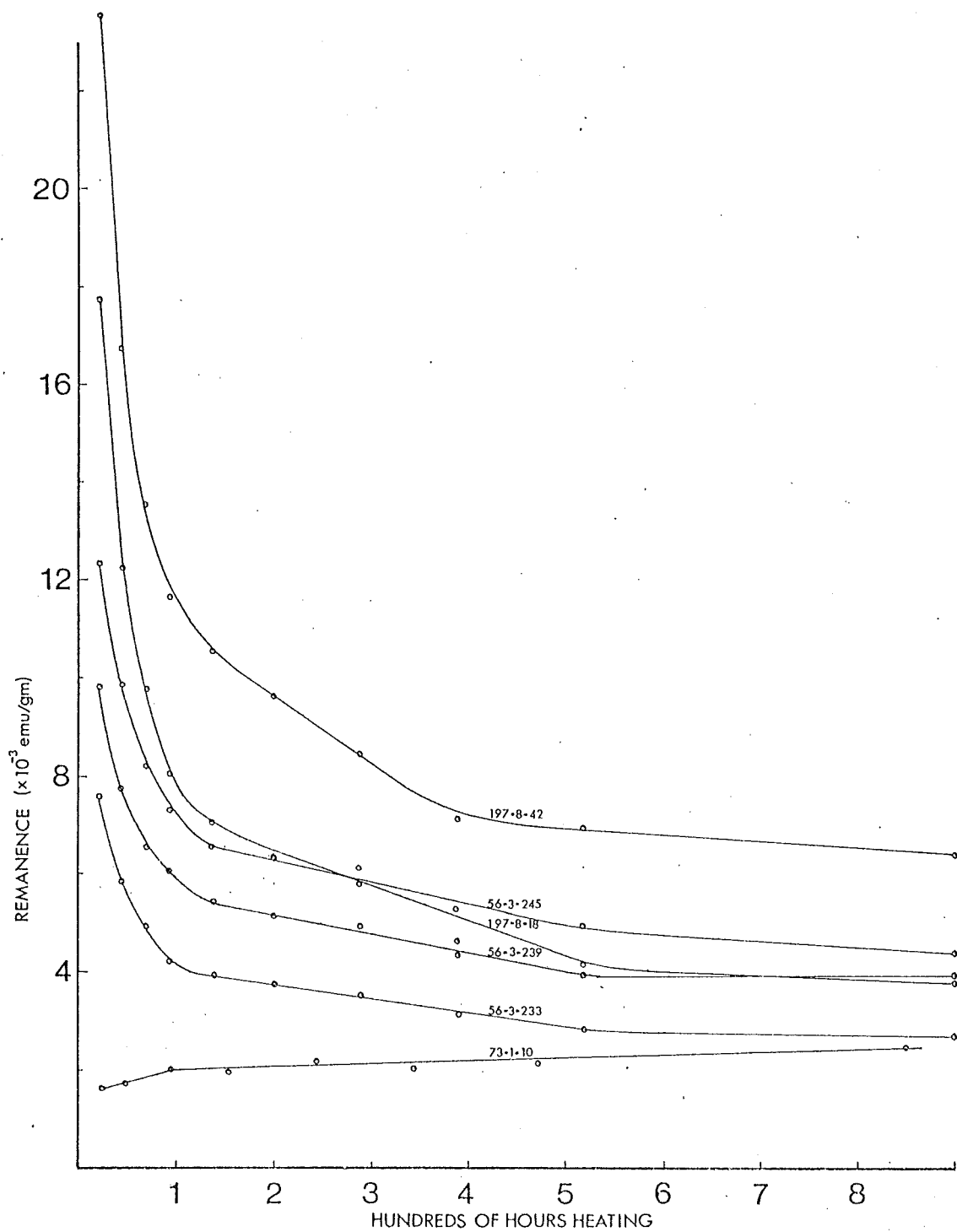


Figure 29. Variation of PRM acquired by various slices in cooling from 210°C in a 1.00 G field as a function of total heating time.

heating time. This increase is caused by the creation of ferrimagnetic material reported in the previous section.

The TRM's shown in Figure 29 were A.F. demagnetized. The normalized demagnetizations are given in Figure 30a-f. Once again the different pillows will be considered separately.

Pillow 56-3: All three samples show an increase in hardness in the first 94.5 hours heating. The MDF increases by 40 Oe. for -233 and by about 10 Oe. for the other two. With further heating there is little systematic change at demagnetizing fields greater than 200 Oe. At demagnetizing fields less than 200 Oe. the TRM decreases more rapidly with increased heating time while at about 200 Oe. there is virtually no change.

Pillow 197-8: Sample 197-8-18 follows the same pattern as the samples from pillow 56-3. There is an increase in the MDF with the first 94.5 hours heating; little change at demagnetizing fields greater than 200 Oe. with subsequent heating but a more rapid initial demagnetization in the first hundred Oersteds or so.

Pillow 73Ma-1: The behaviour of this sample is totally different from the others. There is a marked increase in hardness up to 243 hours heating and a slight decrease thereafter. The MDF's after various heatings are given in Table 4.

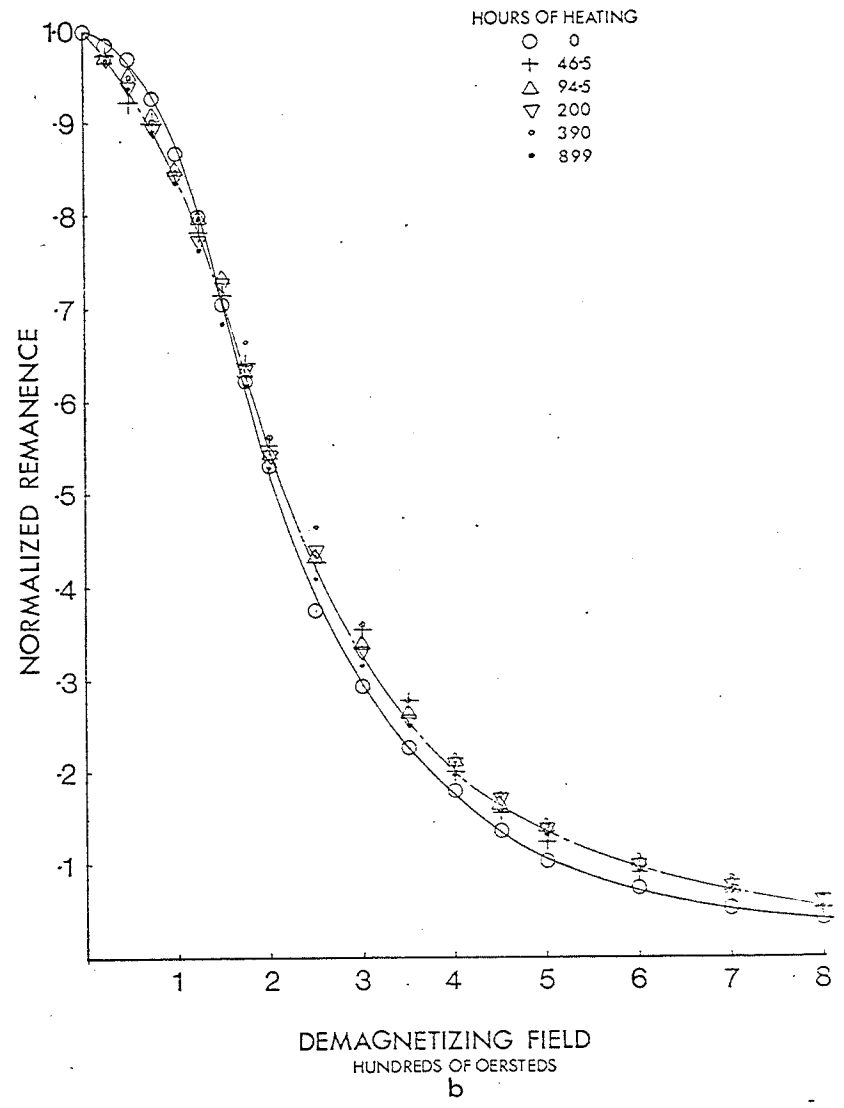
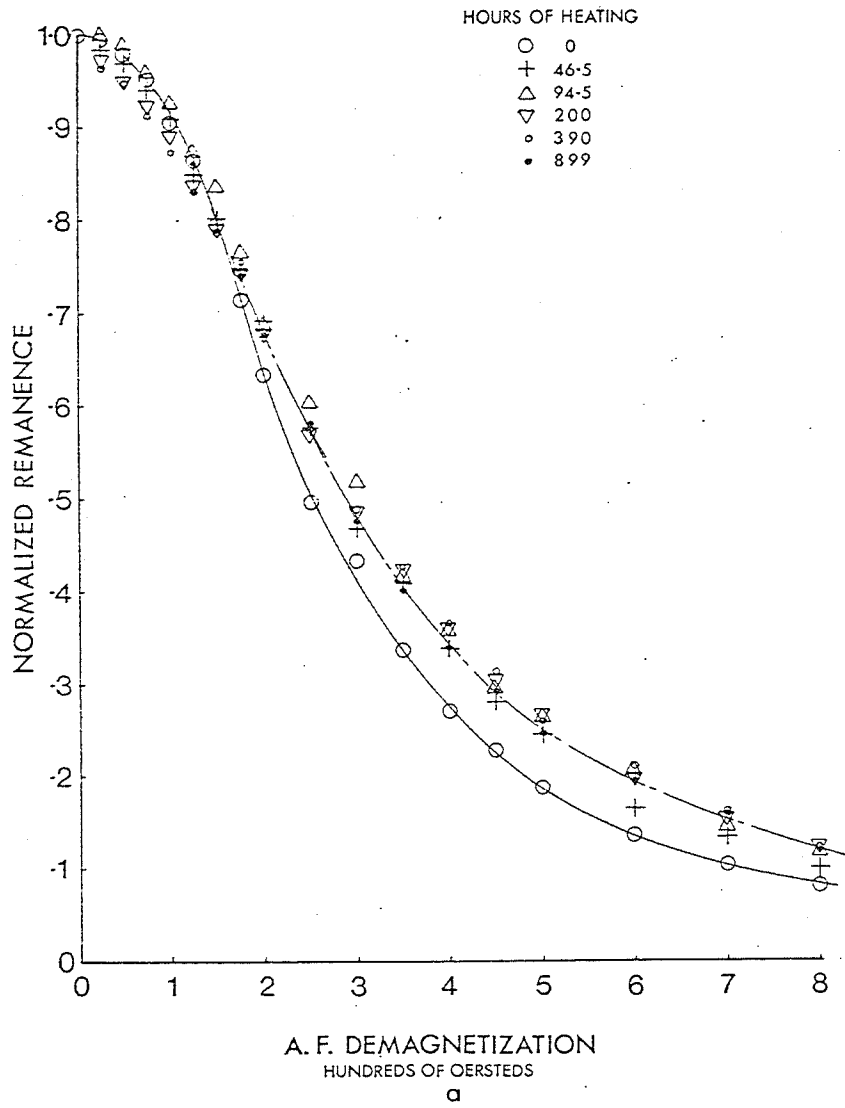


Figure 30. Normalized A.F. demagnetizations of the samples heated at 210°C for various times.
 a) 56-3-233, b) 56-3-239, c) 56-3-245, d) 197-8-18, e) 197-8-42, f) 73Ma-1-10.

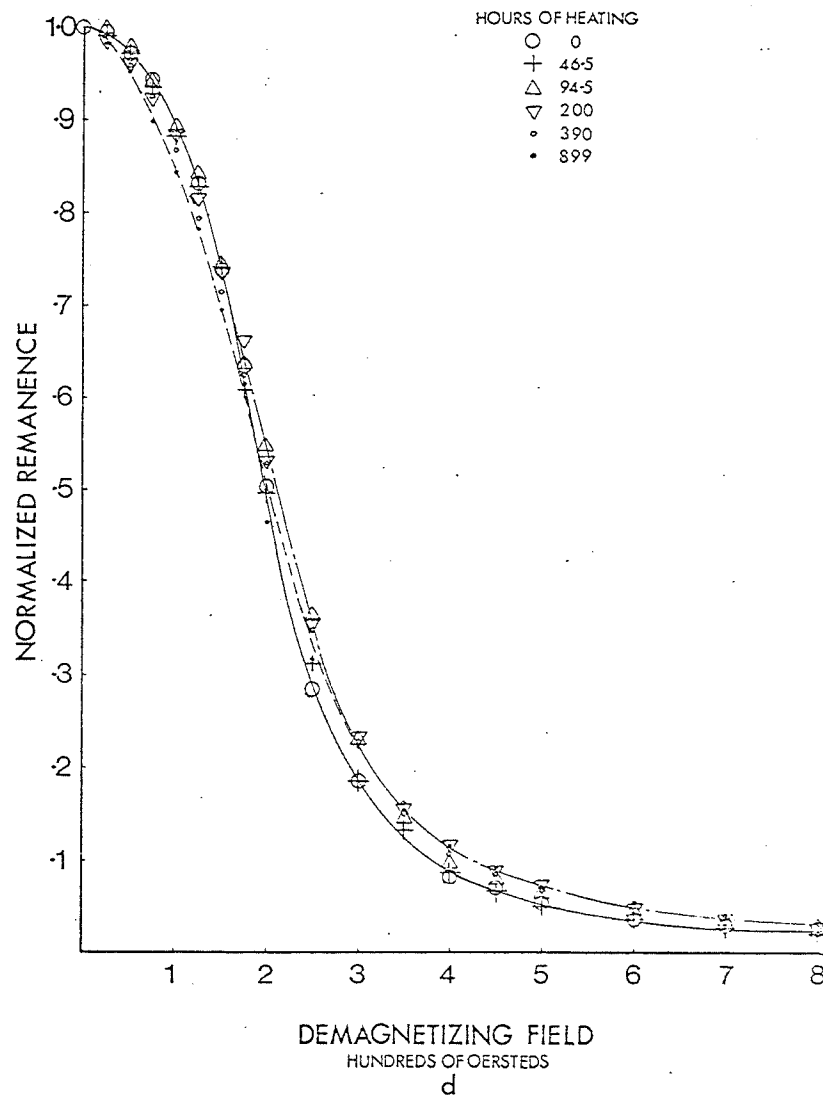
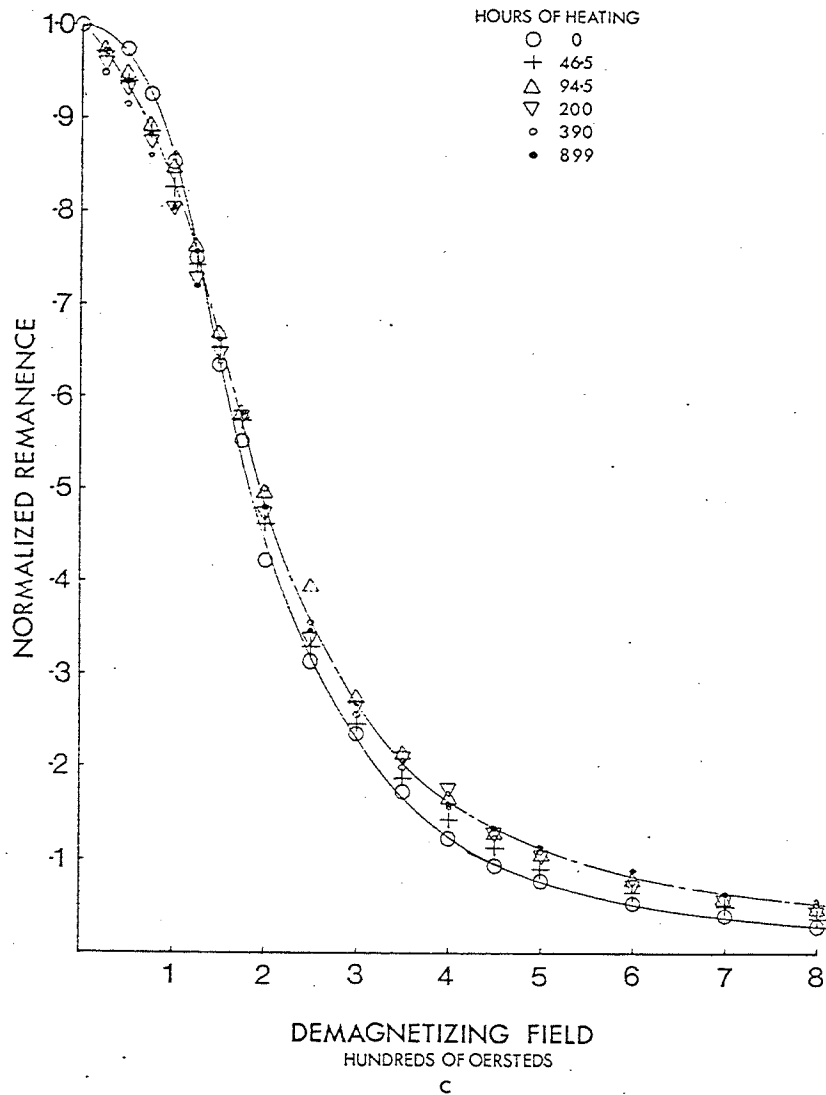


Figure 30 (continued)

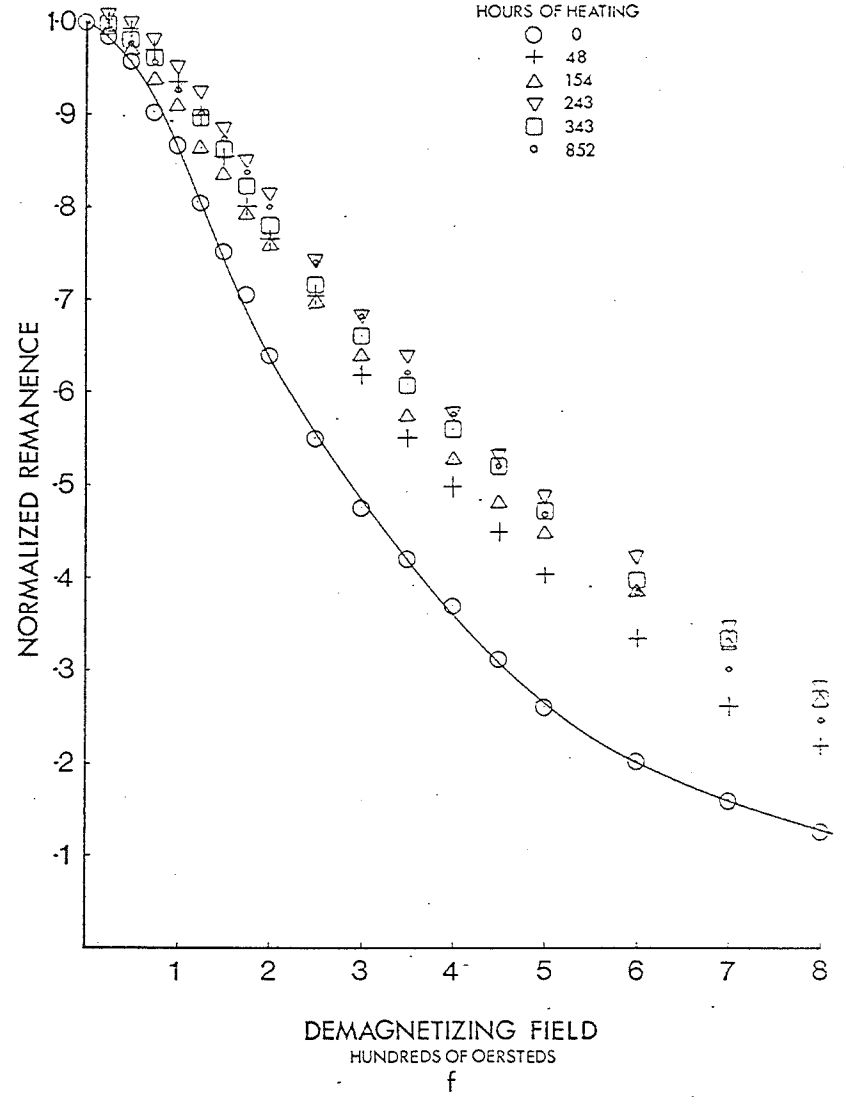
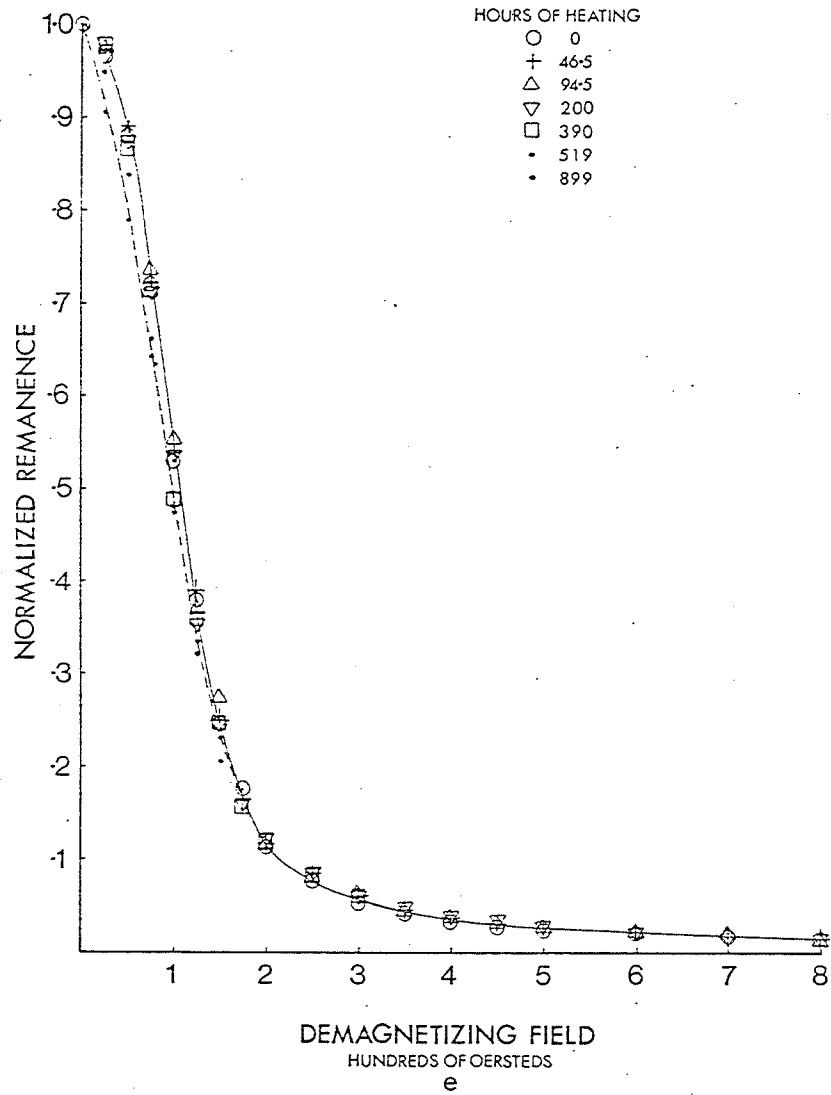


Figure 30 (continued).

TABLE 4
MDF'S OF 73Ma-1-10

Hours at 210°C	0	48	154	243	343	852
MDF (Oe.)	288	400	430	490	470	475

The increase in coercivity of remanence can be attributed to the growth of ferrimagnetic grains from paramagnetic size into the single-domain region. For these very small grains, measured in hundreds of Angstroms, coercivity increases with increasing grain size (Johnson and Lowrie 1974). The stabilization of MDF coincides with the appearance of measureable Curie points in this material.

Considering the Mid-Atlantic Ridge samples, a surprising aspect of these demagnetization curves is the relative constancy despite a change in Curie temperature from less than 200°C to about 400°C with resultant changes in composition of the titanomagnetite and its splitting into two phases. This behaviour is quite unlike that seen in the radial progression in the pillows. At first glance the coercivity of remanence is seemingly insensitive to either the composition or grain size - the latter must change with any phase splitting.

The changes in A.F. demagnetization characteristics are most noticeable for 56-3-233 and least apparent for 197-8-42. Now 197-8-42, as shown in Section II, initially has the least altered titanomagnetite so that it would be expected to alter most easily. On the other hand,

sample 56-3-233 is initially the most altered, but the A.F. demagnetization characteristics suggest that it undergoes the greatest changes.

An explanation for the seemingly anomalous behaviour just outlined is provided by comparing Figures 25 and 29. They show that while J_s increases J_{TRM} decreases. The reason for this is that the amount of high Curie point phase is increasing. Since the remanence measured is a PTRM acquired on cooling from 210°C, then a γ -phase with a Curie point over 300°C will only acquire a few percent of the remanence it would acquire on cooling through its Curie point. On the other hand the original γ -phase with a Curie point around 200°C will acquire its total possible TRM.

Hence the TRM measured is characteristic of the remaining γ -phase of initial composition. With increased heating time the amount of this material decreases so the intensity of TRM decreases. The intensity of TRM is a measure of the amount of unaltered, original γ -phase. Since the TRM is due to the same magnetic material, only in reduced quantities, that shape of the demagnetization curve will not be markedly changed.

An important point for palaeomagnetic studies is that in altered rocks the TRM observed is not necessarily caused by the titanomagnetite most prominent in J_s -T measurements.

4. Second Experiment at 150°C

4.1 Introduction

The first experiment at 150°C with sample 56-3-35 had produced encouraging results. It was thought that the initial results tended to mirror the changes which had been observed in radial sampling of pillows from the Mid-Atlantic Ridge. In addition, further alteration at 150°C had produced an intriguing self-reversal in conditions close to natural conditions. In an attempt to duplicate these results, further experiments had been carried out at 210°C. The higher temperature was used in an effort to reduce the time constants for the alteration effects.

Results at 210°C had not been as expected. While of value in modelling the sort of alteration and phase splitting to be expected in low temperature hydrothermal alteration, they did not represent the alteration effects seen in pillow basalts subject only to halmyrolysis. Nor had there been any indication of the self-reversal as seen in sample 56-3-35.

Despite the longer time constants involved for alteration it was decided to try again at 150°C, this time using sea-water from the North West Arm, the composition of which is given in the appendix.

4.2 Samples

The group of samples was very similar to that used in the 210°C experiment. There were three samples from pillow 56-3: -236, -141, -242 all of which are close to 56-3-35

in composition. There were two samples from pillow 197-8: -30 and -45. The final sample was 73Ma-1-07 from the Hawaiian lava.

4.3 Saturation Magnetization and Curie Temperature

Despite the heating being more than three times as long compared to the experiment at 210°C, the degree of alteration was considerably less. As Figure 31 shows Curie temperatures at the end of the experiment were in general around 320°C, about 100°C less than at the end of the 210°C experiment. While some samples showed an increase in J_s , the increase was less than in the 210°C experiment. All samples from the Mid-Atlantic Ridge pillows follow the same general pattern. The J_s -T curves were reversible even after the first few hundred hours heating. With further heating time at 150°C a higher 'z' cation-deficient titanomagnetite was made with a higher Curie point. This oxidized titanomagnetite was sufficiently unstable that it was decomposed at the high temperature reached in the J_s -T measuring process. Thus the J_s -T cooling curve shows two Curie temperatures. After about a thousand hours there is the appearance of a small amount of titanomagnetite with a Curie temperature near that of magnetite. Apart from this small amount (less than 5% of J_s) of 'magnetite' the J_s -T curves are typical of a high 'z' cation-deficient titanomagnetite.

So far the change in Curie points from the initial value to about 300°C has been treated as the progressive

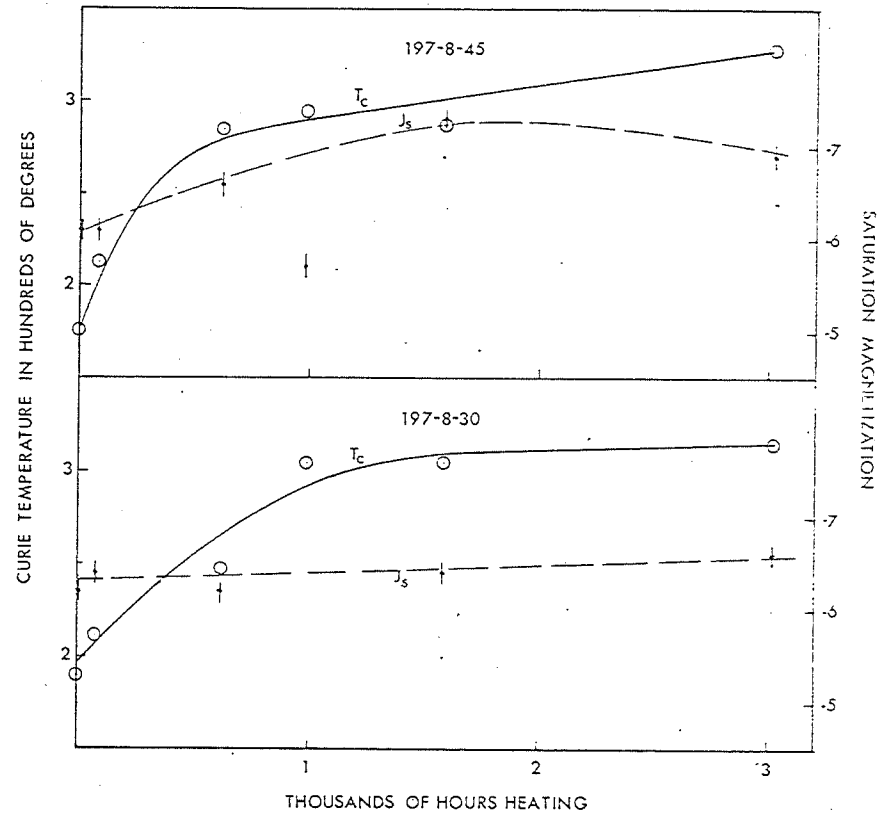
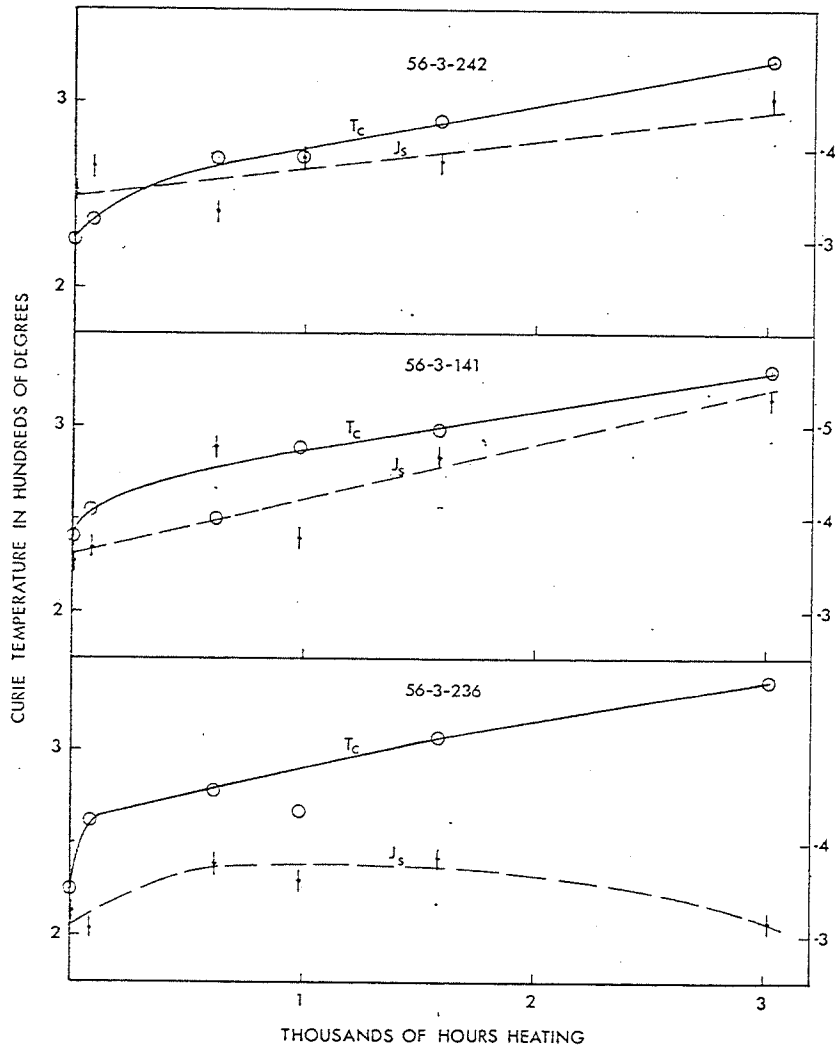


Figure 31. Change in J_s and Curie temperature for five of the samples heated at 150°C as a function of total heating time. Saturation Magnetization is in emu/g.

alteration of all the γ -phase to a γ -phase of progressively higher 'z' until a phase with a Curie point around 300°C is reached which may then unmix. In the case of some of the samples in the 210°C experiment, as illustrated in Figure 27, it was possible to follow the alteration process as one of the formation of an increasing amount of the higher Curie point phase accompanied by a decrease in the amount of the phase of original composition. This behaviour may be more prevalent than is generally realized from J_s -T curves.

Under experimental conditions some of the original γ -phase is converted to a composition on the titanomaghemite line. With longer heating time the amount of original composition converted increases. As the amount of high Curie point phase increases, the J_s -T curve, which is the summation of the J_s -T curves of the two phases, will closely resemble the J_s -T curve of an homogeneous γ -phase of increasing Curie temperature. This behaviour is illustrated in Figure 32.

The lowest Curie point curve is a typical curve for a 175°C Curie point. In successive curves the amount of 175°C Curie point phase is decreased by 20% per curve and the amount of 325°C Curie point phase increased correspondingly. The final curve is for 100% 325°C Curie point material. Only the centremost curves, (if obtained experimentally), are likely to be recognized as containing two Curie points. In actual experimental curves the two Curie points may be less clear because of noise, thermal hysteresis etc.

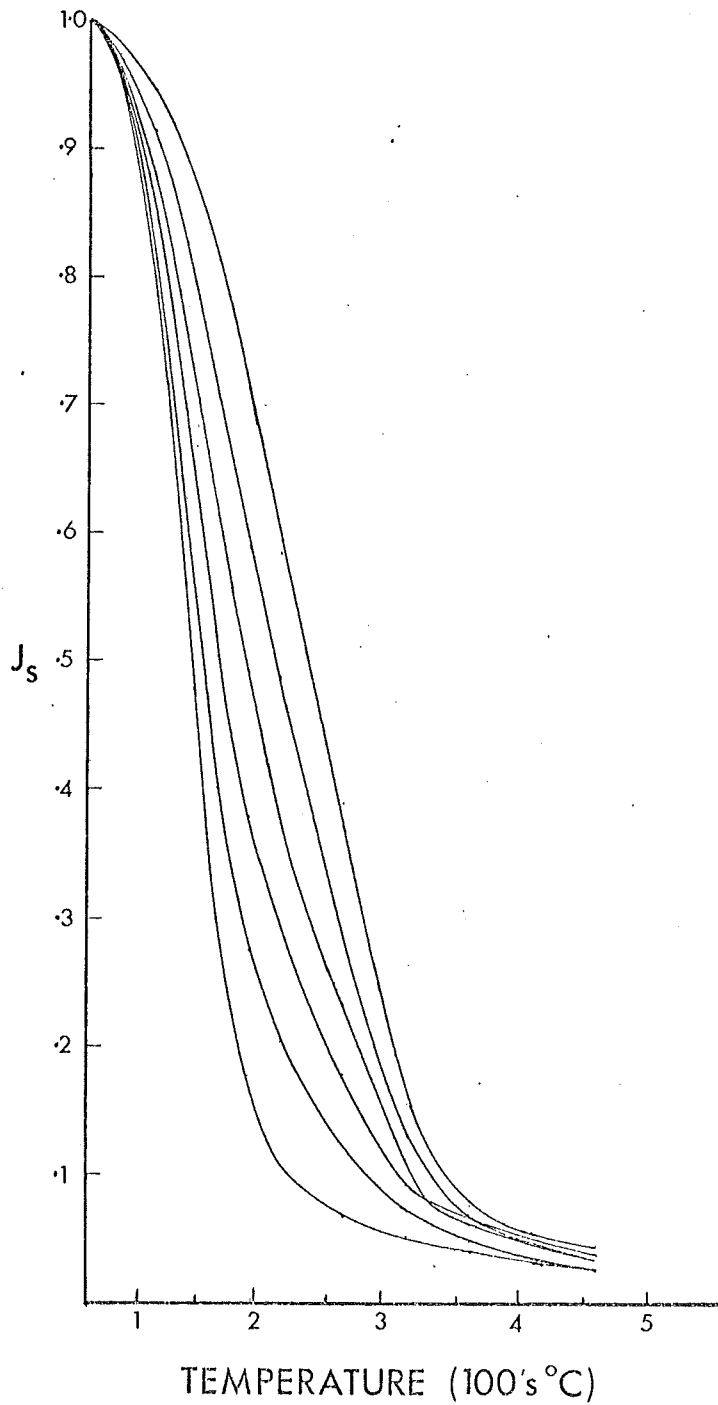


Figure 32. Synthesis of J_s -T curves from varying amounts of phases having Curie points of 175°C and 325°C. The leftmost curve is 100% 175°C phase, the next one 80% 175°C phase +20% 325°C phase and so on to 100% 325°C phase.

There is a suggestion of the sort of behaviour shown in Figure 32 in some of the J_s -T curves for samples 197-8-30 and -45.

Pillow 56-3: The two inner samples -141 and -242 may be considered together. The Curie temperature increases from about 230°C to 325±5°C, while J_s increases by about a quarter in the case of -242 from 0.35 emu/g to 0.44 emu/g and by about a third in the case of -141 from 0.36 emu/g to 0.54 emu/g. For sample -236 Curie temperature increases from 225° to 337°C but J_s shows no systematic increase, its final value being virtually the same as its initial one. The J_s -T curves shown in Figure 33 are typical of all three of these samples, that is typical of a high 'z' cation-deficient titanomagnetite.

Pillow 197-8: Samples -30 and -45 also show an increase in Curie temperature from around 200°C to about 325°C with no systematic increase in J_s . The later J_s -T curves for these samples also show a small amount of magnetite responsible for no more than 5% of the total J_s .

56-3-236

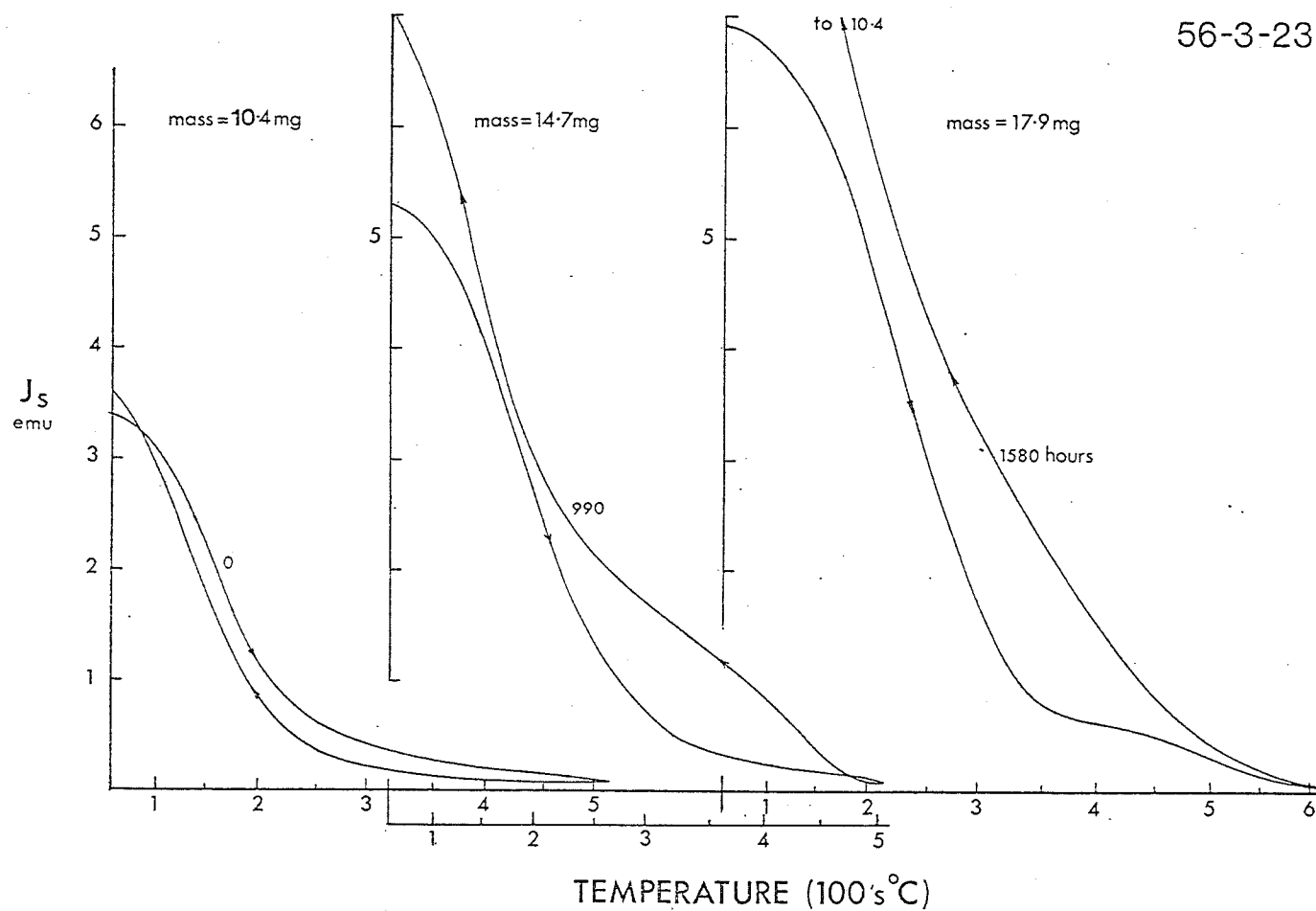


Figure 33. Evolution of J_S -T curves for sample 56-3-236 before heating and after 990 hours and 1580 hours at $150^\circ C$.

Pillow 73Ma-1: Sample 73Ma-1-7 shows no distinct Curie point throughout the entire experiment. As for sample 73Ma-1-10 there must be grains having a range of Curie points in order to produce any PTRM's. However even 3000 hours at 150°C is insufficient to produce enough concentration of any one composition to give a defineable Curie point in the J_s -T curves.

4.4 Concentrations of Ferrites

If one uses the same procedure as was followed in the first 150°C experiment it is possible to monitor the changes in concentration of the ferrites in the samples. It will be assumed that initial oxidation is an homogeneous oxidation along the $x = 0.6$ line. With this assumption made it is possible to obtain 'z' and hence I_s from the Curie point. By dividing I_s for the ferrite into the J_s measured for the rock the concentration of ferrite will be obtained. The results of following this procedure after various heating times are given in Table 5.

TABLE 5

VARIATION OF CONCENTRATION WITH HEATING TIME

Sample	56-3-236	-141	-242	197-8-30	-45
Time					
0	1.42	1.48	1.55	2.3	2.2
82	1.23	1.49	1.59	2.8	2.5
622	1.51	1.70(1.76)	1.32	2.5	2.5
990	1.44	1.25(1.35)	1.41(1.46)	-	2.4
1587	1.40(1.47)	1.72(1.79)	1.42(1.47)	2.4(2.5)	2.9
3023	1.56(1.59)	2.31(2.39)	1.76(1.82)	2.7(2.8)	3.1(3.2)

Note: Concentrations given in percent ferrite by weight.

Note: These concentrations were obtained after subtracting the small contribution, if any, due to 'magnetite'. Concentrations in brackets include the 'magnetite'.

Up to 1587 hours there is no clear trend in the concentration, just the usual between-chip scatter. Up to this point there is homogeneous oxidation with the development of a γ -phase with a Curie point about 300°C.

A γ -phase with a Curie point about 300°C and $x = 0.6$ will have a composition on the ilmenite-hematite join, i.e. it is a titanomaghemite. With further heating time Curie point increases and concentration, assuming continuing homogeneous oxidation, also increases in samples 56-3-141, -242 and 197-8-45. For these three samples the assumption of continuing homogeneous oxidation must be wrong. If unmixing

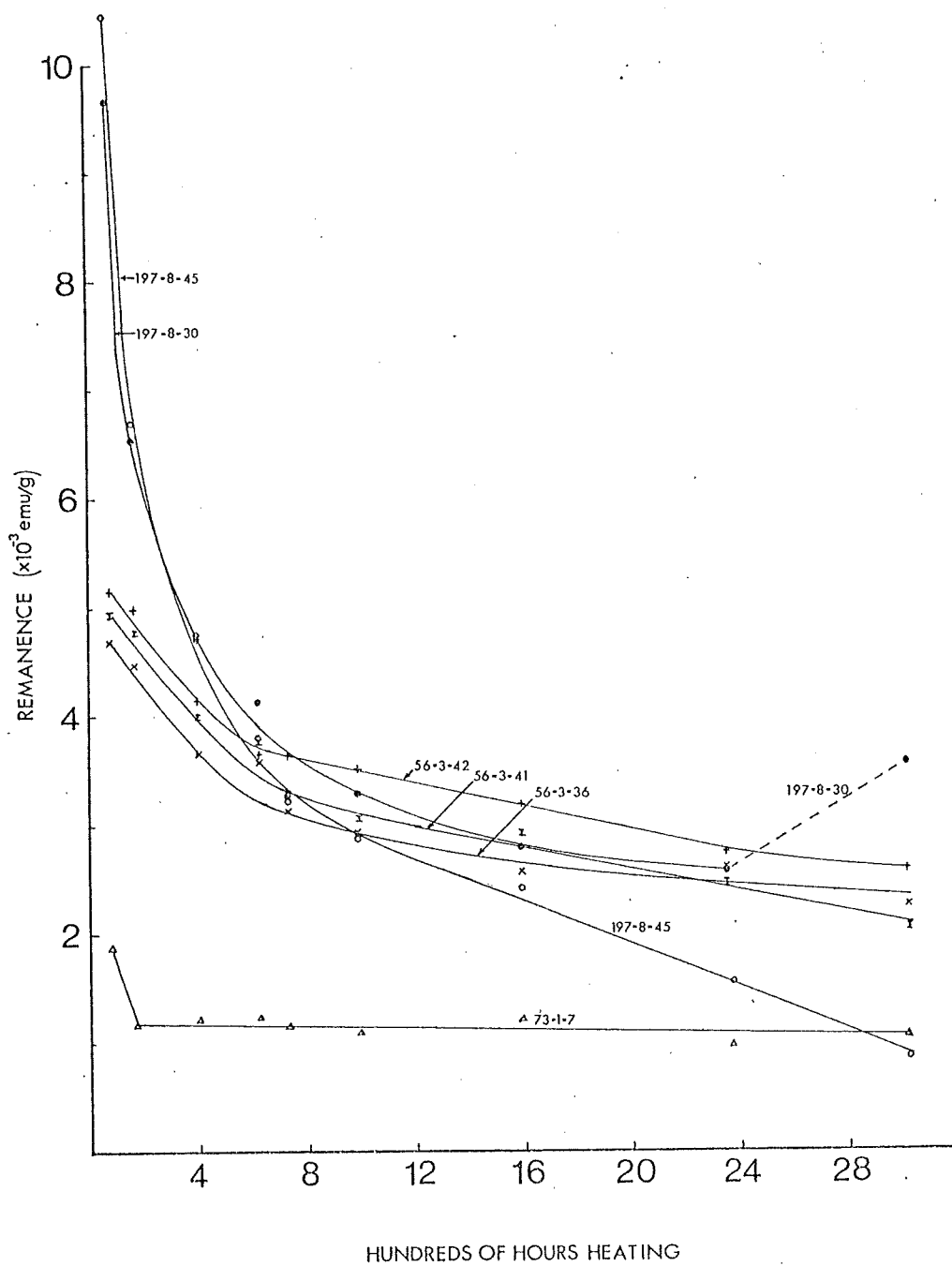


Figure 34. Variation of PTRM acquired by various slices in cooling from 150°C in a 1.00 G field as a function of total heating time.

along the ilmenite-hematite join is considered then an increase in Curie point will be accompanied by an increase in I_s which would have the result of allowing the concentration to remain constant.

Hence the mechanism of alteration is one of homogeneous oxidation from the original composition until a titanomaghemite is made at which point further heating produces unmixing.

4.5 A.F. Demagnetization of Successive TRM's

The intensity of the remanence acquired in cooling from 150°C in a 1.00 G field is shown in Figure 34. As in the case of the 210°C heating the TRM acquired decreases with heating time. Once again the decrease is most rapid in the first few hundred hours. The drop is to about half the initial value for samples from pillow 197-8 in the first four hundred hours. Samples for pillow 56-3 are less affected dropping only about a quarter in the same period. For sample 73Ma-1-07, the TRM remains constant after a drop in the first two hundred hours. Overall the pattern of decrease in Figure 34 is very similar to that in Figure 29. Comparisons are complicated by reverse components of varying size for 197-8-45 and 56-3-141 and -242 after 2400 hours.

The TRM's shown in Figure 34 were A.F. demagnetized. The normalized demagnetizations are given in Figure 35a-f. The demagnetizations will be considered in two groups: those which show no reversed component: 56-3-236 and 197-8-30 and those which show some reversed component:

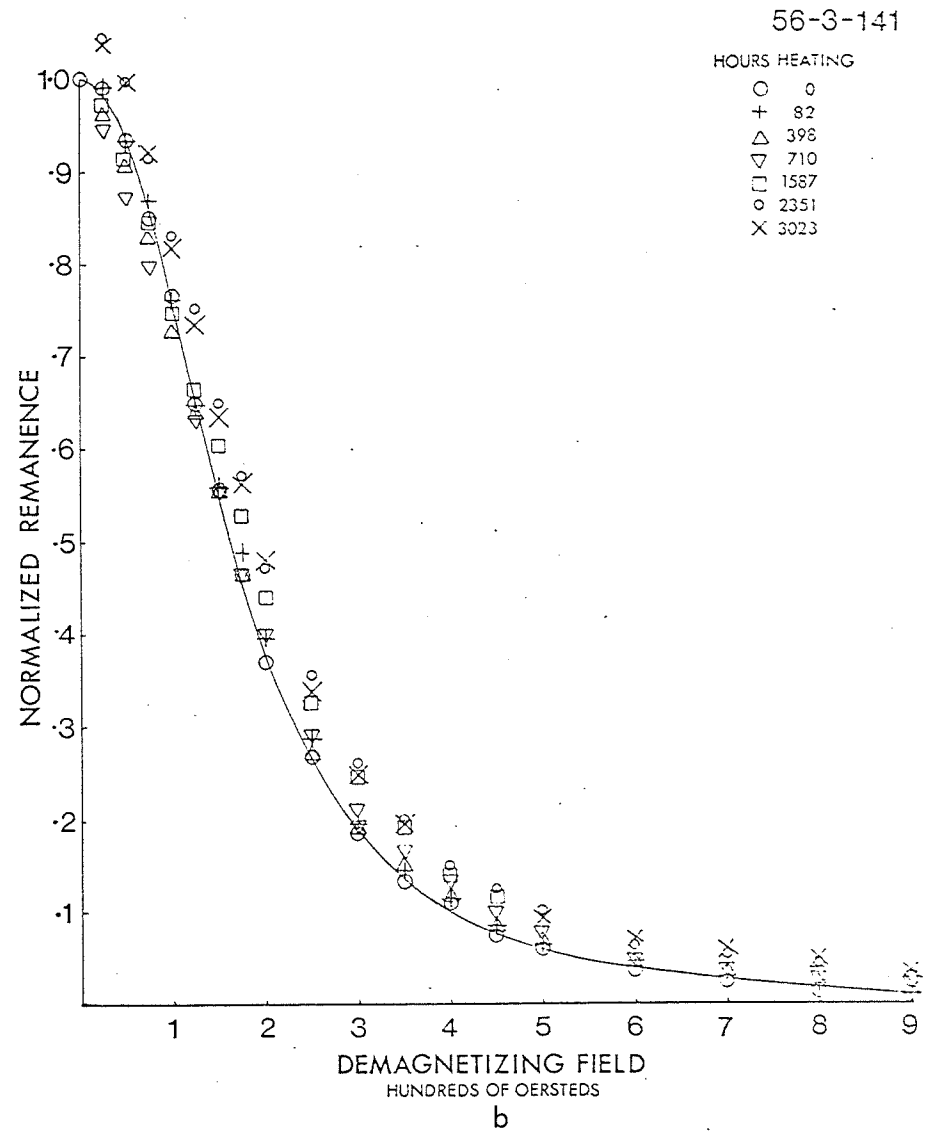
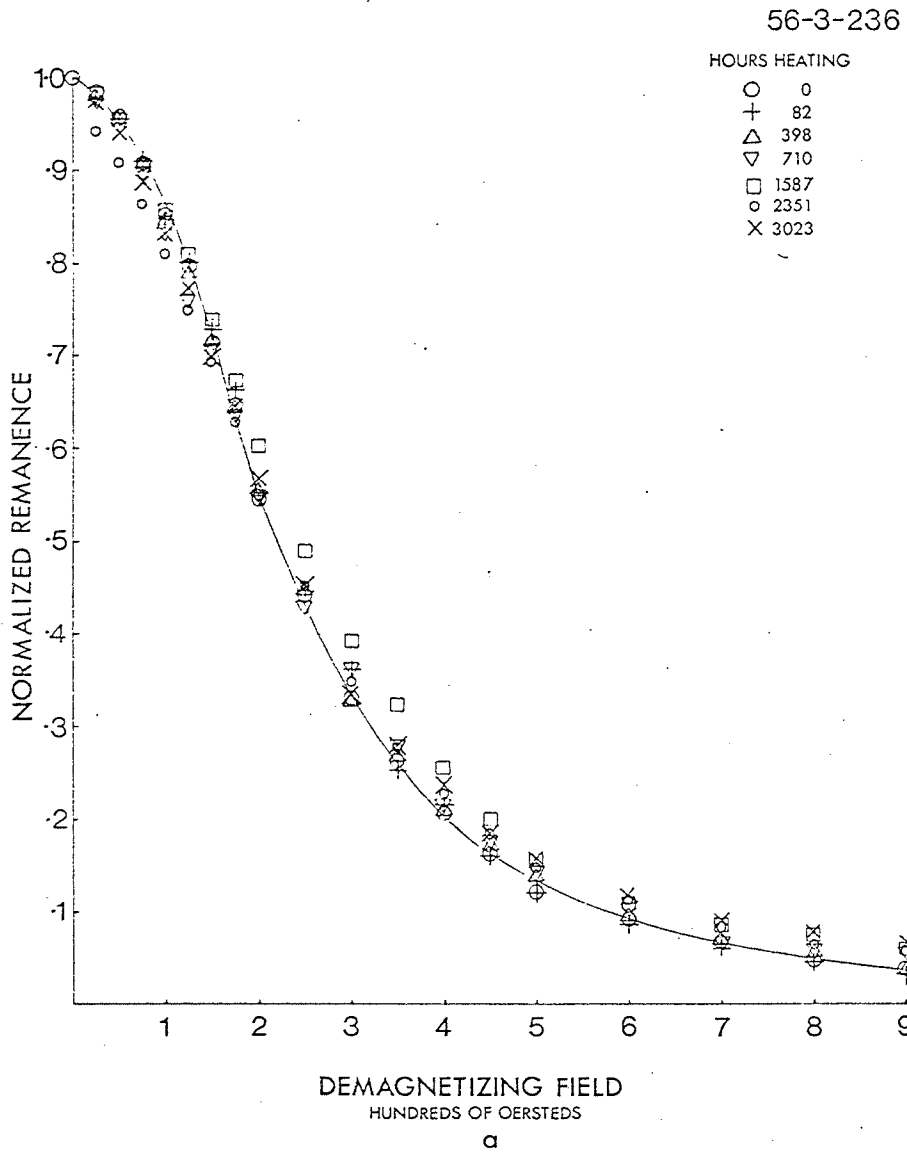
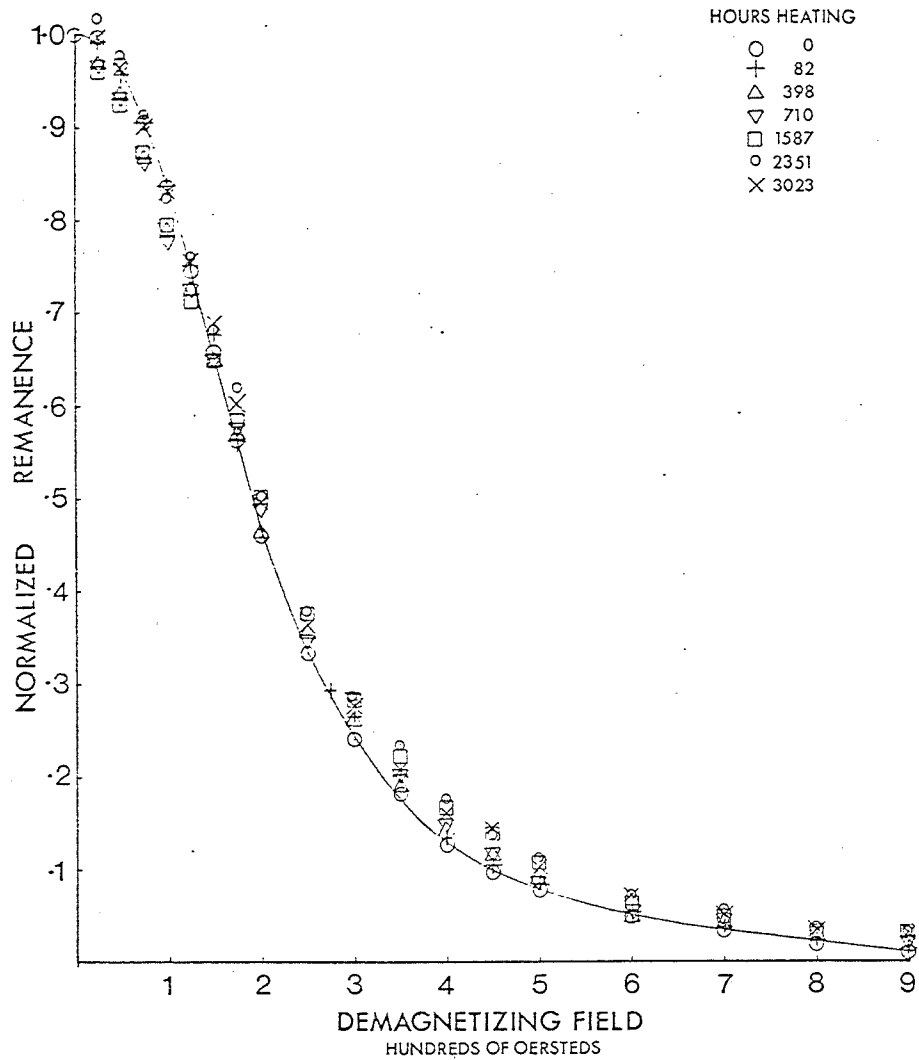


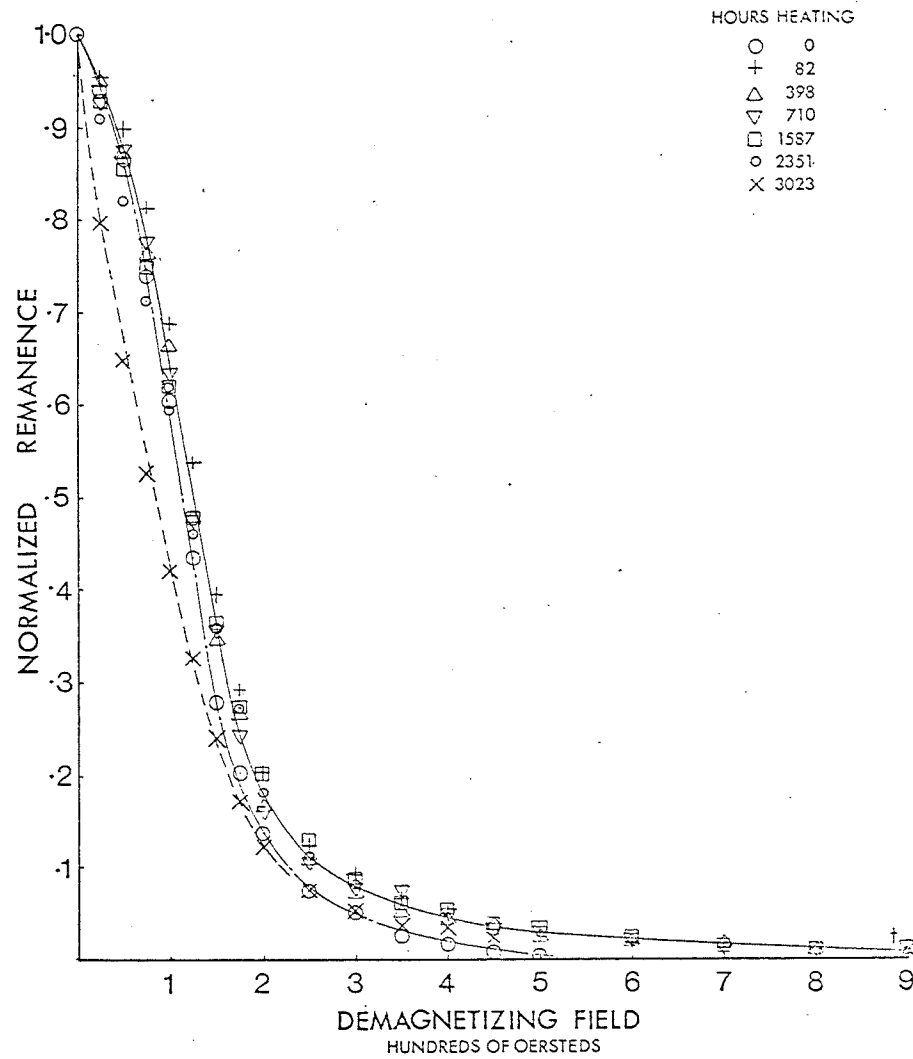
Figure 35. Normalized A.F. demagnetizations of the samples heated at 150°C for various times.
 a) 56-3-236, b) 56-3-141, c) 56-3-242, d) 197-8-30, e) 197-8-45, f) 73Ma-1-7.

56-3-242



c

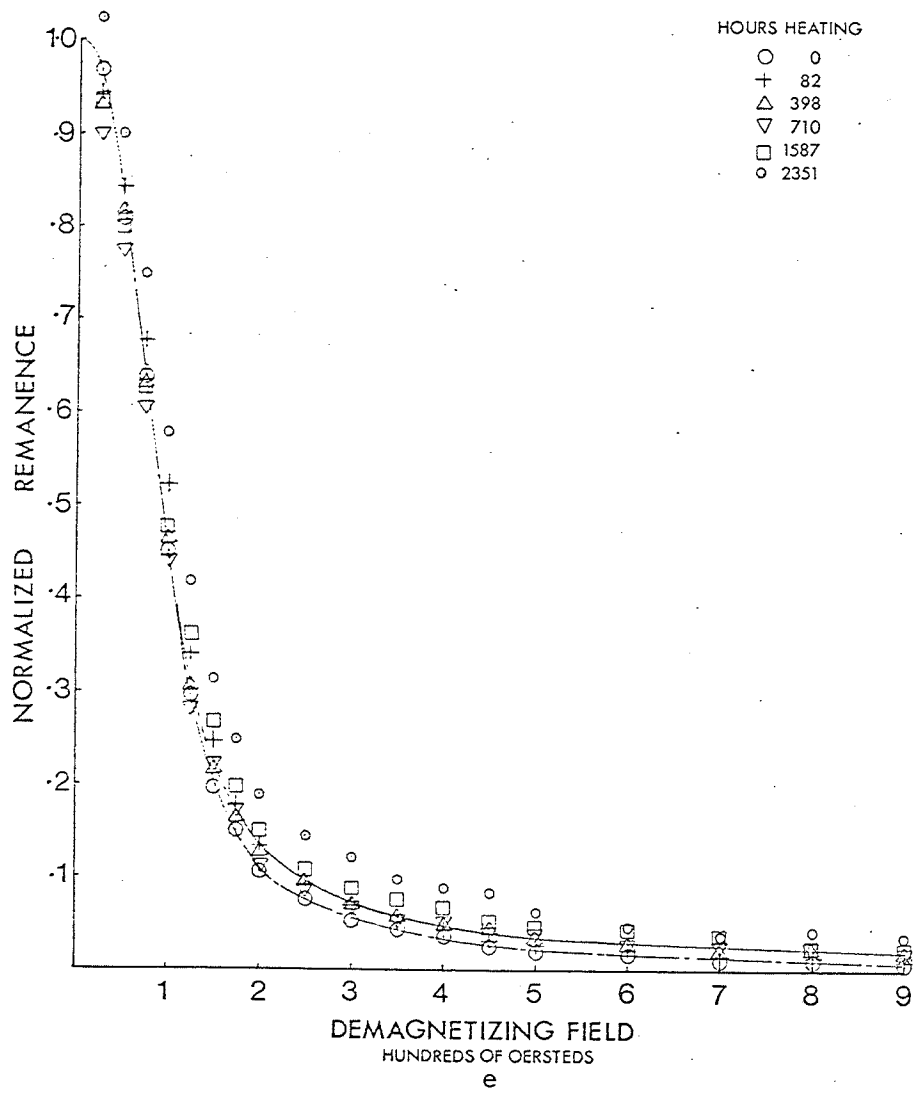
197-8-30



d

Figure 35 (continued).

197-8-45



73Ma-1-7

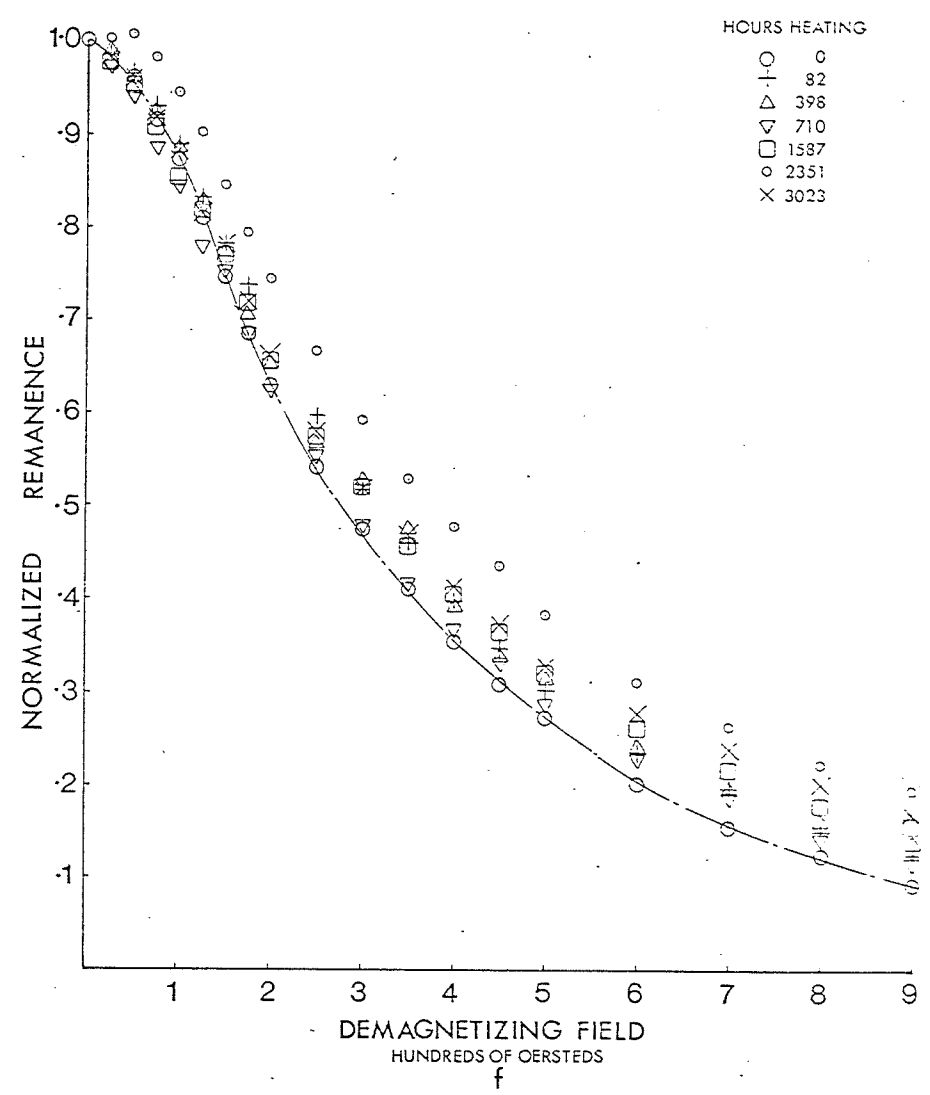


Figure 35 (continued).

56-3-141, 56-3-242, 73Ma-1-07 and 197-8-45.

No reversed component:

Sample 56-3-236. There is little systematic change in the shape of the A.F. demagnetization curve. After 1587 hours the sample is notably harder, MDF up 20 Oe. to 240 Oe., but this increase does not persist through further heating.

Sample 197-8-30. All demagnetizations after the initial one are harder but with some scatter until 3023 hours. At 3023 hours the TRM is much softer, MDF decreases from 120 Oe. to 85 Oe., while intensity increases from 2.6×10^{-3} emu/g to 3.6×10^{-3} emu/g.

Some reversed component:

Pillow 56-3: Samples -141 and -242. Both these samples show a slight increase in normalized TRM above 200 Oe. demagnetizing field. At 2351 hours both have a small reversed component which persists to 3023 hours in -141 but disappears in -242.

Sample 73Ma-1-07. This sample shows much the same behaviour as 73Ma-1-10, that is a steady hardening of TRM with heating. The MDF reaches a peak of 375 Oe. at 2351 hours heating, a curve which shows a very slight reversed component. With the next heating the curve is virtually identical to that after 1587 hours with an MDF of 320 Oe. All of these MDF's are much lower than those encountered in 73Ma-1-10 which was heated at 210°C.

Sample 197-8-45. For the first 1587 hours there is not much difference between this sample and 197-8-30. At 2351 hours a small reversed component is acquired which gives an impression of greater hardness. At 3023 hours this sample is completely reversed and normalized plots like Figure 35e lose their usefulness. The TRM acquired parallel to the magnetizing field by this sample is plotted in Figure 36. This set of curves shows a clear progression from the original state to a self-reversed condition. The last step recorded here is probably the sort of curve which would have been seen for sample 56-3-35 at some time between 1070 hours and 3110 hours in Figure 23 had a measurement been made then. Presumably further heatings would show the development of a remanence which preserves its self-reversal to higher demagnetizing fields. Due to time and equipment limitations it is not possible to follow this alteration any further at the moment.

5. Summary

5.1 Alteration Processes

Up to this point the three heating experiments have been considered separately. Considering the results of the three experiments together it can be seen that one scheme of oxidation and unmixing can explain them all. The first phase of this scheme is the homogeneous oxidation of the original γ -phase to a γ -phase with a composition on the ilmenite-hematite join, i.e. a titanomaghemite, and with the

197-8-45

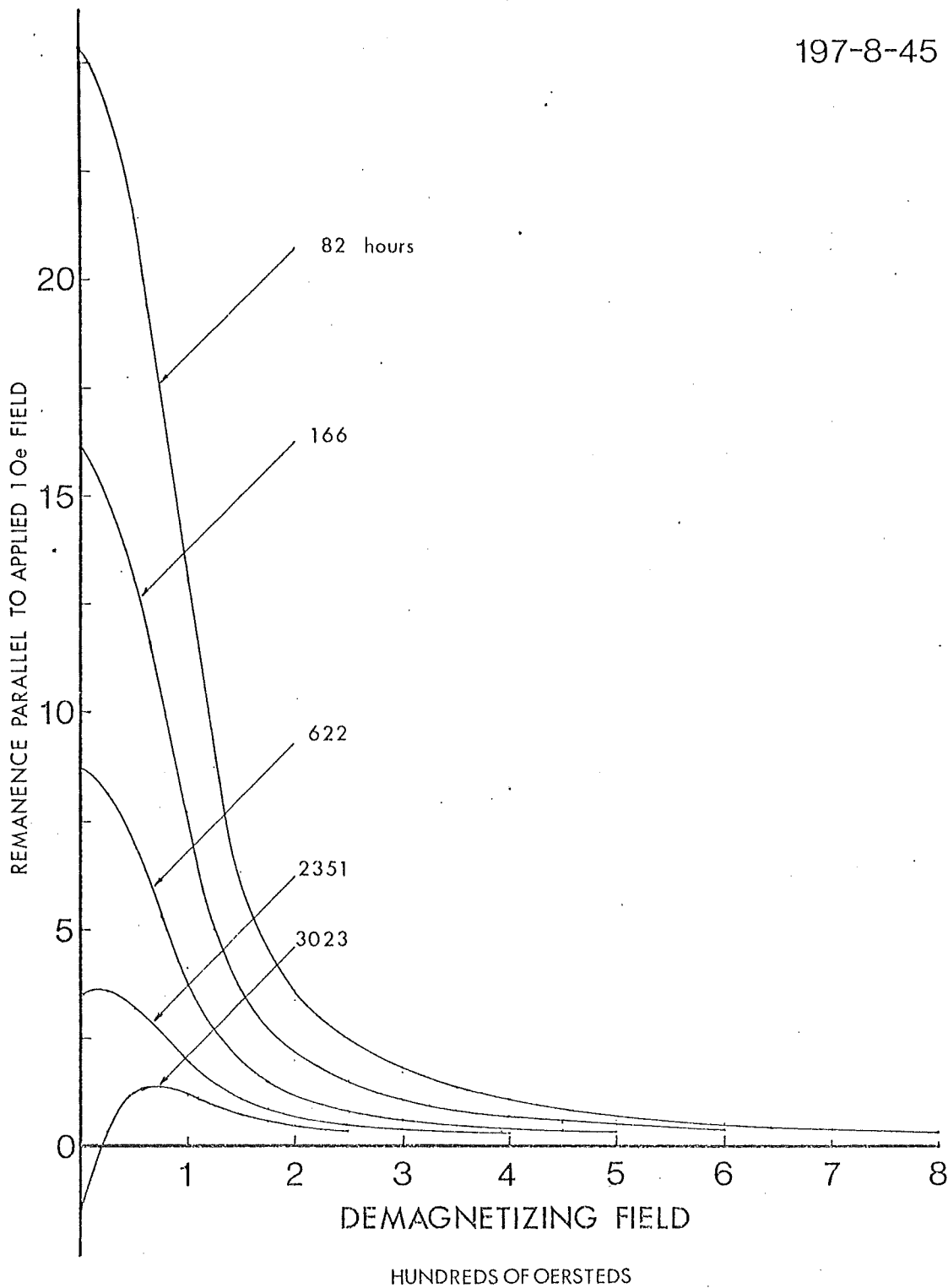


Figure 36. A.F. demagnetization of successive TRM's for 197-8-45.

same 'x' as the original material. The second phase of the alteration is the unmixing of the titanomaghemite into Fe-rich and Ti-rich components.

The first phase of the alteration is supported by evidence from the increase in Curie temperature accompanied by relatively constant J_s . In addition, if one considers the different times required for maghemitization at the two different temperatures, it is possible to work out the activation energy for the process.

Following Ozima and Ozima (1972) the reaction time constant of the process can be described by the expression:

$$\lambda = \lambda_0 \exp - \frac{E_s}{kT}$$

in which λ_0 , E_s , k and T denote a constant, the activation energy, Boltzman's constant and the temperature respectively. If one considers the attainment of a Curie temperature of 300°C as the completion of maghemitization then from Figures 25 and 31 the average times required at 210°C and 150°C are 45 hours and 1560 hours respectively. Putting these values into the equation gives:

$$0.022 = \lambda_0 \exp(- \frac{E_s}{0.0415})$$

$$\text{and } 0.00064 = \lambda_0 \exp(- \frac{E_s}{0.0364})$$

from which $E_s = 1.04 \text{ eV}$ and $\lambda_0 = e^{21.3}$. This value for the activation energy at $x = 0.6$ is in good agreement with Readman and O'Reilly's (1970) values of 1.5, 1.4 and 1.2 eV

for $x = 0, 0.2$ and 0.4 respectively. This agreement is further evidence that the alteration to a phase with a Curie point of 300°C is a process of maghemitization.

After the bulk of the original γ -phase is altered to titanomaghemite it begins to unmix. The presence of a γ -phase with a Curie point greater than 300°C is indicated and because of the higher J_s measured, then the titanomaghemite must be unmixing to produce an Fe-rich phase with higher I_s . The unmixing is also energetically favourable requiring only 0.033 eV (Ozima and Ozima 1972) instead of the 1.0 eV for continuing to produce a cation-deficient phase.

Plots of the PTRM's acquired after various heating runs, Figures 29 and 34, confirm that the mechanism is a two-stage process with a much slower change in PTRM's after the maghemitization is complete. Initially the intensity of the PTRM decreases while the shape of the A.F. demagnetization curve remains relatively constant because the PTRM is primarily due to the decreasing amount of the original γ -phase. The newly formed γ -phase with Curie point around 300°C contributes little to the PTRM because most of its grains will have blocking temperatures higher than the experimental heating temperature. In all of the samples in the 210°C experiment the remaining original γ -phase continues to dominate the PTRM. In some samples at 150°C , namely 56-3-35 and 197-8-45 there is a complete reversal in the direction of the PTRM while 56-3-141 and -242 show small partial reversals.

5.2 Self-reversal Mechanisms

Many possible self-reversal mechanisms have been proposed (Néel 1955) and discussed in the literature (Uyeda 1958, Nagata 1961, Stacey 1963) as well as being used by several workers dealing with self-reversed rocks. Possible self-reversal mechanisms fall into two broad categories:

1) A one-constituent model in which the direction of J_s reverses spontaneously due to the thermal characteristics of the sub-lattices as in Néel N-type ferrimagnetics.

2) A two-constituent model involving either:

a) magnetostatic interaction between a domain of one constituent and a domain of the other

b) exchange interaction between the lattices of each constituent across the boundary between the domains.

One-constituent model

The self-reversing properties, if any, of a titanomagnetite depend on the cation distribution. A model was proposed by Verhoogen (1962) and later modified by O'Reilly and Banerjee (1966) which gives the self-reversal regions shown in Figure 37. It can be seen that the self-reversal regions are restricted to values of x greater than 0.6. The x -value would not need to be much greater than 0.6 for self-reversal to be possible at high z -values. Likewise a slight change in the model might make self-reversal possible at $x = 0.6$. However it has been shown in the experiments described in this work that at 150°C the γ -phase unmixes at a z -value corresponding to the ilmenite-hematite join so

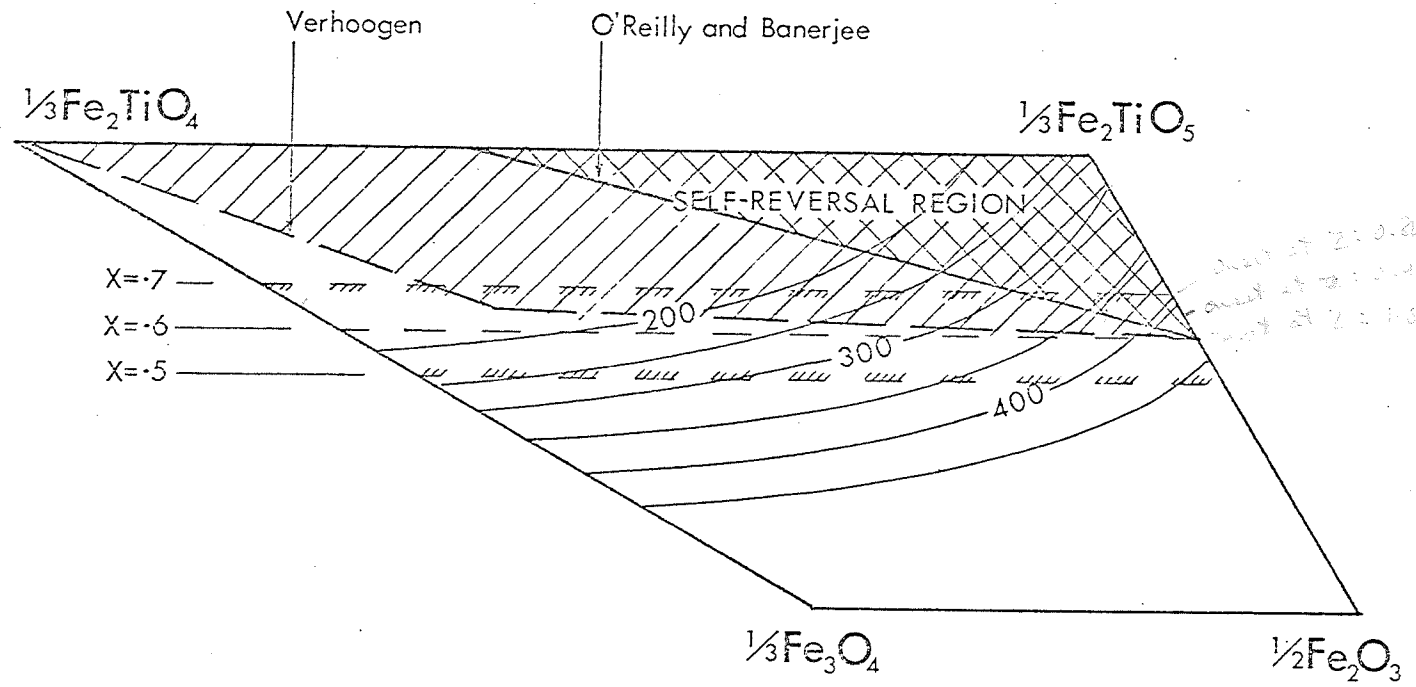


Figure 37. Section of FeO-TiO₂-Fe₂O₃ ternary diagram showing self-reversal regions. That area suggested by Verhoogen is shown hatched, that by O'Reilly and Banerjee cross hatched.

the γ -phase is unlikely to have a z high enough to enter the self-reversal region.

While not a cause of self-reversal in the laboratory experiments at 150°C, a one-component mechanism cannot be ruled out in nature where, as is seen in pillow 47A-1, and as reported by Grömmé (1975), high z -values may be obtained.

Two-constituent model

In the case of the present experiments self-reversal only occurred during a transitory period during which there were two constituents present as shown by the two Curie temperatures in the samples. Hence a two-constituent model is likely to provide the answer.

a) Magnetostatic Interaction

The small size of the grains in these samples limits the number of mechanisms of interaction which need be considered. For example, interaction between lamellae of alternate constituents such as considered by Uyeda (1958) can be ignored because the grains are simply not large enough to contain such interleaved, interacting domains. Likewise Néel's (1951) model involving interactions between elongate single domain grains of two constituents can be ignored because it requires the magnetic constituent to make up at least 27% of the whole rock while in these samples there is only a few percent of titanomagnetite.

Néel (1955) considered, in addition to reversal due to interaction between two previously existing constituents, the possibility of a negative TRM being developed while an

original mineral splits into two phases. Consider a spherical single domain grain of a constituent A with spontaneous magnetization J_s and suppose that exsolution occurs precipitating a second magnetic phase B, accompanied of course by a change of composition of A. The first crystallites of the new phase B grow in the demagnetizing field of A, given by $\frac{4}{3}\pi J_s$. If the magnetocrystalline field of B is less than this, which it usually is, and if the exchange coupling between A and B is negligible, the spontaneous magnetization of the crystallites of B will necessarily be oriented antiparallel to that of A. Once the process has started exchange interaction within B ensures that it will continue automatically during the formation of phase B from phase A.

In an assemblage of grains of A, having a TRM in a particular direction, this process necessarily implies that as the B-phase is formed TRM will decrease in intensity, and when the concentration of B is high enough, will change sign.

This process of development of reversed TRM can accompany any exsolution into two phases. Graham (1953) suggested that such a mechanism might be responsible for self-reversal during the oxidation of magnetite to maghemite.

Stacey (1963) considers a grain sub-divided into two regions, each a single domain composed of minerals A and B. Suppose that in a simple case A and B are adjacent cubes of side 'd' and that B becomes magnetized first. (The following arguments do not require equal cubes, a large range of

adjacent shapes will do.) The region of B will acquire a moment $M = d^3 I_{SB}$. By approximating the volume of B to a dipole, its field at the centre of A is $H' = -\frac{M}{d^3} = -I_{SB}$ under the arrangement shown in Figure 38a.

At this point Stacey (1963) substitutes I_{SB} for hematite of 0.5 cm/cm^3 - which must be a misprint because I_S of hematite is $0.5 \text{ emu/g} \approx 2.0 \text{ emu/cm}^3$. Substituting 2 emu/cm^3 then H' is -2.0 Oersted which can easily outweigh the Earth's field rather than just possibly outweigh it as suggested by Stacey. Furthermore there is no reason to consider only such a weakly magnetic mineral as hematite. The predominant magnetic phases seen in this experiment and in most basalts are titanomagnetites having $I_S \approx 25 \text{ emu/g} \approx 100 \text{ emu/cm}^3$ thereby giving rise to fields of the order of -100 Oersted, similar to Uyeda's (1958) estimate.

Because of the relatively weak value of H' obtained by Stacey, he considered that the effective field on A would be negative only if the line joining the centres of the domains is nearly perpendicular to the external field, as shown in Figure 38a. As shown in Figure 38b the interaction field in opposition to H_{ex} is $-\frac{M}{d^3} \sin\theta$ so if $H \approx H'$ then Stacey's condition applies. If however $H' > 10H_{ex}$ then it will have a component antiparallel to and greater than H_{ex} for all orientations except where $\sin\theta < 0.1$, i.e. the line joining the centres of the domains is within 5° of being parallel to the external field.

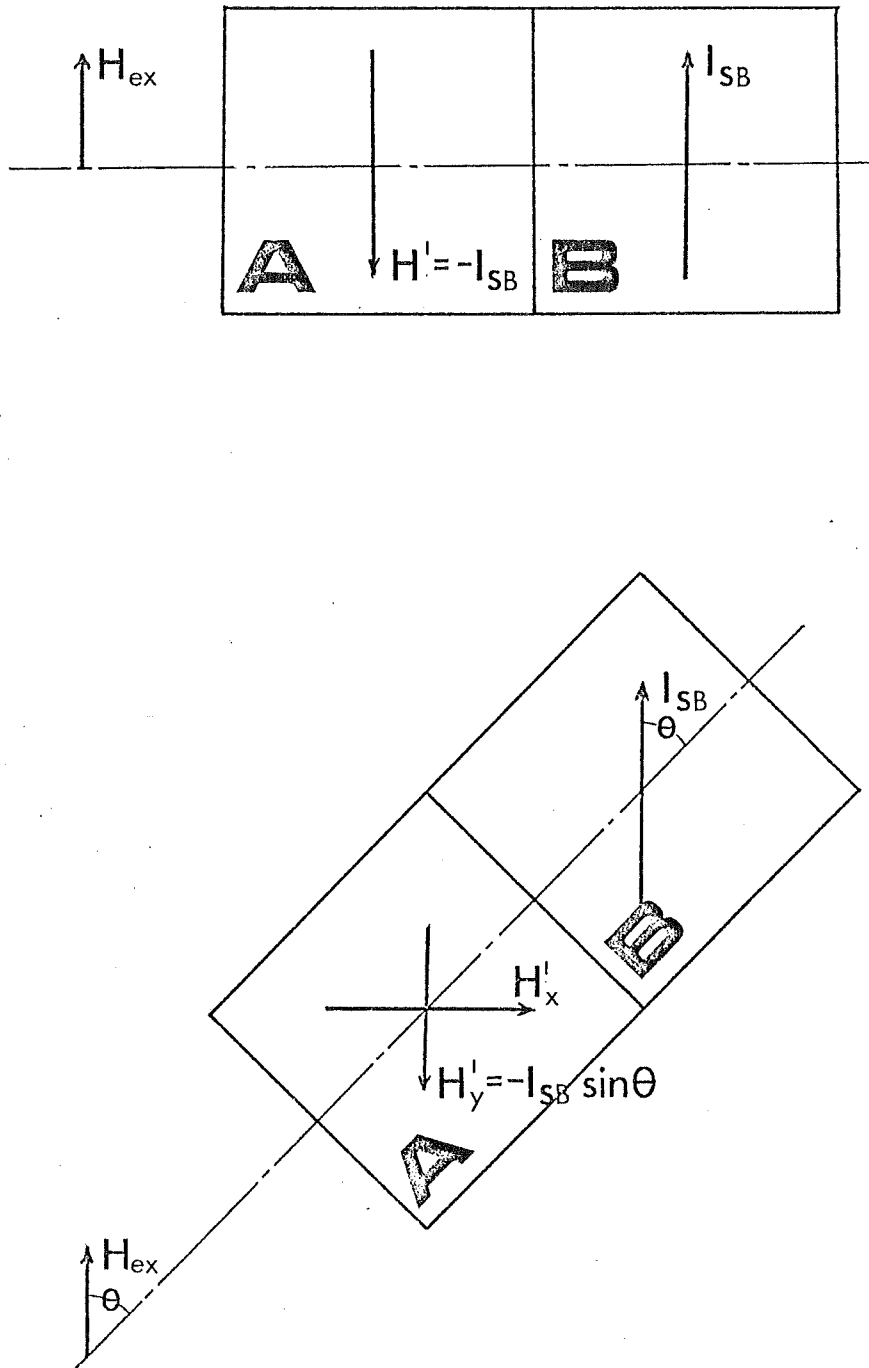


Figure 38. A model for negative magnetostatic interaction. In (a) the line joining the two domains is perpendicular to the applied field in (b) the line joining the two domains makes an angle θ with the applied field.

The model of two adjacent cubes is obviously a very simplified version of reality. More complicated situations are possible some of which may be less favourable to magnetostatic interaction and some which will be more favourable. Since the simplified model gives such a clear possibility of magnetostatic interaction then it cannot be ruled out as a likely mechanism for the self-reversals.

b) Exchange Interaction

Néel (1955) suggested the possibility of exchange interaction across the boundary between the two constituents that could give rise to the production of reverse TRM providing that the crystal lattices are in good registry. In such a case the reversing force can be as strong as the order of the molecular field, thousands of Oersteds. A synthetic ilmenohematite ($0.48\text{FeTiO}_3 \cdot 0.52\text{Fe}_2\text{O}_3$) has been shown by Nagata and Uyeda (1959) to have an effective internal reverse field greater than 16,000 Oersteds. This synthetic is very similar to the ilmenohematite from the famous Haruna dacite so that self-reversal of this rock as well as self-reversal of the α -phase with $0.45 < y < 0.63$ is attributed to this mechanism.

In the course of heating samples from submarine basalts containing γ -phase at 300°C which unmixed to two phases, Ozima and Larson (1968) were able to produce self-reversals in the presence of an external field of 2600 Oe. Since no conceivable magnetostatic interaction would produce a field of that order they concluded that the reversal could only

be due to exchange interaction. In addition they pointed out that A.F. demagnetization of reversed TRM produced by exchange interaction should give a coercivity spectrum much harder than that of normal TRM. It is this last point which makes exchange interaction an unlikely cause of self-reversal in samples 56-3-35 and 197-8-45. Examination of Figures 23 and 39 show that the MDF of the self-reversed TRM is only about half that of the normal TRM.

Thus the most probable mechanism for self-reversal in these samples is magnetostatic interaction.

5.3 Self-reversals in Mid-Atlantic Ridge Samples

The samples which have self-reversed in the present series of experiments have undergone a two stage oxidation process. First they have been homogeneously oxidized to a titanomaghemite, i.e. a γ -phase with a composition on the ilmenite-hematite join, and second the titanomaghemite is unmixed. The self-reversal coincides with the unmixing of the titanomaghemite.

In some two-constituent models it has been assumed that one of the components acquires its magnetization before the other when they are cooled down from a temperature greater than the Curie point. However the present experiments were carried out at temperatures lower than the Curie temperatures of both components. For any particular grain the relevant temperature is not the Curie temperature but rather the blocking temperature. The blocking temperature is the temperature at which the relaxation time becomes of the

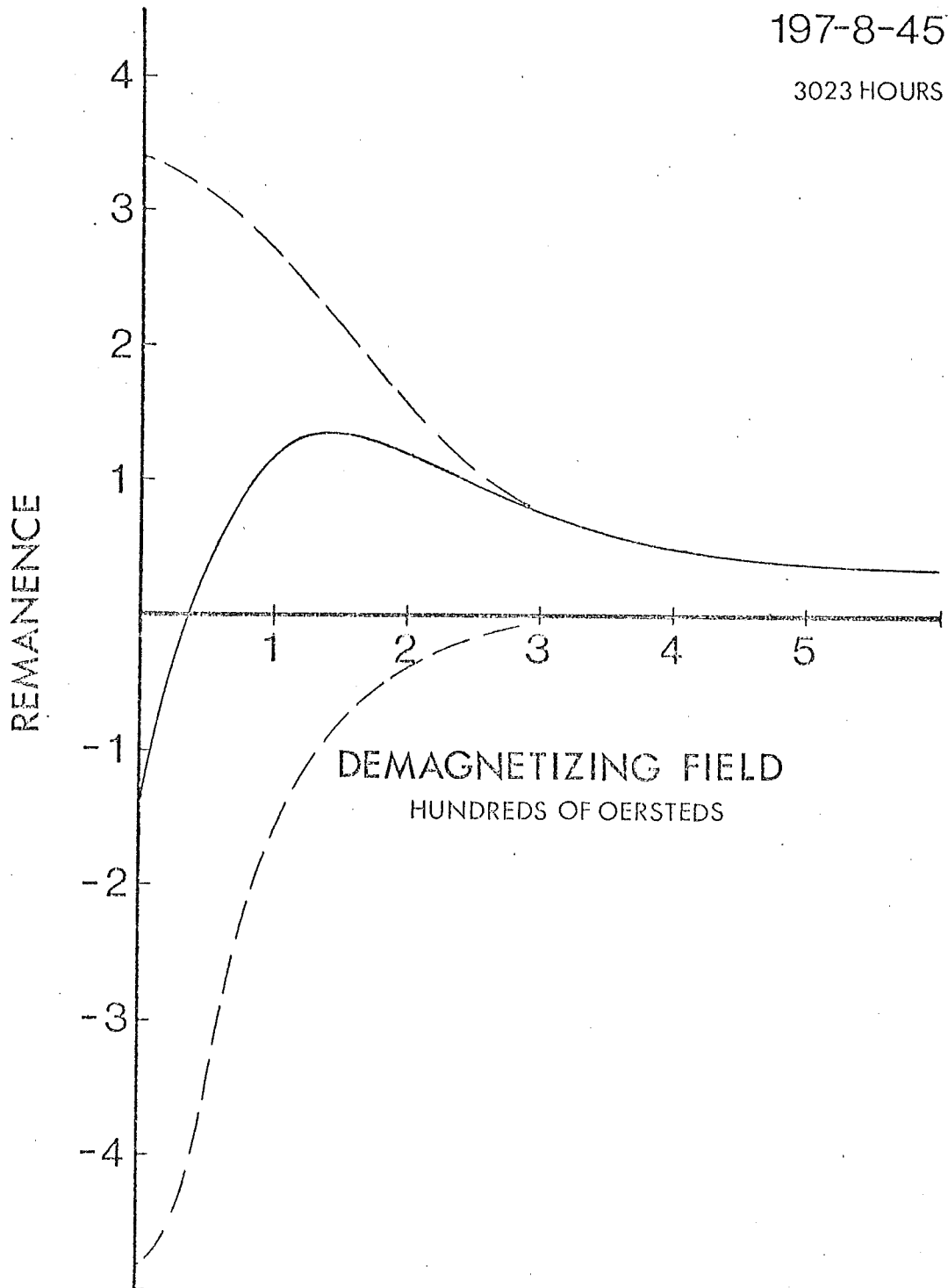


Figure 39. Analysis of PTRM for sample 197-8-45 after 3023 hours of 150°C into normal and reverse components.

order of the duration of the experiments made on the rock. The relaxation time, τ_0 , is given by Néel (1955) as:

$$\frac{1}{\tau_0} = C \exp \left(- \frac{v H_c J_s (T)}{2kT} \right)$$

where 'v' is the volume of the grain, ' H_c ', the coercive force, ' J_s ', saturation magnetization, 'k', Boltzman's constant and 'T', temperature. It can be seen that increasing the volume has the same mathematical effect as lowering the temperature. Thus as unmixing proceeds at a temperature less than Curie temperature grains of the daughter phase, B, will acquire a magnetic moment as they grow through their blocking volume at that temperature.

In the present experiments the samples are A.F. demagnetized to 1000 Oe. prior to each heating which reduces their magnetization to less than 5% of its original value. Thus when heated to 150°C the samples have virtually zero magnetic moment. Providing the γ -phase is mostly titanomaghemite unmixing into an Fe-rich and a Ti-rich phase will occur at 150°C. The Ti-rich phase can be ignored because either its Curie point will be below room temperature or it may invert into α -phase. The Fe-rich component definitely remains a γ -phase because of the high I_s measured. As the grains of this new γ -phase grow through their critical volume they will acquire a magnetic moment parallel to the external field at 150°C. When the sample is cooled the remaining mother phase will be under the influence of both the external field and the interaction field of the daughter, B. It has

been shown in the previous section that there are many situations in which the interaction field can dominate and thus the mother phase, A, will be magnetized in a direction antiparallel to that of the applied field. Whether or not the total magnetization is parallel or antiparallel will depend on the relative concentrations and exact arrangements of the two components.

A possible process is outlined in Figure 40. Figure 40a shows the case where only phase A is present. As the amount of A decreases but grains of B are not yet large enough to acquire a remanence, then the resulting moment will be simply due to the lesser amount of A as seen in Figure 40b. Once grains of B can grow through their critical volume during one experimental cycle then they will acquire a moment, J_B which will depend on how much of B grows through the critical volume during the heating. As the sample is cooled the parent, A, will be magnetized possibly antiparallel to the applied field as in Figures 40c, d, e, the resultant magnetization depending on the relative amounts of A and B and their arrangement which will determine the effective field. Eventually all the A-phase will have unmixed to B-phase and the B-phase grains will have grown through their critical volumes in previous heating cycles and so there will simply be a PTRM acquired on cooling from 150°C to room temperature. Thus the final situation is very similar to the initial case.

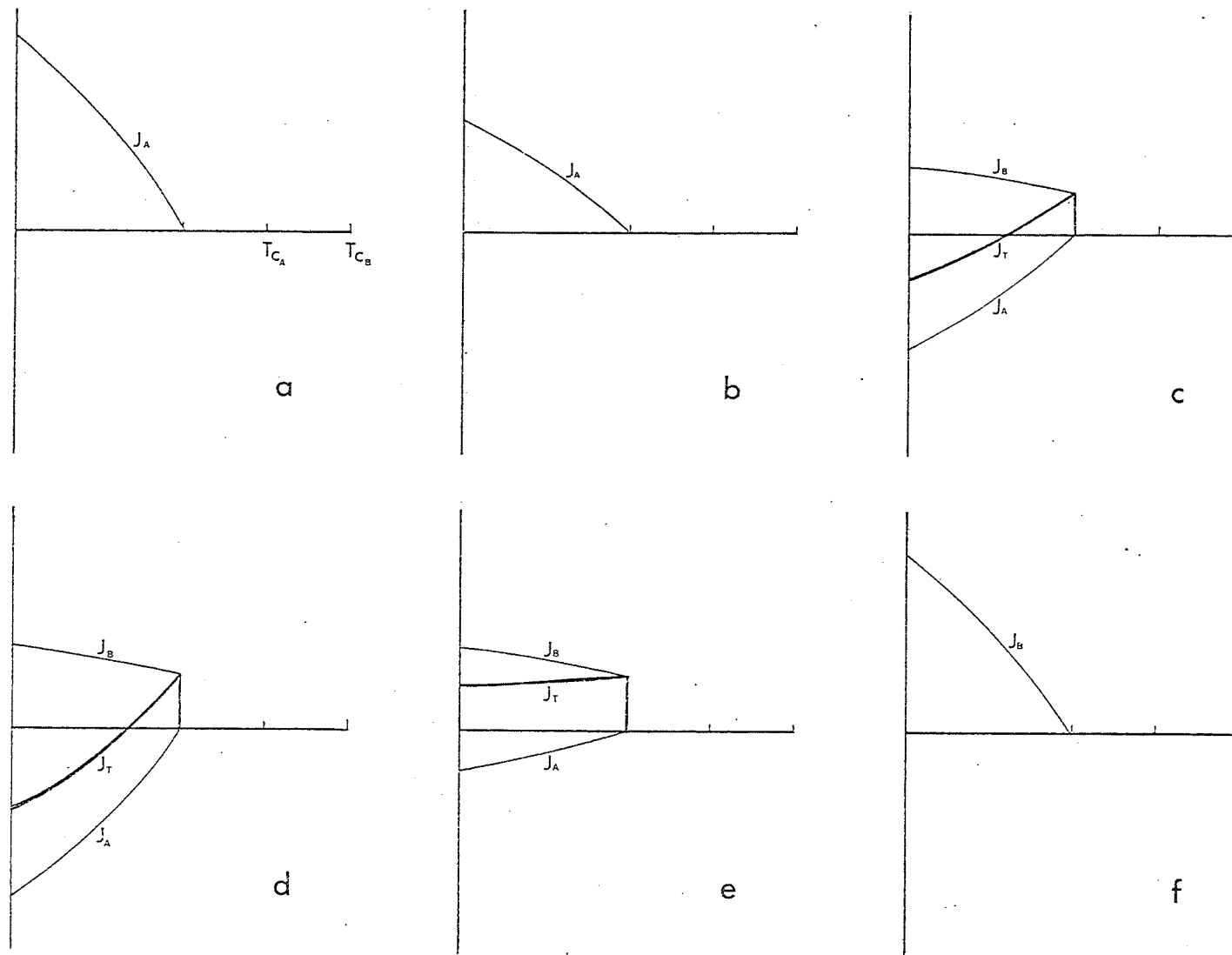


Figure 40. A magnetostatic interaction model for self-reversal. In (a), the original situation, there is only mother phase A present. In (b) some daughter B has been made but grains of B are not large enough to be single domain. In (c), (d) and (e) grains of B acquire varying amounts of magnetization at 150°C . A is then magnetized in the field of B and self-reversal may occur. In (f) only phase B is present.

The nature of the PTRM depends on the relative abundances of the two phases and so it is controlled by the duration of the heatings. Firstly the cumulative heating time controls the composition of the γ -phase. Secondly the length of the individual heating period is important since it controls the amount of daughter which acquires stable magnetization at 150°C and is then available to produce the interaction. Although the growth of grains of the daughter phase is cumulative, the magnetization is reset to essentially zero with each A.F. demagnetization between heatings. Thus the magnetic field available for interaction at 150°C after several short heatings would have arisen only during the last heating while the magnetic field after one long heating equal to the sum of the short ones might be much larger since it is caused by all the grains of daughter phase which have grown.

It is noteworthy that the fully reversed TRM for sample 56-3-35 occurred after the longest heating period, namely 2000 hours. In contrast, samples from 56-3 used in the second 150°C heating experiment acquired only weak reversals perhaps because their longest heating period was only several hundred hours. Finally in the 210°C experiment there were no reversals because the individual heating periods were only a few tens of hours while the γ -phase was in the neighbourhood of the 300°C Curie point.

In nature the process would be slightly different, more akin to Néel's and Graham's mechanism. The mother phase

would remain magnetized while the daughter phase would grow under the influence of the mother's interaction field, and possibly acquire reverse magnetization. Although the roles of the two phases would be reversed the result is the same: during phase splitting a reverse magnetization is acquired.

The important point to be gathered from these laboratory experiments is that they have shown that phase splitting of a cation-deficient titanomagnetite may be accompanied by self-reversal. Hence any direction of remanence resulting from an unmixed titanomagnetite must be considered possibly reversed.

IV BERMUDA SEAMOUNT LAVAS

1. Introduction

In previous sections of this work the variations of magnetic properties both within a single pillow and between different pillows has been examined. Then alterations were produced in the laboratory in an attempt to reproduce some of the changes seen in nature. Finally it was decided to examine some older submarine lavas to give a natural reference for the end product of the alteration processes.

The lava of the Bermuda seamount was formed at least 91 million years ago (Reynolds and Aumento, 1973) through a massive outpouring of lava either soon after or contemporaneously with the creation of new ocean floor on the axis of the Mid-Atlantic Ridge. Later, 33 million years ago, when the seamount was a great distance from the ridge a new phase of igneous activity subjected the seamount to massive intrusions. The original lava makes up 64% by volume of the 767.5 metres of the core drilled through basalt. There were a total of about 600 lava units, but it is thought by Aumento and Gunn (1974) that many of these 'units' are individual pillows lying one above the other which had originated from the same lava flow. Thin sections examined by Aumento and Gunn (1974) have shown the majority of the lava to be fine-grained, typical of submarine pillow lavas or thin rapidly cooled flows. Aumento and Gunn (1974) suggest that the alteration of Bermuda lavas was primarily controlled by the

length of time each flow was exposed to sea water. If such were the case, then this material would certainly be a good natural reference end product for low temperature alteration. If, however, the alteration of the titanomagnetites was primarily controlled by the subsequent reheating at 33 million years ago, then the titanomagnetites may not be typical of oceanic pillow basalts.

Two lava units, 38.1 and 122.6, each slightly thicker than a metre, were chosen from depths of 230 m and 730 m respectively. Samples were obtained by transversely drilling one inch diameter by one inch long measuring cores from the drill core. These measuring samples were numbered according to their distance in centimetres from the top of the unit.

2. Magnetic Properties of Two Flows

2.1 Bermuda Flow 38.1, NRM and Saturation Magnetization

The general magnetic properties and core description are given in Figure 41. This unit may be considered in two separate sections, first the two small pillows comprising the upper 30 centimetres and second the massive flow material from the 42 cm mark to the bottom of the unit at 115 cm. The material between 30 and 42 centimetres is rubble which has got broken up in the drilling. The 63 centimetre thick flow is coarse grained in the centre but has finer grained chilled margins.

Comparing the pillows and flows in Figure 41, it can be seen that saturation magnetization at about 1.2 emu/g in the flow is about twice that of 0.6 emu/g in the pillows. However

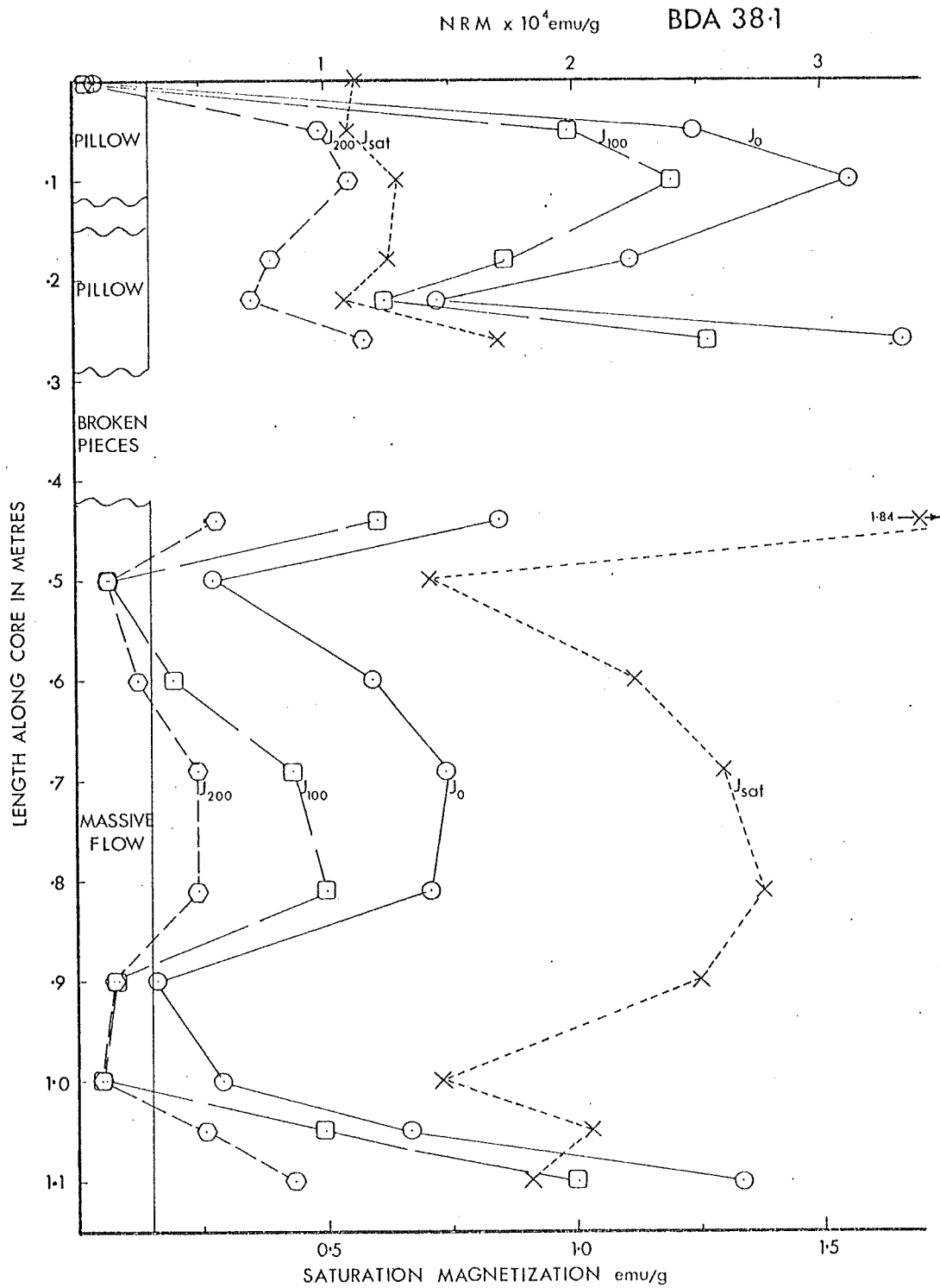


Figure 41. Magnetic properties of flow 38.1.
 J_0 , J_{100} , J_{200} are NRM before A.F. demagnetization
 and after demagnetization to 100 and 200 oersteds
 respectively. J_{sat} is the saturation magnetization.

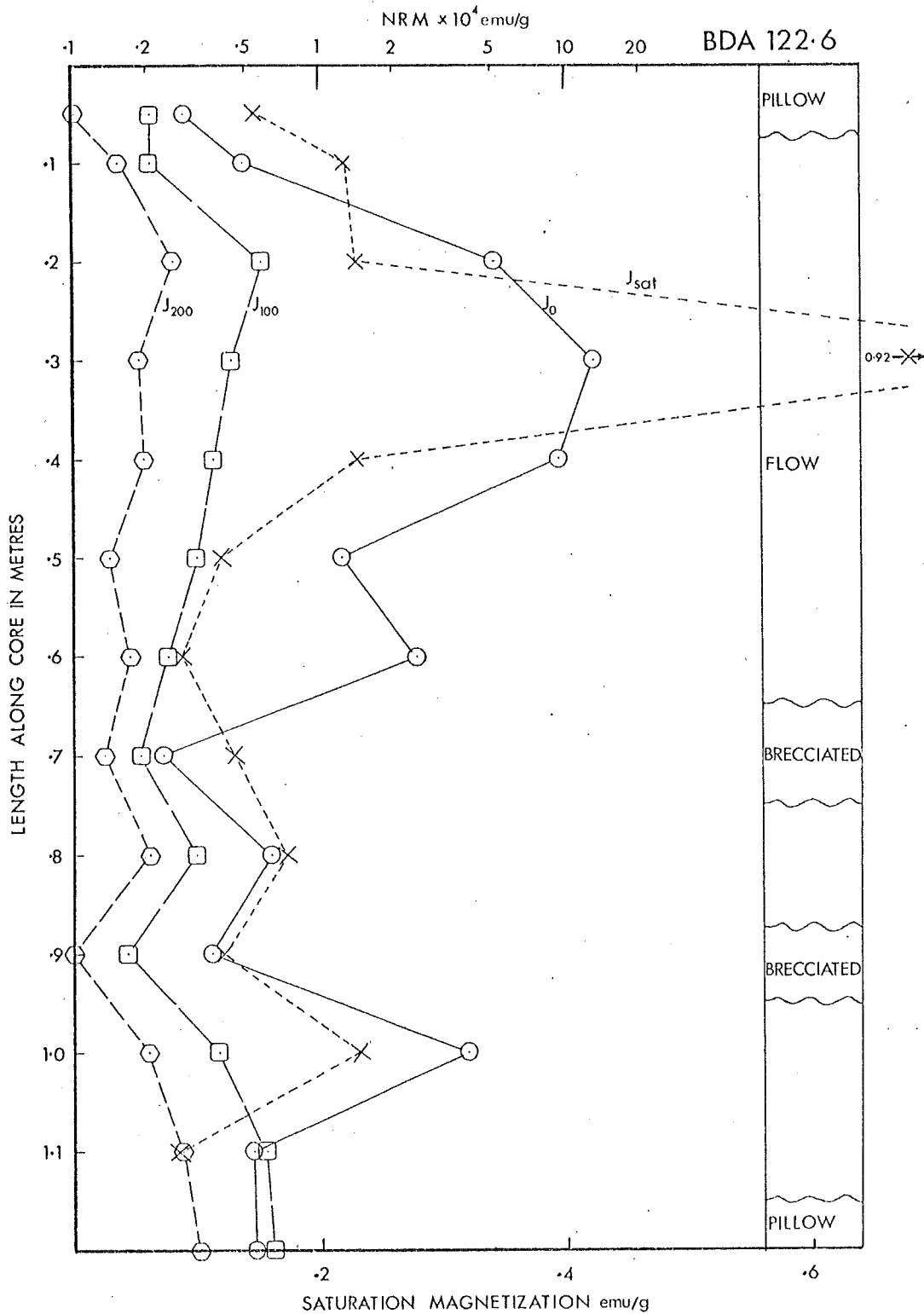


Figure 42. Magnetic properties of flow 122.6.
 J_0 , J_{100} , J_{200} are NRM before A.F. demagnetization
 and after demagnetization to 100 and 200 oersteds
 respectively. J_{sat} is the saturation magnetization.

the NRM intensity of the flow at about 1×10^{-4} emu/g is half that of pillows. The difference in effectiveness as a carrier of NRM can be attributed to different magnetite grain sizes in the flow and pillows as seen in polished sections. The grains in the pillows are generally less than two microns in maximum dimension with a length to width ratio around three and so are probably single or pseudo-single domain. Within the flow grains are generally larger and more equidimensional with some grains as large as 20μ across. At the chilled margins of the flow the grains are smaller, more like those of the pillows. Within this range of sizes the larger grains would be less efficient carriers of NRM as shown in Figure 4a.

The major magnetic mineral as identified from Curie temperature and microscope observation is magnetite. In most samples there is also some hematite visible either in veins or finely disseminated, giving a reddish colour to areas tens of microns across.

2.2 Bermuda Flow 122.6, NRM and Saturation Magnetization

The general magnetic properties are given in Figure 42. The unit is broken up by two brecciated zones at around 70 cm and 92 cm down the core. In this unit there are large variations in the amount of NRM intensity removed in the first 100 Oe. demagnetization. There are large direction changes as this soft component is removed. This soft component may be acquired either while the rock is sitting in storage in the laboratory prior to measurement or during

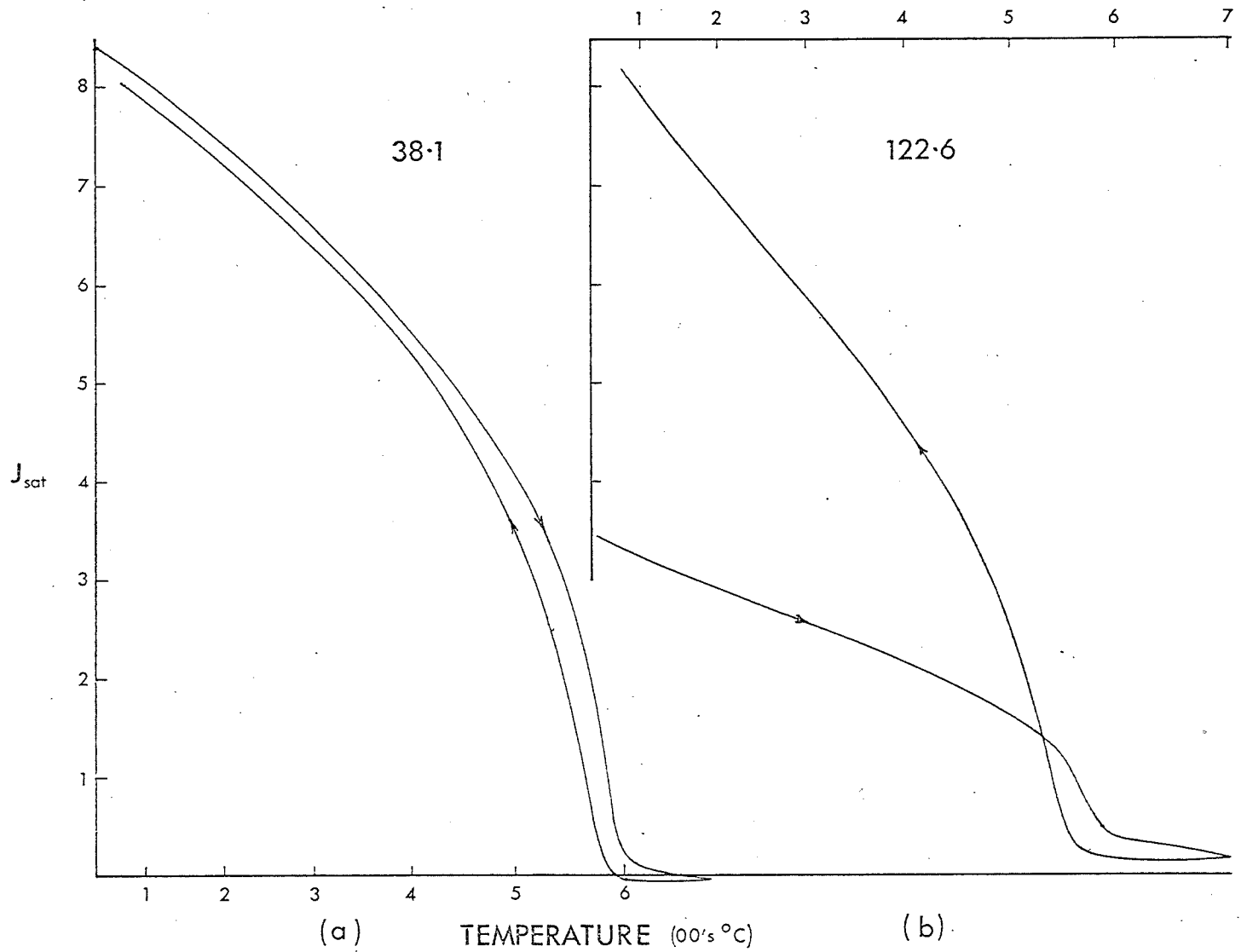


Figure 43. Typical J_s -T curves for flows 38.1 and 122.6. Those for 38.1 are reversible while those for 122.6 show an increase in J_{sat} on cooling.

the drilling process in a manner similar to that reported by Rainbow et al. (1972). These possibilities will be further considered in a following subsection on viscous remanent magnetization.

For this unit saturation magnetization was generally a fifth of that in flow 38.1, while the NRM intensity was comparable to values for flow 38.1.

The major magnetic mineral was again magnetite with minor hematite - less hematite than in 38.1. There is also abundant sulphide. Micron sized sulphide grains are present in all samples with a few larger grains occasionally. The highest concentration of sulphides is in sample 090 which had cubic grains of 60μ across. One area of the polished section for this sample was yellow-gold to the naked eye, so concentrated were the sulphide grains.

The same apparatus was used for J_s -T measurement of the Bermuda samples as described in Section 3.2 with the exception that the diffusion pump had been replaced with a rotary pump and nitrogen backfill capability. In this arrangement the system would be pumped down to less than 10^{-1} torr pressure, filled with nitrogen to atmospheric pressure and pumped out again. By repeating the cycle three times it is possible to get oxygen partial pressure lower than with the diffusion pump alone.

The J_s -T curves for flow 122.6 were quite different from those of flow 38.1. All samples from flow 38.1 had a typical magnetite curve as seen in Figure 43a, that is a Curie

temperature slightly less than 600°C and an essentially reversible curve, the difference between heating and cooling being due to thermal hysteresis of the measuring system. In contrast, samples from flow 122.6 had a J_s after cooling about three times as great as before heating as shown in Figure 43b. This effect could be produced both at the low oxygen partial pressures after the system had been repeatedly backfilled with nitrogen and also at atmospheric oxygen pressure. It would seem that the increase in J_s is due to the conversion of some other mineral to magnetite, perhaps some of the abundant sulphide or an iron bearing silicate. In support of this idea, more sulphides are seen in the polished sections for flow 122.6 than in those for flow 38.1 or the Mid-Atlantic Ridge pillows. In particular, sample 122.6.090, which has by far the greatest amount of sulphide showed the greatest increase in J_s , by a factor of 10, during J_s -T measurement. Only sample 122.6.030 did not exhibit an increase in J_s . This sample had a high J_s prior to heating and showed more abundant skeletal magnetite grains up to 20 μ than other samples so probably the sulphides were proportionately less important in this region.

3. Viscous Remanent Magnetization

3.1 Introduction

It can be seen in Figure 42, that while some of the samples have a relatively high NRM, it is a soft magnetization as shown by the large decrease in intensity to J_{100} and also

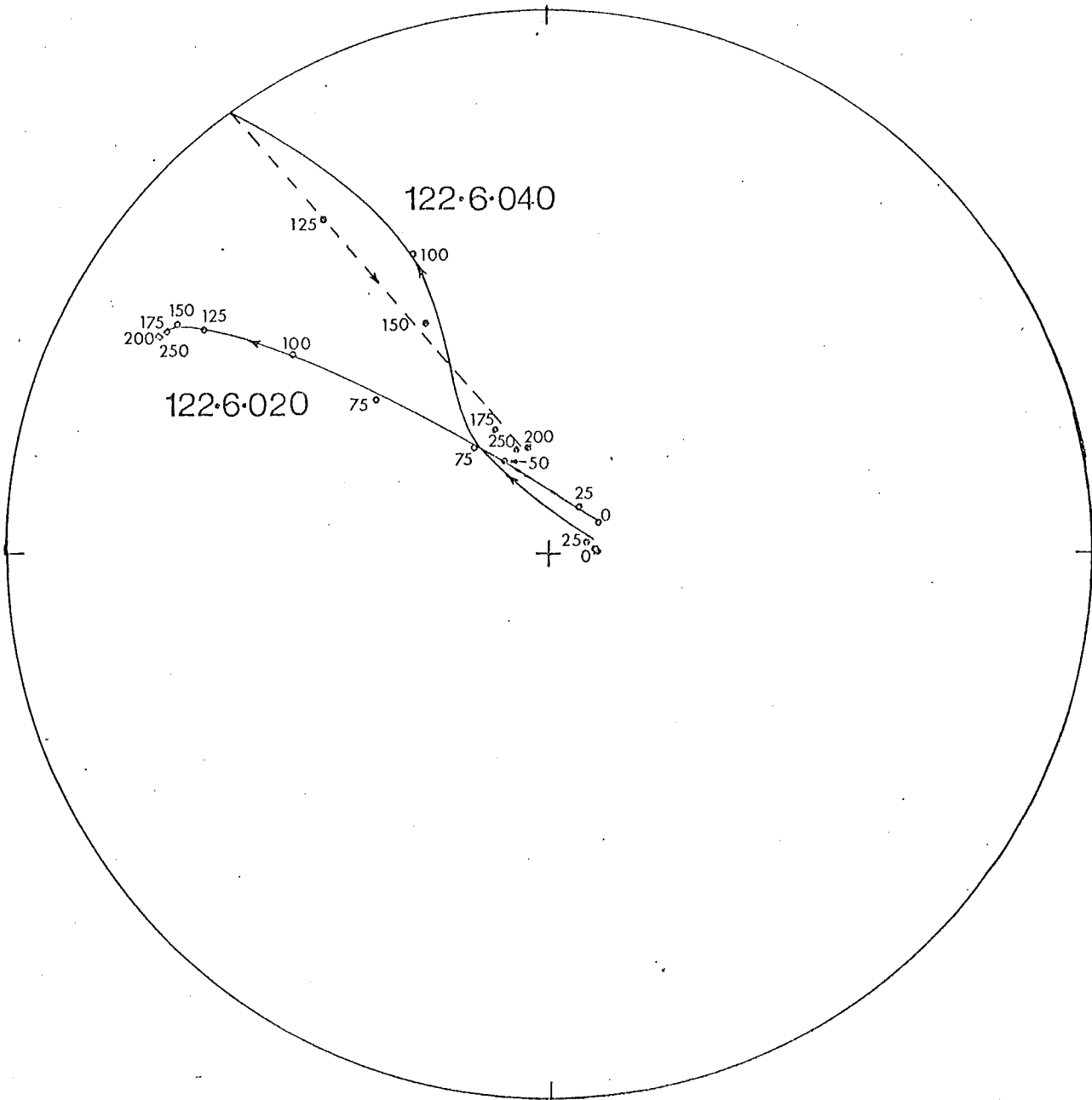


Figure 44. Change of direction in two samples from flow 122.6 with A.F. demagnetization. Both are initially aligned with the drill barrel. On demagnetization one remains normal while the other reverses. The numbers opposite the points are the A.F. demagnetization in oersteds.

by large direction changes during demagnetization. Figure 44 shows two samples which have almost the same steep direction before demagnetization, aligned closely with the axis of the drill barrel, yet which have quite different directions after demagnetization, these different directions are further discussed in Section 4. While these two samples had acquired a remanence aligned along the drill core axis, some other samples from Bermuda have picked up a component of remanence in the direction of the Earth's magnetic field in which they had been stored (Ade-Hall, pers. comm.). Because of these indications and considering Lowrie's (1974) results in which he showed there to be significant VRM in basalt from DSDP hole 57 and in view of the possible importance of VRM as a contributor to marine magnetic anomalies, it was decided to test some of the Bermuda samples for VRM acquisition.

3.2 Procedure

The acquisition of isothermal viscous remanent magnetization generally follows the law:

$$I_{r,H}(t) = I_{r,H}(0) + S(\log t - \log t')$$

where S is the viscosity coefficient, t is the time during which a field H is applied and t' is the time required for the measurement of the VRM (Nagata, 1961). Therefore in order to determine the viscosity coefficient S , a sample would be placed in a known field for various times and the resulting VRM after each time plotted against it on semi-logarithmic paper.

Prior to the VRM experiment, the NRM was demagnetized as far as possible. This would usually be to a percent or so of the original NRM except for sample 38.1.022 which started to acquire an ARM when it still had 12% of the original NRM. Samples 122.6.020 and 030 were demagnetized to less than one percent of their NRM. Immediately after the A.F. demagnetization the sample was placed in a 5.0 Gauss field where it was kept for the required time. A 5.0 Gauss field was used to produce as large a VRM as possible in a relatively short time. The acquisition of VRM is linear with small fields (less than 10G) as shown by Shimizu (1960) and confirmed for typical Bermuda samples by Kitazawa (pers. comm.). After the desired time the sample moment was measured in the spinner magnetometer which would take four to five minutes for a six-spin determination. The sample would be A.F. demagnetized generally to about 350 Oe. after which the moment was usually dominated by ARM's.

3.3 Results

The VRM's acquired were plotted against time as shown in Figure 45. From these plots the coefficient S was determined and this coefficient used to calculate the VRM which would be acquired in a 0.5 Oe. field over a period of 7×10^5 years, the length of the present normal epoch. This provides an estimate of the VRM which could be acquired by these rocks while in situ. The results are given in Table 6.

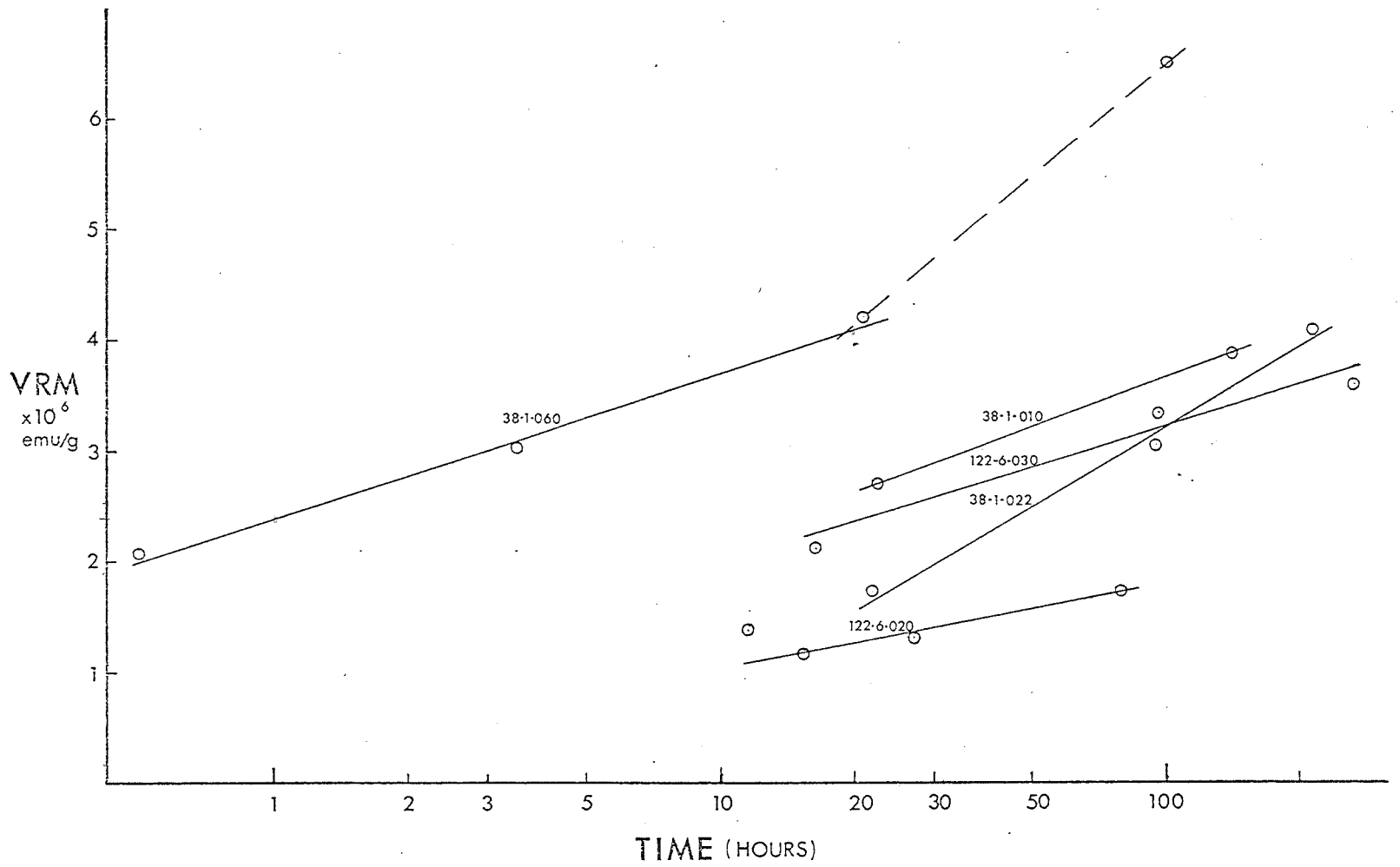


Figure 45. Acquisition of VRM by Bermuda samples.

TABLE 6
ACQUISITION OF VRM

	38.1.010	022	060a	060b	122.6.020	030
VRMx10 ⁴ emu/g in 7x10 ⁵ yr	.14	.22	.15	.21	.08	.13
NRMx10 ⁴ emu/g measured	3.1	1.45	1.18	1.18	5	15
VRM/NRM(%)	4.5	15	13	18	1.6	1.0

Note: 060a and 060b denote the two segments drawn in
Figure 45.

From these results it is unlikely that the VRM of the lavas could have made a significant contribution to the magnetization.

The VRM aligned along the axis of the drill barrel is very soft with MDF of the samples from the upper 60 cm of 122.6 being less than 50 Oe. The laboratory induced VRM is even softer, only 10-15 Oe. The differing hardness between drilling induced and laboratory VRM may be due to the drilling induced VRM being acquired at slightly elevated temperatures caused by the drilling process. According to VRM theory the MDF should increase with the time over which the VRM is acquired. There was no clear indication of such hardening of VRM in this experiment even though the acquisition times ranged over three orders of magnitude.

Unfortunately there is some doubt about the hardness of the laboratory VRM's due to the experimental techniques used.

This uncertainty arises because as soon as the sample is removed from the magnetizing field the VRM will start to decay, hence the term t' in the VRM equation. As the A.F. demagnetization proceeds the time since removal from the magnetic field, t' , is constantly increasing. Thus one will be measuring a total decrease due to both the A.F. demagnetization and also the viscous decay of the VRM. So, by the time the remanence remaining at some demagnetizing field is measured, the amount left will be less than what would be expected if the VRM did not decay. Hence the apparent hardness of the VRM depends on the speed with which it is measured. If components of the VRM over the entire coercivity spectrum decay at equal rates, which they probably do not, and the time of measurements were accurately recorded then it may be possible to separate the two effects. However, the times were not recorded and cannot be estimated with sufficient accuracy to make such a separation attempt worthwhile.

It had been expected that samples from 122.6 which had the largest drilling induced VRM would acquire the largest VRM in the laboratory - such was not the case. It seems then that the mechanisms for these remanences must be different or perhaps the difference is a result of acquisition at slightly different temperatures. Dunlop (1973) claims that single domain particles should be the most efficient at acquiring VRM yet the most obvious feature in polished sections from DSDP hole 57, which shows most VRM acquisition,

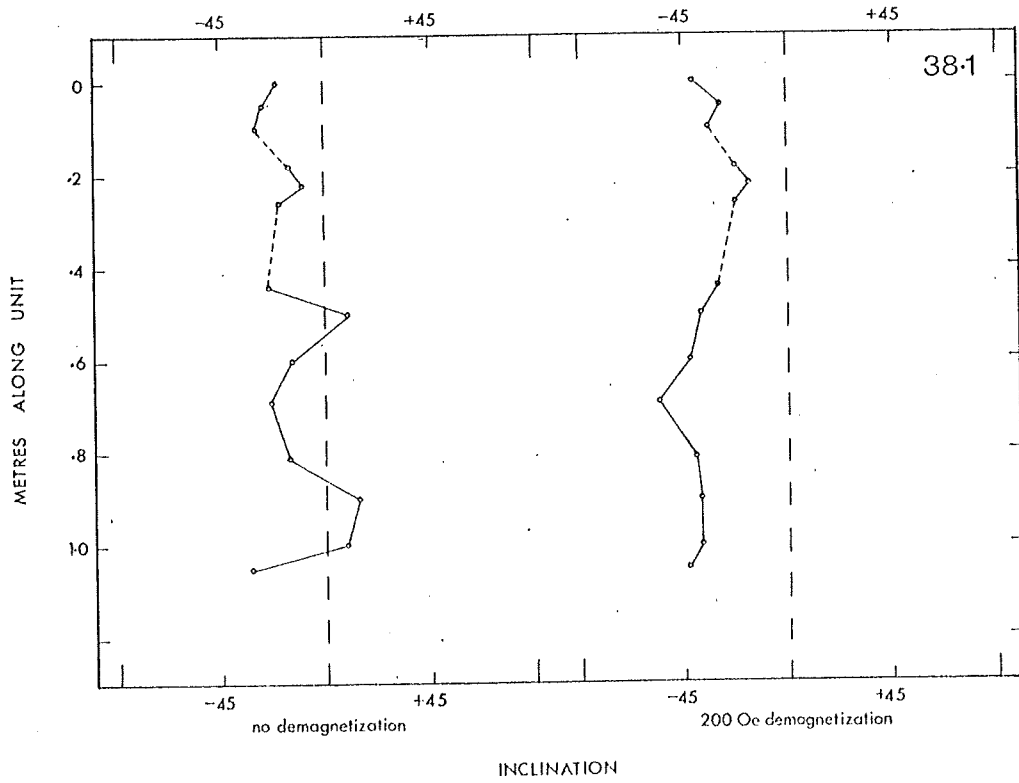
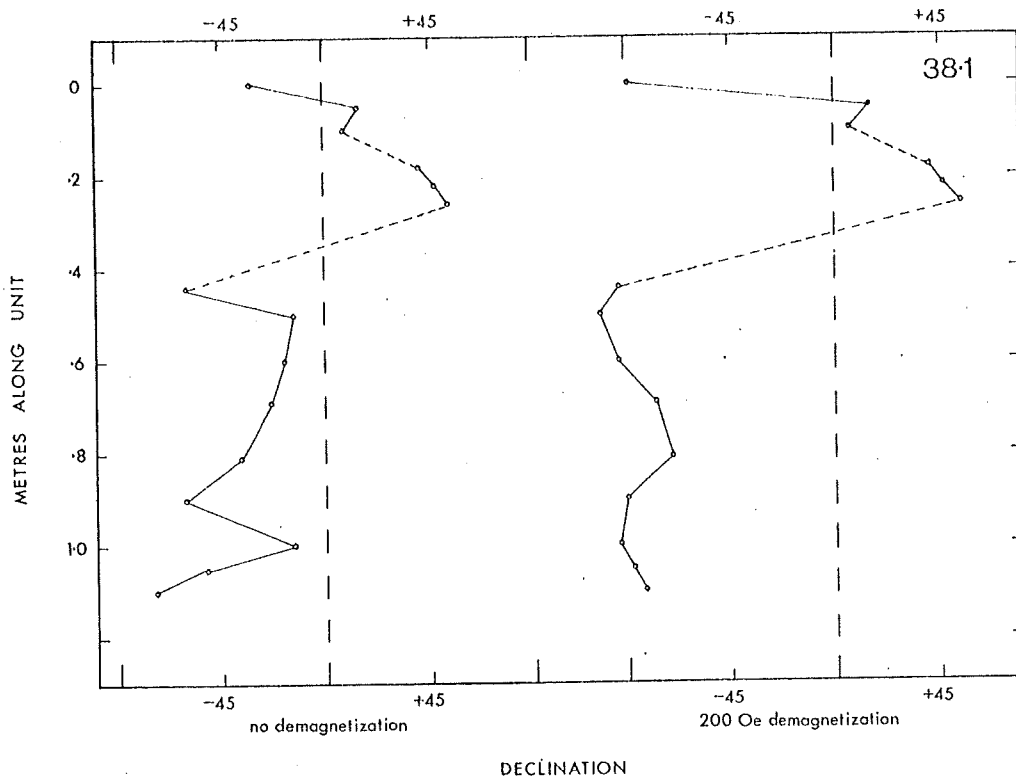


Figure 46. Declination and inclination for flow 38.1.

is the abundance of large titanomagnetite grains measured in tens of microns (Kitazawa, pers. comm.). The very fine grained pillows are notably poor at acquiring NRM.

The mechanism for the acquisition of both VRM and the drilling induced moment is not well understood and requires a great deal of further study.

4. NRM Directions

The declinations and inclinations for flows 38.1 and 122.6 are shown in Figures 46a and 47a. respectively. The directions are plotted both before demagnetization and after demagnetization to 200 Oe. The latter value was chosen because, in general, it was sufficient to remove the strong but soft drilling VRM but sufficiently low to avoid inducing ARM.

The directions for unit 38.1 are divided into three sections by the dotted lines which indicate breaks in the core across which orientation cannot be carried. There were three cores drilled from each pillow at the top of the core. The variation within each pillow is much larger than would be expected from Mid-Atlantic Ridge pillow results. Within the flow the maximum scatter of both the declination and inclination after demagnetization has brought the directions closer together than they were initially.

The directional behaviour of 122.6 is quite different. Sample 110 should be neglected from these considerations since its directions are so different and being from the

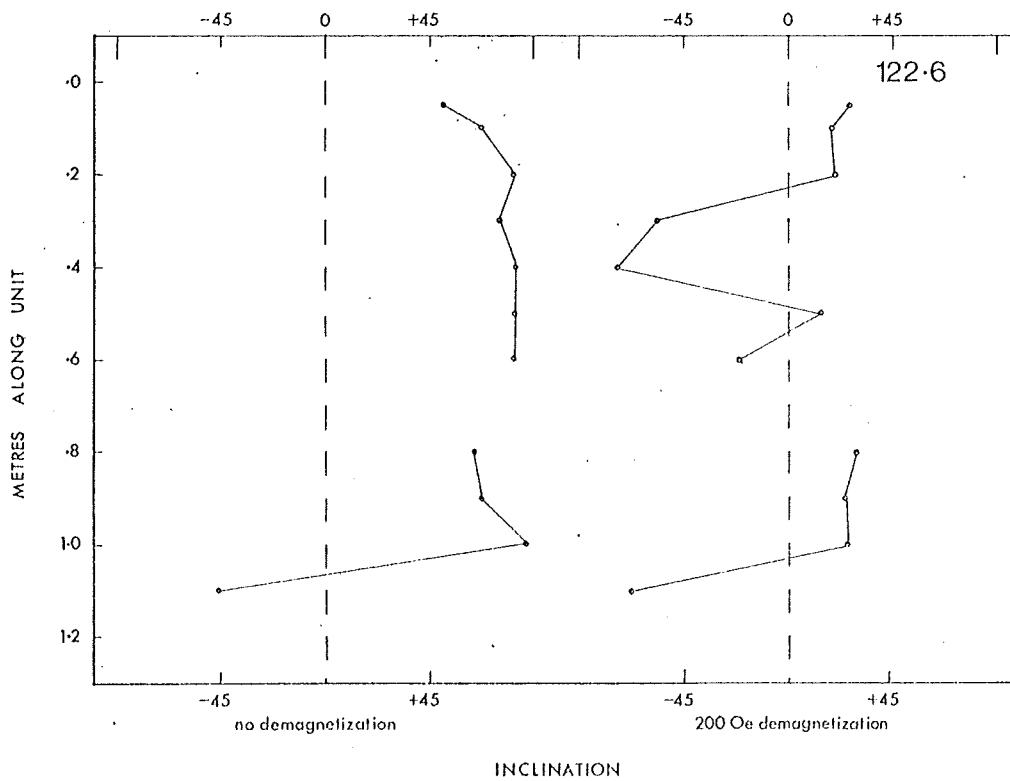
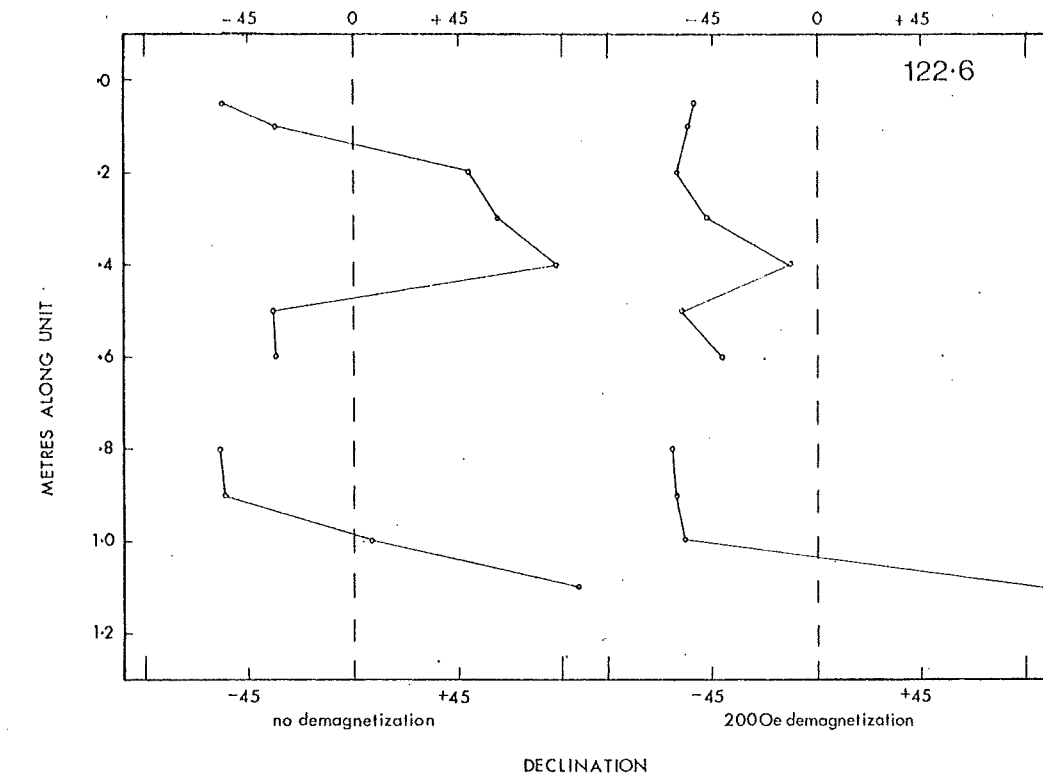


Figure 47. Declination and inclination for flow 122.6.

margin it has probably been remagnetized at some different time from the rest of the flow. Considering the other samples there is a large scatter in declination but all inclinations are positive before demagnetization. At the 200 Oe. level the declinations are more closely grouped together as would be expected but the inclinations, now that the dominance of the drilling VRM has been removed, have diverged into two groups; one positive and one negative. While the inclinations are positive and negative, the moments are not antiparallel. For example, samples 030 and 090 have declination -60° but sample 030 has inclination of -54° while sample 090 has an inclination of $+24^\circ$.

Since the vertical components of these samples are in opposition they will cancel out. Thus the net magnetic effect of the flow will be less than would be expected if all of the flow were magnetized in the same direction. It is difficult to see how such a distribution of angles could be caused if the unit were cooled together in the same field. It is more likely that the magnetization is not original but rather a magnetization which has been acquired at some time long after the original outpouring of the lava at the ridge.

It is possible that the lava has been reheated at two different times by intrusions, once from above and once from below. This would cause the upper and lower halves of the flow to be magnetized in antiparallel directions if the Earth's field had reversed. However the directions in the flow are not antiparallel since the greatest difference in

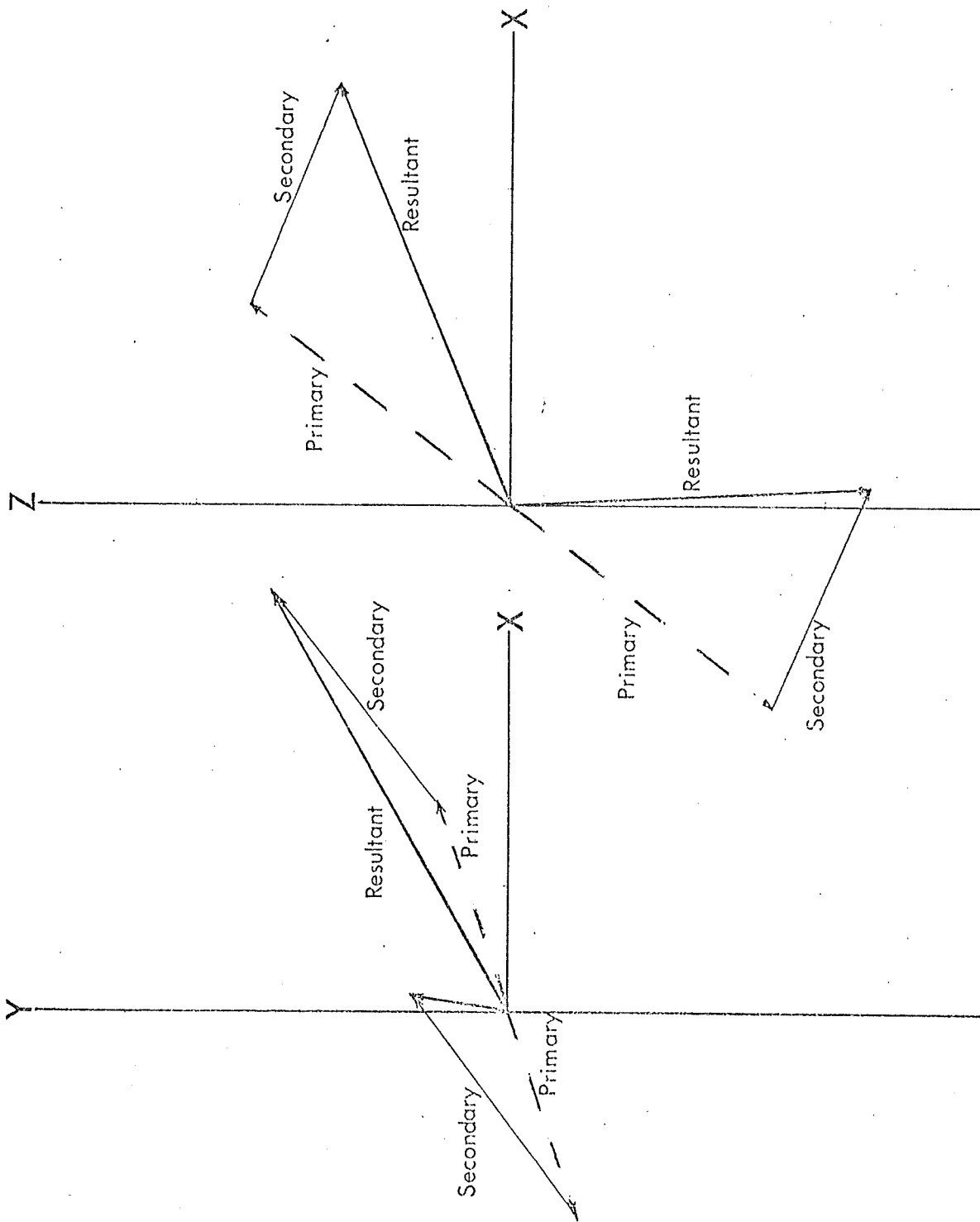


Figure 48. A model showing how the addition of a secondary component to antiparallel vectors could produce the directions measured in flow 122.6.

declination is 50° not 180° . A similar distribution of directions has been reported by Ade-Hall et al. (1973) between the lavas along the Bermuda core. The same mechanism put forward by Ade-Hall could explain the variations within the one flow; namely that a stable shallow CRM is added to antiparallel moments to give the resultant vectors as shown in Figure 48. There is, however, no obvious source for the CRM vector.

5. Summary

Although the saturation moment of the Bermuda lava flows is about the same order as the Mid-Atlantic Ridge pillows the intensity of the NRM is much lower. Although some of this difference may be due to the larger grain size in the Bermuda material, the most important cause is probably that the NRM is not the original TRM acquired when the lava cooled. The remanence in the Mid-Atlantic Ridge pillows is undoubtedly original TRM acquired by the titanomagnetites cooling through their Curie point. This remanence may have been modified and reduced in older pillows as maghematization proceeds but it is still a considerable fraction of the original remanence.

The remanence in the Bermuda lavas is due to magnetite which is almost certainly secondary considering the extensive hydrothermal and subsequent alterations reported by Aumento and Gunn (1974) in their study of the petrology. The remanence is acquired by the magnetite when it is altered at a temperature well below its Curie point and hence it is

only a small fraction of the remanence the magnetite would have acquired had it been above its Curie point.

The Bermuda flows exhibit considerable differences. Flow 38.1 while weakly magnetized is relatively stable. Flow 122.6 shows both positive and negative inclinations after a large drilling induced moment has been removed. There are more abundant sulphides in 122.6 than are usually seen in pillow lavas so perhaps they are the source of some magnetite which acquires a CRM to account for the variability of direction. The deeper burial and hence higher temperatures experienced by 122.6 probably accounts for its more confused and complicated magnetism.

V. REVIEW AND DISCUSSION

1. Introduction

The original intention of this work had been to study, in three steps, the alteration processes affecting the magnetic minerals in submarine pillow lavas. The intention had been to use a detailed study of young pillow lavas from the Mid-Atlantic Ridge to establish both the initial magnetic mineralogy and the alteration of the magnetic minerals due to reaction with sea-water. Next it was hoped to duplicate in the laboratory the type of alteration seen in the pillows and then to extend it through increased reaction time to a state equivalent to millions of years. Finally it was proposed to check the final state reached in the laboratory alteration through comparison with very altered submarine lavas from Bermuda.

From the work described in Sections II and III several points emerge. The magnetic minerals in pillow basalts are altered by reaction with sea-water and this reaction is accompanied by a decrease in NRM intensity. This alteration process causes not only a decrease in NRM intensity with increasing distance from the ridge axis but also, in conjunction with other factors, a radial variation in NRM intensity within each young pillow. The laboratory experiments have shown that there is a strong temperature dependence in the rate of reaction. Further, it is seen that at temperatures as low as 150°C phase-splitting

eventually occurs.

The cores from Bermuda, of which those described in Section IV are typical, are important because they give a picture of many hundreds of thin intrusive and extrusive units.

It is necessary now to consider how these facts might be applied to obtain a better understanding of the magnetized part of layer 2.

2. Effect of Radial Variations within Pillows

The pillow lavas examined in Section II show a radial variation in NRM intensity such as shown in Figure 16. In the course of obtaining values of NRM for use in modelling of magnetic anomalies it is often the practice to use the values for the fresh interiors as typical, on the premise that this will be representative of the bulk of the material. With the use of Figure 16 and estimating the radii of the pillows it is possible to carry out the sort of numerical integration done by Marshall and Cox (1971b) and obtain the average pillow intensities given in Table 6.

TABLE 6

Average Pillow Intensities

Pillow	197-8	56-3	9-18	47A-1
Distance from Axis (km)	0	0	10	25
Highest J_{NRM} (emu/cm^3)	0.13	0.042	0.020	0.0022
Average J_{NRM} (emu/cm^3)	0.08	0.024	0.015	0.0021

Thus high values from the fresh interiors may be higher than truly representative values by almost a factor of 2. These values agree reasonably with Talwani et al. (1971) values obtained from mathematical analysis of profiles along magnetic anomalies: 0.03 emu/cm^3 on the axis and 0.012 emu/cm^3 off the axis. However the use of a value as high as 0.012 emu/cm^3 at distances more than 20 km from the axis does not agree with the low intensity of 47A-1.

3. Effect of Temperature Dependence of Reaction Rate

From examination of the natural magnetization of these pillow basalts a decrease in intensity with distance from the ridge is evident. The laboratory alteration experiments have shown that the rate of reaction for the alteration process, which causes the decrease in intensity, is strongly temperature dependent. By using the constants obtained in Section 5.1 (page 108) and applying them at lower temperatures one obtains the relation between time for maghemitization and temperature shown in Figure 49.

From Figure 49 it can be seen that a pillow which had been exposed to sea-water at about 4°C should have titanomaghemite with a Curie point of 300°C after 6.4×10^5 years. Pillow 47A-1 is dated at 7.4×10^5 years and has Curie points between 300°C and 350°C . From this agreement between prediction and observation one is encouraged to make further predictions concerning the maghemitization of the titanomagnetites in layer 2. The similar time-dependence of the

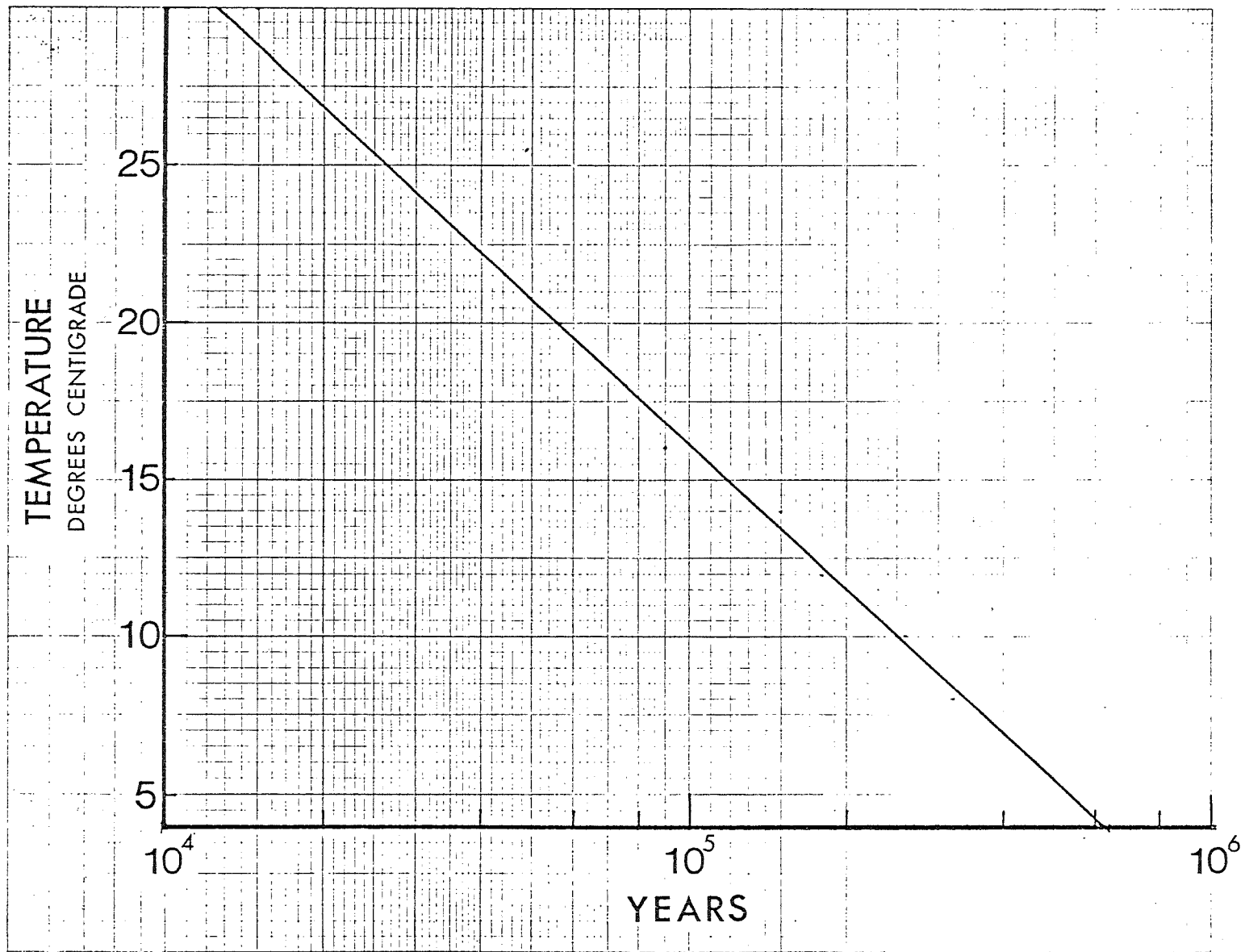


Figure 49. Relation between temperature and time required for maghemitization.

intensity of the PTRM's acquired on cooling from 150°C and the NRM intensity of basalts recovered from different stations (Figure 50) is further evidence that alteration at 4°C and 150°C is by the same process.

Figure 50 shows an intensity of 0.006 emu/cm³ for laboratory time at 150°C equivalent to the age of pillow 47A-1. This intensity is typical of values for pillows of that age. Hence the time calculated from Figure 49 for maghemitization to a state with a Curie temperature of 300°C may also be interpreted as the time for intensity to decrease to 0.006 emu/cm³. From the shape of the line in Figure 50 it is possible to calculate the time required for any particular intensity. For example: at 150°C, 500 hours heating results in an intensity of 0.012 emu/cm³, that is 20% of the time required for 0.006 emu/cm³. Consequently, at 10°C which requires 2.5x10⁵ years to reduce intensity to 0.006 emu/cm³ then 20% of that time, i.e. 5x10⁴ years would have lowered intensity to 0.012 emu/cm³.

Using Figures 49 and 50 in this fashion one may construct Figure 51 which is a plot of contours of constant intensity in a time-temperature plane. Such a diagram is easily transferred to a geological setting by applying a known spreading rate along the horizontal axis to convert time to distance and a temperature gradient will similarly convert the vertical axis. For the spreading rate a typical value for the Mid-Atlantic Ridge would be 1.5 cm y⁻¹. It is expected that temperature gradients at a spreading ridge

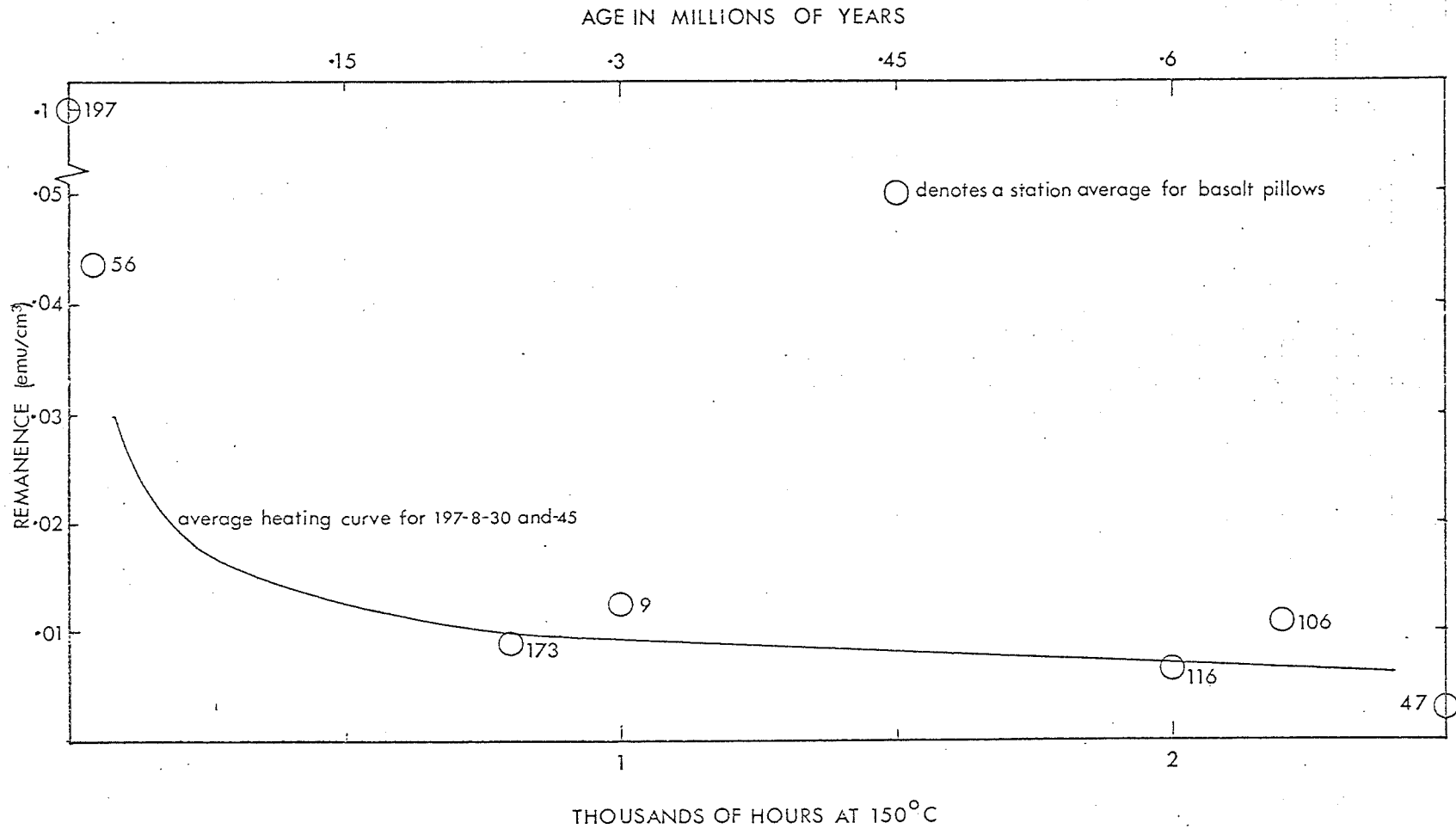


Figure 50. A comparison between the PTRM acquired in the laboratory as a function of heating time to the intensity (station average) of dredge haul basalts as a function of age.

crest will vary strongly from place to place. If one assumes a conservative, perhaps even minimal gradient of $0.03^\circ/\text{m}$ a temperature of 30°C would occur at a depth of 1 km, the order of thickness of layer 2.

It is anticipated that very close to a ridge axis the intensity of magnetization is not constant in a vertical section but decreases sharply with depth. If one assumes that the intensity, does not decrease much below $0.003\text{emu}/\text{cm}^3$ at distance - as suggested by measurements of pillows (Irving et al. 1970) - then at distance the intensity will be weak but constant with depth.

This mechanism of the temperature-dependence of the rate of alteration is perhaps the explanation for Irving's (1970) thin intensely magnetized layer at the ridge and thicker more weakly magnetized layer at distance. Actually the thickness of the magnetic layer is constant but the high intensity near-surface region dominates at the ridge crest.

Implicit in these arguments is that all of layer 2 can be treated as a pile of pillow lavas which has access to an excess of sea-water for reaction. Studies of Leg 34 D.S.D.P. basalts (Ade-Hall et al. 1975) have shown that where there are pillows, there is sufficient water available for alteration but it has also been shown that not all of the lava is in the form of pillows. A sizeable fraction is in the form of massive units which are not so readily altered.

It is interesting to speculate what effect the distribution of intensities shown in Figure 51 would have

METRIC

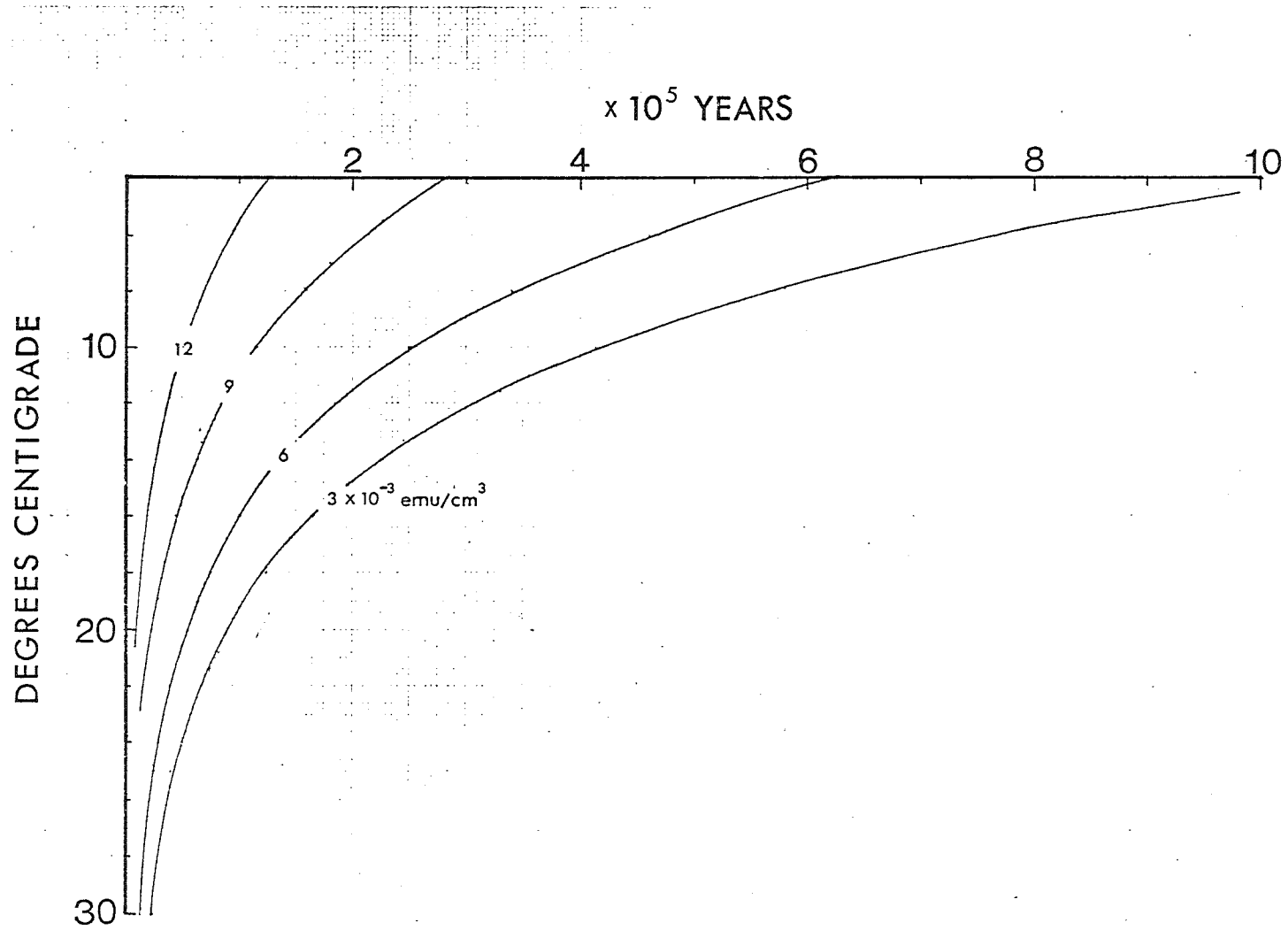
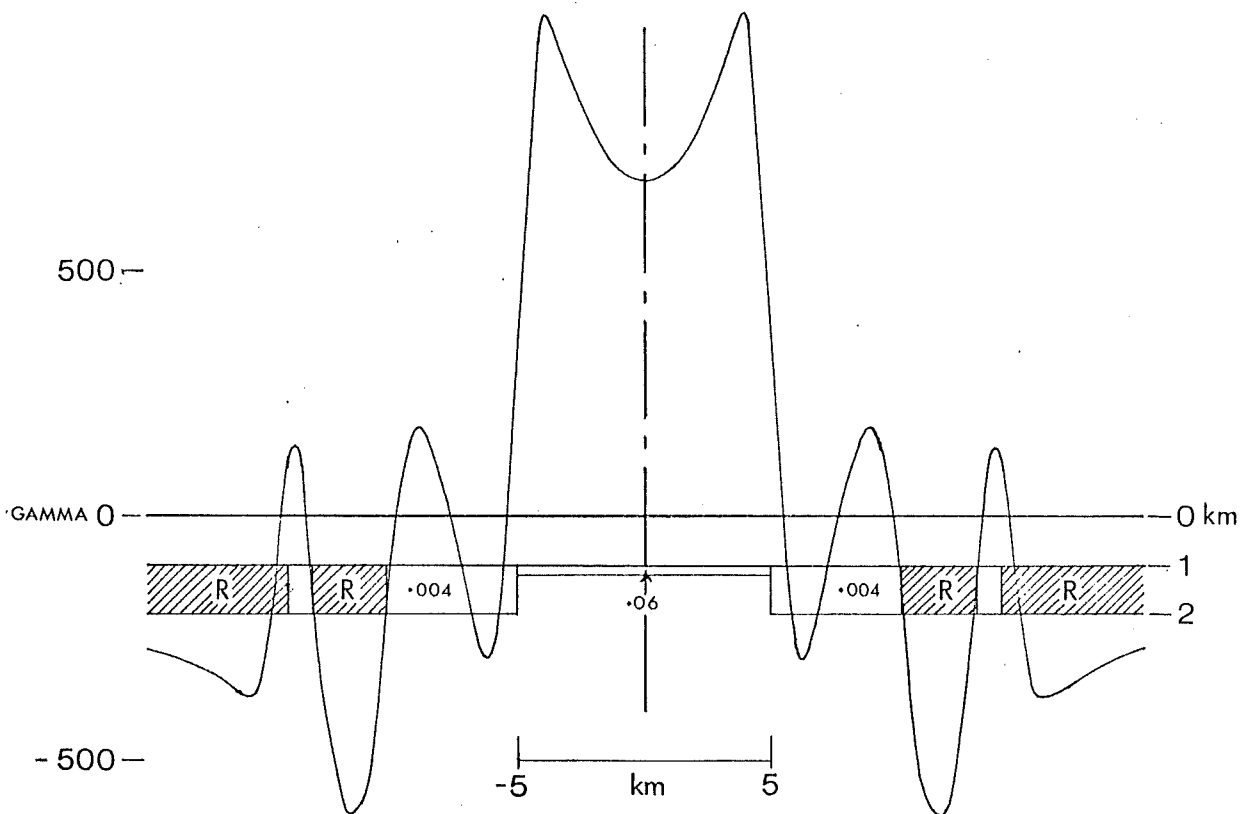


Figure 51. Contours of constant intensity of magnetization.

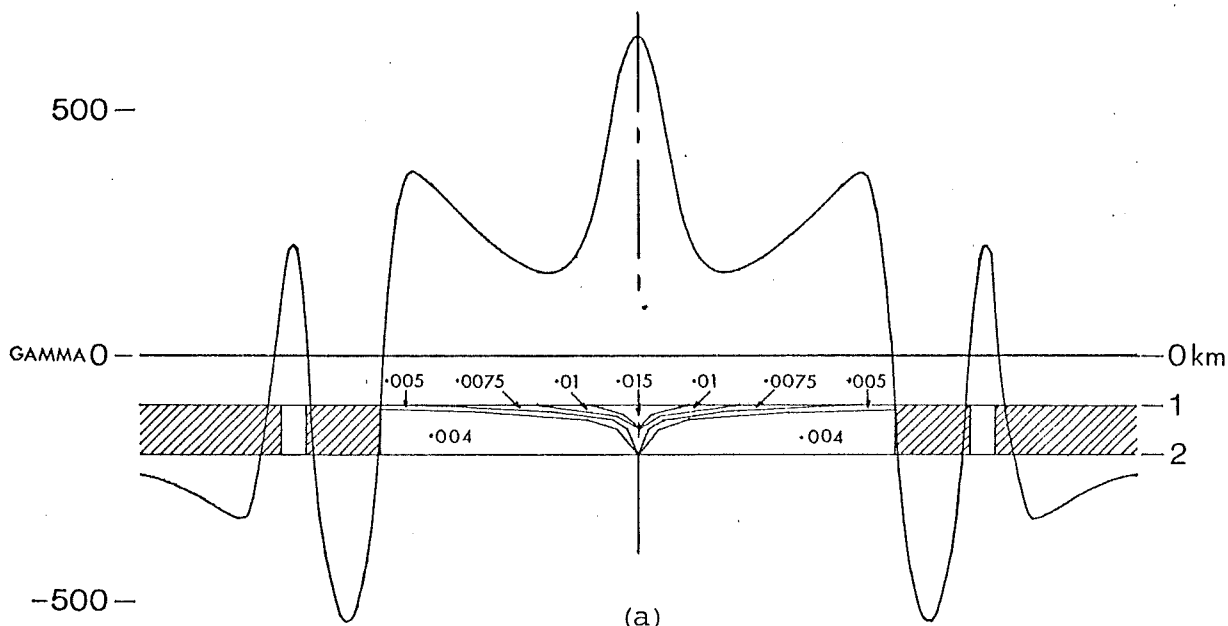
on the shape of the axial magnetic anomaly. Figure 52 shows a comparison between anomalies perpendicular to a N-S ridge produced by: a) the model given in Figure 51 and b) a model similar to that suggested by Irving et al. (1970). Figure 53 illustrates the anomalies produced by the same models perpendicular to a ridge trending N 15°E, such as the Mid-Atlantic Ridge. The change in direction of the ridge introduces asymmetry but does not change the basic characteristics. These characteristics are: in the case of the new model, three peaks in the central anomaly; in the case of the earlier model, two peaks with a central depression.

Various attempts at modelling central anomalies are shown in Figure 54. Figure 54a is from Dickson et al. (1968). Here the authors' model has a smaller central dip than is observed. They were using relatively thick (2 km) central block with 0.01 emu/cm^3 ; a thinner, more strongly magnetized block would have a more pronounced depression. There is also a small central peak in the observed profile unexplained by their model. Figure 54b from Heirtzler et al. (1968) shows a generally confused central region with several peaks within the central region compared to the smooth depression in the model. Figure 54c from Vacquier (1972) shows a profile across the Juan de Fuca ridge. Clearly the model presented in Figure 51 would give far better agreement in the central block than the model actually used for this profile.

It can be seen that many profiles have complex median peaks not explained by simple models with uniform intensity



(b)



(a)

Figure 52. Profiles across N-S Ridge.

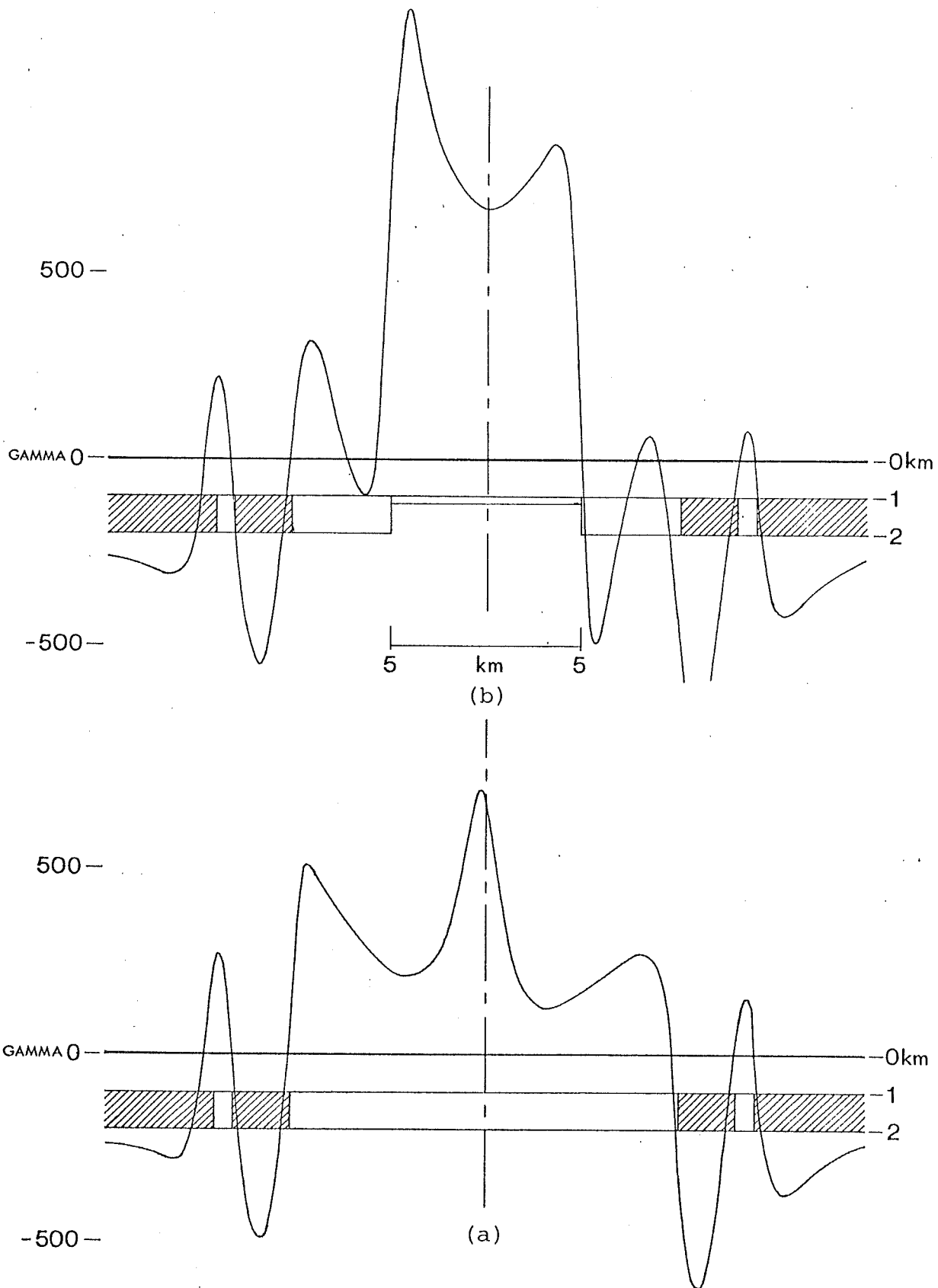
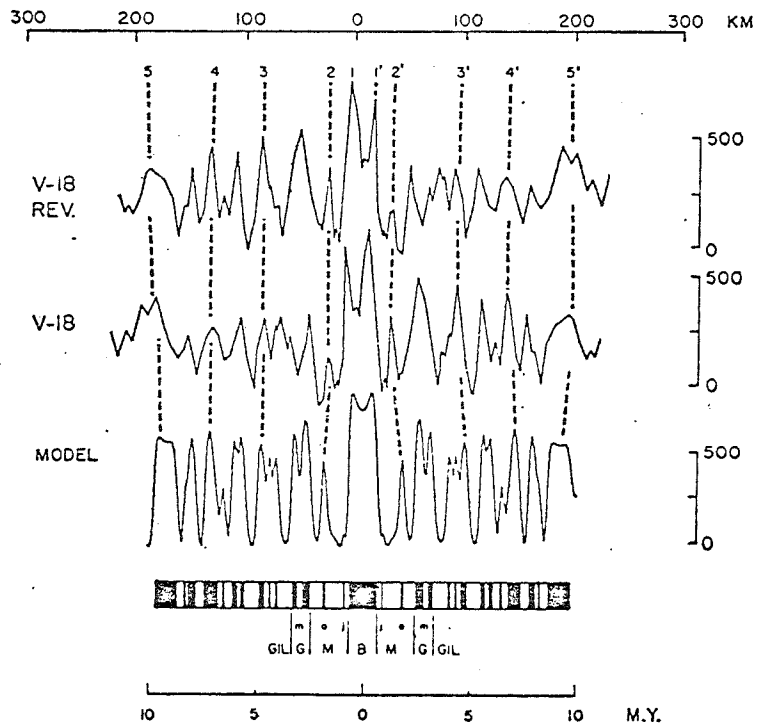
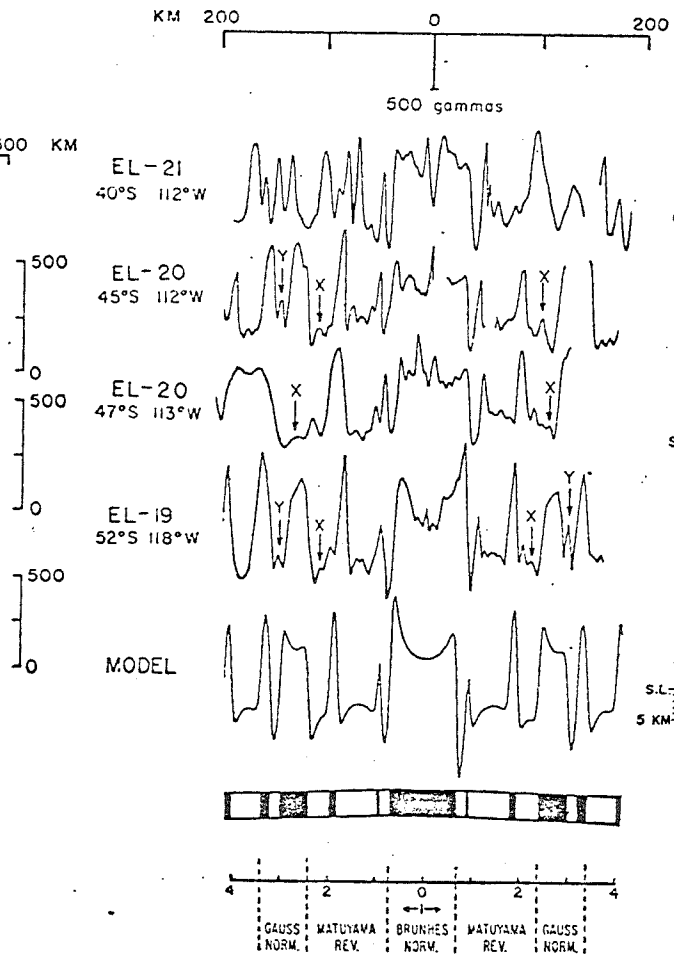


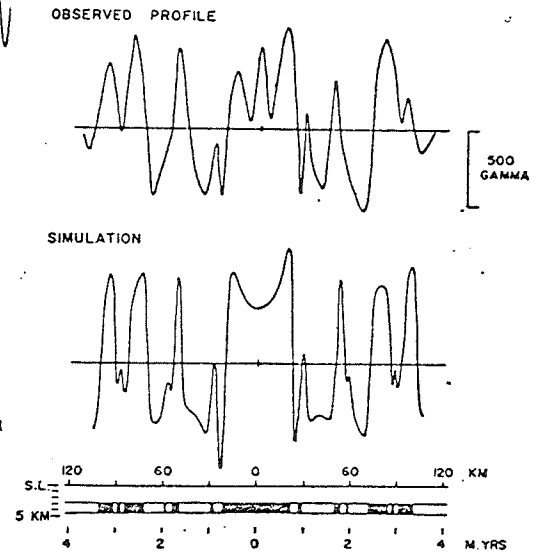
Figure 53. Profiles across a N15°E trending Ridge.



(a)



(b)



(c)

Figure 54. Profiles and their models across several ridges.

in the central block. On the other hand a model such as that presented here can produce a central peak directly over very young basalts of the active spreading centre and in the case of the Juan de Fuca ridge would produce a better fit to the observed profile.

Speculating further one might even suggest that since the peaks within the central block are caused by basalts less than about 3×10^5 years old then the presence of such peaks is an indication of volcanic activity during that period and that multiple peaks, as in Heirtzler et al. (1968) show multiple centres of volcanic activity within that period.

4. Effect of Possible Self-reversals

In Section III some consideration was given to the "self-reversal" phenomena encountered in the laboratory alteration. What has to be decided is whether this is merely an interesting laboratory phenomenon or whether it is of geologic significance. The important factor in making this decision is the comparison between the conditions under which the reversal occurred in the laboratory and the conditions which pillow basalts may encounter in nature.

The self-reversal seen in the laboratory occurs when the original titanomagnetite is oxidized and splits into two phases. Apparently the reversal is due to an interaction between the daughter phase and the previously demagnetized mother phase. There is no evidence as yet for such phase-splitting at sea-bottom temperatures; also under natural

conditions the pillows will not be demagnetized as they were in the laboratory. If the pillows are magnetized and phase-splitting of the titanomagnetite does occur, then the mother and daughter phases might merely interchange roles, with the daughter exsolved in the interaction field of the mother, and self-reversal might still occur. This mechanism has already been proposed by Graham (1953).

The minimum temperature for phase-splitting is not known - it may only be a few tens of degrees, certainly it is little more than a hundred (Johnson and Merrill 1973, this thesis). It is very likely that such temperatures, and hence phase-splitting occur widely at depth within layer 2, certainly where hydrothermal alteration is taking place. The experiments described here indicate that during phase-splitting, conditions are such that self-reversal may occur.

If the cores recovered from Bermuda are at all typical then there are indeed literally hundreds of thin intrusive and extrusive units with many opportunities for reheatings so that adjacent units or even regions within one unit may be magnetized in up and down directions. Such different directions were, in fact, seen in Bermuda although there the magnetic mineral was almost exclusively magnetite, perhaps one of the end products of phase-splitting.

5. Summary

When the results of the experiments described in this thesis are considered, it is clear that the current simple picture of the magnetized part of layer 2 require modification. Up to now this magnetized layer has been visualized as a thin, uniformly magnetized layer, with a magnetization decreasing laterally from the ridge. This picture has been based on dredge hauls and, as far as the top few metres is concerned, it has been confirmed by examination of the pillows described in Section II. These pillows have shown a change in magnetization within each pillow and between the pillows as a result of alteration by sea-water.

Up to this time it has been considered that the magnetization is uniform vertically downwards to the bottom of the magnetic source layer, however, the experiments described in Section II and the Bermuda results show that such is not necessarily the case. Reactions which may take hundreds of thousands of years at 4°C will require only a few thousand hours at 150°C. Thus, near a ridge, the magnetization will be reduced at depth when compared to surface magnetization.

The self-reversals further complicate the picture. They open the possibility that not only does the magnetization decrease in a vertical column - at least near a ridge - but also that under certain conditions some flows, pillows or perhaps only parts of them may have self-reversed magnetization.

Both the decrease in intensity with depth and the possibility of the occurrence of self-reversals mean that a thicker magnetized layer may be necessary to account for the observed anomalies - something closer to a kilometre or two than the more recently proposed 400-500 m. Results from Bermuda roughly confirm this picture. There are many thin volcanic units and not only are some magnetized normally and some reversely but also within one unit (122.6) there are both up and down magnetizations.

In summary then, the measurements in this work lead to a picture not only of lateral decrease in magnetization from a ridge but also of downwards decrease from the high values measured at the surface. Under certain conditions it is possible that self-reversals will occur at depth in some regions further reducing the effective magnetization. Because of these factors the values of intensity of NRM from the "fresh" parts of near surface pillows are almost certainly much higher than values to be used in model building.

6. Future Work

Some of the extrapolations just outlined are speculative, to extrapolate from a few grams of rock in the laboratory to kilometres of rock in the crust is always dangerous but one would be remiss not to make the attempt. The degree of cation deficiency of the titanomagnetites will depend on the availability of water. This will doubtless vary from place to place. Hopefully a clear picture can be built up when several deep holes into layer 2 have been analyzed.

The actual heating experiments described in this work are incomplete simply due to lack of time to pursue them further. These experiments have focussed attention on a very important dependence of the state of cation deficiency on the temperature of reaction. At sea-water temperatures very high 'z' values are attainable, at moderate temperatures, 210°C, $z \approx 0.6$ seems to be an upper limit while at very high temperatures z is very small and the titanomagnetites are essentially stoichiometric. It would be useful not only to rock magnetism to determine such a relation but it may be possible to then use such an index for other mineralogical purposes.

Finally there is the tantalizing question of self-reversal. Why do some samples self-reverse and others not? Perhaps a more detailed examination of the titanomagnetite grains might prove the answer. It may also be possible to carry out the experiment in a high magnetic field and test conclusively if the mechanism of self-reversal is exchange interaction.

BIBLIOGRAPHY

- ADE-HALL, J. M. Khan, M. A., Dagley, P. and Wilson, R. L.
1968. A detailed opaque petrological and magnetic investigation of a single Tertiary lava from Skye, Scotland, Parts I, II, III. Geophys. J. R. astr. Soc. 16, 374, 389 and 401.
- ADE-HALL, J. M., Palmer, H. C. and Hubbard, T. P. 1971.
The magnetic and petrological response of basalts to regional hydrothermal alteration. Geophys. J. R. astr. Soc. 24, 137-174.
- ADE-HALL, J. M., Lowrie, W., Opdyke, N. D. and Aumento, F.
1973. Deep Drill-72: The palaeomagnetism of a long succession of submarine lavas from Bermuda. EOS (Trans. Am. Geophys. Un.) 54, 486 (abstract).
- ADE-HALL, J. M., Aumento, F., Ryall, P.J.C., Gerstein, R. E., Brooke, J. and McKeown, D. L. 1973. The Mid-Atlantic Ridge near 45°N. XXI. Magnetic results from basalt drill cores from the Median Valley. Can. J. Earth Sci. 10, 679-696.
- AKIMOTO, S., Katsura, T. and Yoshida, M. 1958. Magnetic properties of the $\text{TiFe}_2\text{O}_4 - \text{Fe}_3\text{O}_4$ system and their change with oxidation. J. Geomag. and Geoelectr. 9, 165-178.

- AUMENTO, F. 1968. The Mid-Atlantic Ridge near 45°N. II. Basalts from the area of Confederation Peak. Can. J. Earth Sci. 3, 1-21.
- AUMENTO, F. 1969. The Mid-Atlantic Ridge near 45°N. V. Fission track and ferro-manganese chronology. Can. J. Earth Sci. 6, 1431-1440.
- AUMENTO, F. and Ade-Hall, J. M. 1973. Deep Drill-1972: Petrology of the Bermuda drill core. EOS (Trans. Am. Geophys. Un.) 54, 485 (abstract).
- AUMENTO, F. and Gunn, B. 1974. Deep Drill-1972: Petrology and Geochemistry of the Bermuda Seamount. (in press).
- BARTH, T.F.W. and Posnjak, E. 1932. Spinel structure with and without variable atom equipoints, Zeit. Krist. 82, 324.
- BROOKE, J., Irving, E. and Park J. K. 1970. The Mid-Atlantic Ridge at 45°N. XIII. Magnetic properties of basalt bore-core. Can. J. Earth Sci. 7, 1515-1527.
- CHIKAZUMI, S. 1964. Physics of Magnetism. John Wiley, New York.
- COX, A. 1969. Geomagnetic Reversals. Science 163, 237-245.
- CREER, K. M., Petersen, N. and Petherbridge, J. 1970. Partial self-reversal of remanent magnetization and anisotropy of viscous magnetization in basalts. Geophys. J. R. astr. Soc. 21, 471-483.

- CREER, K. M. 1971. Geophysical interpretation of remanent magnetization in oxidized basalts. *Z. für Geophysk.* 37, 383-407.
- DAVIES, H. L. 1968. Papuan ultramafic belt: 23rd Internat. Geol. Congr. Prague, Rep., Sec. 1, 209-220.
- DICKSON, G. O. 1968. Magnetic Anomalies in the South Atlantic and Ocean Floor Spreading. *J. Geophys. Res.* 73, 2087-2100.
- DUNLOP, D. J. and West, G. F. 1969. An experimental evaluation of single domain theories. *Rev. of Geophys.* 7, 709-757.
- DUNLOP, D. J. 1973. Thermoremanent magnetization in sub-microscopic magnetite. *J. Geophys. Res.* 78, 7602.
- DUNLOP, D. J. 1973. Theory of magnetic viscosity of lunar and terrestrial rocks. *Rev. of Geophys. and Space Phys.* 11, 855-901.
- EVANS, M. E., McElhinny, M. W. and Gifford, A. C. 1968. Single domain magnetite and high coercivities in a gabbroic intrusion. *Earth and Planet. Sci. Lett.* 4, 142.
- EVANS, M. E. and McElhinny, M. W. 1969. An investigation of the origin of stable remanence in magnetite bearing igneous rocks. *J. Geomag. and Geoelectr.* 21, 757-773.
- EVANS, M. E. and Wayman, M. L. 1970. An investigation of small magnetic particles by means of electron microscopy. *Earth Planet. Sci. Lett.* 9, 365-370.

- EVANS, M. E. and Wayman, M. L. 1972. The Mid-Atlantic Ridge near 45°N. XIX. An electron microscope investigation of the magnetic minerals in basalt samples. *Can. J. Earth Sci.* 9, 671-678.
- GASS, I. G. 1968. Is the Trudos massif of Cyprus a fragment of Mesozoic ocean floor? *Nature* 220, 39-42.
- GRAHAM, J. W. 1953. Changes of Ferromagnetic Minerals and their Bearing on Magnetic Properties of Rocks. *J. Geophys. Res.* 58, 243-260.
- GROMME, C. S., Wright, T. L. and Peck, D. L. 1969. Magnetic properties and oxidation of iron titanium oxide minerals in Aloe and Mahaopulic lava lakes, Hawaii. *J. Geophys. Res.* 74, 5277-5293.
- GROMME, C. S. 1975. Rock Magnetism of Leg 34 Basalts in Initial Reports of the Deep Sea Drilling Project. (in press).
- HART, R. 1970. Chemical exchange between sea-water and deep ocean basalts. *Earth Planet. Sci. Lett.* 9, 269.
- HART, R. A. 1973. A model for chemical exchange in the basalt-seawater system of oceanic layer II. *Can. J. Earth Sci.* 10, 799.
- HEIRTZLER, J. R. and LePichon, X. 1965. Crustal structure of the Mid-ocean ridges. Magnetic anomalies over the Mid-Atlantic Ridge. *J. Geophys. Res.* 70, 4013-4033.
- HEIRTZLER, J. R. and Hayes, D. E. 1967. Magnetic boundaries in the North Atlantic Ocean. *Science* 157, 185-187.

- HEIRTZLER, J. R., Dickson, G. O., Herron, E. M., Pitman, W. C. III and LePichon, X. 1968. Marine Magnetic Anomalies, Geomagnetic Field Reversals, and Motions of the Ocean Floor and Continents. *J. Geophys. Res.* 73, 2119-2136.
- HEKINIAN, R. 1971. Chemical and mineralogical differences between abyssal hill basalts and ridge tholeiites in the Eastern Pacific Ocean. *Mar. Geol.* 11, 77-91.
- IRVING, E., Robertson, W. A. and Aumento, F. 1970a. The Mid-Atlantic Ridge near 45°N. VI. Remanent intensity, susceptibility and iron content of dredged samples. *Can. J. Earth Sci.* 7, 226-238.
- IRVING, E., Park, J. K., Haggerty, S. E., Aumento, F. and Loncarevic, B. D. 1970b. Magnetism and opaque mineralogy of basalts from the Mid-Atlantic Ridge at 45°N. *Nature* 228, 974-976.
- IRVING, E. 1970. The Mid-Atlantic Ridge at 45°N. XIV. Oxidation and magnetic properties of basalts; review and disucssion. *Can. J. Earth Sci.* 7, 1528-1538.
- JENSEN, S. D. and Shive, P. N. 1973. Cation distribution in sintered titanomagnetites. *J. Geophys. Res.* 78, 8474-8480.
- JOHNSON, H. P. and Merril, R. T. 1973. Low-Temperature Oxidation of a Titanomagnetite and the Implications for Palaeomagnetism. *J. Geophys. Res.* 78, 4938-4949.

- JOHNSON, H. P. and Lowrie, W. 1974. Stability of Anhyseretic remanent magnetization in fine and coarse magnetite and maghemite particles. (in press).
- KEEN, M. J. 1963. Magnetic anomalies over the Mid-Atlantic Ridge. *Nature* 197, 888-890.
- KUSHIRO, I. 1960. γ - α Transition in Fe_2O_3 with pressure. *J. Geomag. and Geoelectr.* 11, 148-151.
- LARSON, E., Ozima, M., Ozima, M., Nagata, T. and Strangway, D. 1969. Stability of remanent magnetization of igneous rocks. *Geophys. J. R. astr. Soc.* 17, 263-292.
- LONCAREVIC, B. D., Mason, C. S. and Matthews, D. H. 1966. Mid-Atlantic Ridge near 45°N. The Median Valley. *Can. J. Earth Sci.* 3, 327-349.
- LOWRIE, W. 1973. Viscous remanent magnetization in oceanic basalts. *Nature* 243, 7.
- LOWRIE, W., Lovlie, R. and Opdyke, N. D. 1973. The magnetic properties of Deep Sea Drilling basalts from the Atlantic Ocean. *Earth Planet. Sci. Lett.* 17, 338-349.
- LUYENDYK, B. P., MacDonald, K. C. and Moore, J. C. 1974. Near bottom investigations of the rift valley floor of the Mid-Atlantic Ridge at 36°31'N. *EOS (Trans. Am. Geophys. Un.)* 55, 446 (abstract).
- MARSHALL, M. and Cox, A. 1971a. Effect of oxidation on the natural remanent magnetization of titanomagnetites in suboceanic basalt. *Nature* 230, 28-31.

- MARSHALL, M. and Cox, A. 1971b. Magnetism of pillow basalts and their petrology. Geol. Soc. Am. Bull. 82, 537-552.
- MARSHALL, M. and Cox, A. 1972. Magnetic changes in pillow basalt due to sea-floor weathering. J. Geophys. Res. 77, 6459-6469.
- MASON, R. G. and Raff, A. D. 1961. Magnetic survey off the West coast of North America, 32°N. latitude to 42°N latitude. Bull. Geol. Soc. Amer. 72, 1259-1266.
- MOORE, J. G. and Fiske, R. S. 1969. Volcanic substructure inferred from dredge samples and ocean-bottom photographs, Hawaii. Geol. Soc. Amer. Bull. 80, 1191-1201.
- MOORE, J. G., Phillips, R. L., Grigg, R. W., Peterson, D. W. and Swanson, D. A. 1973. Flow of lava into the sea, 1969-1971, Kilauea Volcano, Hawaii. Bull. Geol. Soc. Amer. 84, 537-546.
- NAGATA, T. and Uyeda, S. 1959. Exchange interaction as a cause of reverse thermoremanent magnetism. Nature 184, 890-891.
- NAGATA, T. 1961. Rock Magnetism, Maruzen, Tokyo.
- NEEL, L. 1955. Some theoretical aspects of rock magnetism. Adv. Phys. 4, 191-243.
- O'REILLY, W. and Banerjee, S. 1966. Oxidation of titanomagnetite and self-reversal. Nature 221, 26-27.
- OZIMA, M. and Ozima, M. 1967. Self-reversal of remanent magnetization in some dredged submarine basalts. Earth Planet. Sci. Lett. 3, 213-215.

- OZIMA, M. and Larson, E. E. 1968. Study of self-reversal of TRM in some submarine basalts. J. Geomag. and Geoelectr. 20, 337-351.
- OZIMA, M. 1971. Magnetic processes in oceanic ridge. Earth and Planet. Sci. Lett. 13, 1-15.
- OZIMA, M. and Ozima, M. 1972. Activation energy of unmixing of titanomaghemite. Phys. Earth and Planet. Interiors 5, 87-89.
- PARK, J. K. and Irving, E. 1970. The Mid-Atlantic Ridge near 45°N. XII. Coercivity, secondary magnetization, polarity and thermal stability of dredge samples. Can. J. Earth Sci. 7, 1499-1514.
- PARRY, L. G. 1965. Magnetic properties of dispersed magnetite powder. Phil. Mag. 11, 303.
- PETERSEN, N. 1969. Calculation of diffusion coefficients and activation energy in some titanomagnetites. Phys. Earth Planet. Sci. Lett. 4, 175-178.
- PETERSEN, N. and Bleil, U. 1973. Self-reversal of remanent magnetization in synthetic titanomagnetites. Z. für Geophysik. 39, 965-977.
- RAFF, A. D. and Mason, R. G. 1961. Magnetic survey off the west coast of North America, 40°N latitude to 52°N latitude. Bull. Geol. Soc. Amer. 72, 1267-1270.

- RAINBOW, R. R., Fuller, M. and Schmidt, V. A. 1972.
Palaeomagnetic orientation of borehole samples. EoS
(Trans. Am. Geophys. Un.) 53, 355 (abstract).
- READMAN, P. W. and O'Reilly, W. 1970. The synthesis and
inversion of non-stoichiometric titanomagnetite. Phys.
Earth and Planet. Interiors, 4, 121-128.
- READMAN, P. W. and O'Reilly, W. 1972. Magnetic properties
of oxidized (cation-deficient) titanomagnetites
(Fe, Ti, □)₃O₄. J. Geomag. and Geoelectr. 24, 69-90.
- REYNOLDS, P. H. and Aumento, F. 1973. Deep Drill-1972:
Geochronology of the Bermuda Drill Core. EoS (Trans.
Am. Geophys. Un.) 54, 485 (abstract).
- SCHAEFFER, R. M. and Schwarz, E. J. 1970. The Mid-Atlantic
Ridge near 45°N. IX. Thermomagnetism of dredged
samples of igneous rocks. Can. J. Earth Sci. 7, 268-273.
- SCHIMIZU, Y. 1960. Magnetic Viscosity of Magnetite. J.
Geomag. and Geoelectr. 11, 125.
- SOFFEL, H. 1971. The single domain - multidomain transition
in natural intermediate titanomagnetites. Z. für
Geophysik. 37, 451-470.
- STACEY, F. D. 1963. The physical theory of rock magnetism,
Adv. in Phys. 12, 45-133.

- TALWANI, M., Windisch, C. C. and Langseth, M. G. 1971.
Reykjanes Ridge Crest: A detailed geophysical study.
J. Geophys. Res. 76, 473-517.
- UYEDA, S. 1958. Thermoremanent magnetism as a medium of
palaeomagnetism, with special reference to reverse
thermoremanent magnetism. Jap. J. of Geophys. 2, 1-123.
- VACQUIER, V. 1972. Geomagnetism in Marine Geology.
Elsevier, Amsterdam.
- VERHOOGEN, J. 1962. Oxidation of iron-titanium oxides in
igneous rocks. J. Geol. 70, 168-181.
- VINE, F. J. and Matthews, D. H. 1963. Magnetic anomalies
over ocean ridges. Nature 199, 947-949.
- WATKINS, N. D. and Richardson, A. 1971. Intrusives,
Extrusives and Linear magnetic anomalies. Geophys.
J. R. astr. Soc. 23, 1-13.
- WATKINS, N. D. and Paster, T. P. 1971. The magnetic properties
of igneous rocks from the ocean floor. Phil. Trans. Roy.
Soc. Lond. A. 268, 507-550.
- WILLIAMS, H. 1972. The Appalachian structural province,
stratigraphy. In 'Variation in tectonic styles in Canada'.
ed. Price, R.A. and Douglas, R.J.W. Geol. Assoc. of
Canada. Spec. Paper No. 11.
- WILSON, R. L. and Haggerty, S. E. 1966. Reversals of the
Earth's Magnetic field. Endeavour 25, 104.

WILSON, R. L. and Watkins, N. D. 1967. Correlation of
petrology and natural remanent polarity in Columbia
Plateau basalts. Geophys. J. R. astr. Soc. 12, 405.

APPENDIX

MAJOR CONSTITUENTS OF
NORTHWEST ARM SEA WATER

(salinity 31-32 ‰)

	‰
Chloride, Cl^-	17.1
Sulphate, $\text{SO}_4^{=}$	2.38
Bicarbonate, HCO_3^-	.126
Bromide, Br^-	.0582
Flouride, F^-	.0012
Boric acid, H_3BO_3	.0234
Sodium, Na^+	9.50
Magnesium, Mg^{++}	1.14
Calcium, Ca^{++}	.360
Potassium, K^+	.342
Strontium, Sr^{++}	.0120

‰ means parts per thousand.

APPENDIX

TYPICAL ANALYSIS OF HALIFAX WATER
TREATED SUPPLY

Made by
Department of Energy, Mines and Resources
Water Quality Division
5 December 1973

(in parts per million)

Temperature at Testing	(C)	20.9
pH		6.1
Chloride Dissolved	(Cl)	8.4
Copper Extractable	(Cu)	0.03
Fluoride Dissolved	(F)	1.1
Iron Extractable	(Fe)	0.20
Iron Dissolved	(Fe)	-
Lead Extractable	(Pb)	0.010
Magnesium Dissolved	(Mg)	0.6
Manganese Extractable	(Mn)	0.04
Manganese Dissolved	(Mn)	-
Nitrogen Nitrate Nitrite	(Diss) (N)	0.05
Nitrogen Dissolved Ammonia	(N)	L0.005
Phosphorus Dissolved Inorganic Phosphate	(P)	L0.010
Potassium Dissolved	(K)	0.4
Specific Conductance	(umno/cm)	49.4
Alkalinity Total	(CaCO ₃)	3.7
Hardness Total	(CaCO ₃)	13.2
Calcium Dissolved	(Ca)	4.3
Sulphate Dissolved	(Ca)	6.0
Silica Reactive	(SiO ₂)	2.0
Sodium Dissolved	(Na)	3.3

APPENDIX (continued)

Zinc Extractable	(Zn)	0.013
Cadmium Extractable		0.001
Non Carb. Hardness		9.51
Sub Const. PRM		29.04
S A R		0.45
o/o NA (Sodium)		37.62
Saturation Index		4.15
Stability Index		14.39

L refers to less than.